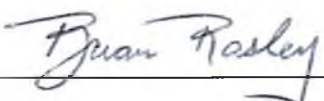



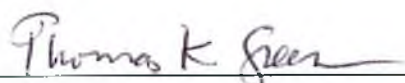
SYNTHESIS AND CHARACTERIZATION OF RANDOMLY 2,3-O-  
SULFOALKYLATED BETA- CYCLODEXTRINS FOR USE IN CHIRAL  
CAPILLARY ELECTROPHORESIS

By

Michael Jaramillo

RECOMMENDED:




Advisory Committee Chair

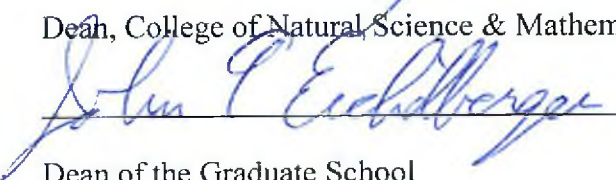


Chair, Department of Chemistry & Biochemistry

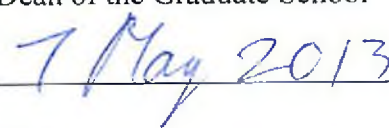
APPROVED:



Dean, College of Natural Science & Mathematics



Dean of the Graduate School



Date

SYNTHESIS AND CHARACTERIZATION OF RANDOMLY 2,3-O-  
SULFOALKYLATED BETA- CYCLODEXTRINS FOR USE IN CHIRAL  
CAPILLARY ELECTROPHORESIS

A

Thesis

Presented to the Faculty  
of the University of Alaska Fairbanks

in Partial Fulfillment of the Requirements  
for the Degree of  
MASTER OF SCIENCE

By

Michael Jaramillo

Fairbanks, Alaska

May 2013

## Abstract

Chiral separation of enantiomers is of vast significance in synthetic chemistry. Determining the enantiomeric purity of a product is necessary in the pharmaceutical industry. Recent studies in capillary electrokinetic chromatography (cEKC) have suggested that anionic cyclodextrins (CDs) are powerful chiral resolving agents. The purpose of this research was to synthesize a series of highly charged heptakis(randomly-2,3-O-sulfoalkyl)- $\beta$ -CDs, characterize the CDs, and apply the CDs to chiral separations of aryl alcohols. The synthesis focused on the sulfobutylation of heptakis(6-O-methyl)- $\beta$ -CD and heptakis(6-O-*tert*-butyldimethylsilyl)- $\beta$ -CD as well as the sulfopropylation of heptakis(6-O-*tert*-butyldimethylsilyl)- $\beta$ -CD. The degree of sulfoalkylation of the final products was determined by hydrophilic interaction chromatography (HILIC) with a low temperature evaporative light scattering detector (LT-ELSD). The synthesis of heptakis(6-O-methyl)- $\beta$ -CD was obtained by a lengthy protection/deprotection reaction scheme utilizing the acetylation of the secondary hydroxyl groups, with an overall yield of 43% in 5 steps. The sulfobutylation of heptakis(6-O-methyl)- $\beta$ -CD and heptakis(6-O-*tert*-butyldimethylsilyl)- $\beta$ -CD produced low degrees of substitution (DS < 1.0). The sulfopropylation of heptakis(6-O-*tert*-butyldimethylsilyl)- $\beta$ -CD in tetrahydrofuran (THF) resulted in much higher degree of substitution, with DS of 3.3, 4.6, and 6.1, which increased with amount of added 18-crown-6 ether. Also, an increase in the DS (6.1 and 8.4) was observed when changing the solvent from THF to N,N-dimethylformamide. Chiral resolution studies of relevant aryl alcohols using potassium heptakis(randomly-

2,3-O-sulfopropyl)-  $\beta$ -CD (DS 8.4), potassium heptakis(2,3-di-O-methyl-6-O-sulfopropyl)-  $\beta$ -CD (DS 4.5) and the single isomer potassium heptakis(2,3-di-O-methyl-6-O-sulfobutyl)- $\beta$ -CD were performed. Resolution of the enantiomers of the aryl alcohols is dependent on the distance of the chiral center from the aromatic ring and the substituent on the secondary rim of the cyclodextrin.

<b>Table of Contents</b>	<b>Page</b>
Signature Page .....	i
Title Page .....	ii
Abstract .....	iii
Table of Contents .....	v
List of Figures .....	vii
List of Tables .....	xi
Acknowledgements.....	xii
Chapter 1. Introduction and Research Goals .....	1
1.1    Introduction to cyclodextrins and their chemistry .....	1
1.2    Hydrophilic interaction chromatography analysis of highly polar molecules ....	10
1.3    Application of highly charged cyclodextrins in chiral capillary electrophoresis separations .....	16
1.4    Summary of research goals .....	21
Chapter 2. Materials and Methods .....	27
2.1    Materials.....	27
2.2    NMR analysis.....	28
2.3    CE analysis.....	29
2.3.1    Characterization of final products with inverse detection CE .....	29

	Page
2.3.2 Chiral analysis of aromatic alcohols .....	29
2.4 HILIC/ LT-ELSD analysis .....	30
2.5 Synthetic procedures .....	30
2.5.1 Synthesis of Methyl triflate .....	31
2.5.2 Synthesis of Heptakis (6-O-methyl)- $\beta$ -CD by acetyl intermediates.....	31
2.5.3 Sulfobutylation of Heptakis (6-O-Methyl)- $\beta$ -CD ( $\beta$ 6).....	44
2.5.4 Optimization of Sulfoalkylation at the secondary face.....	46
Chapter 3. Results .....	51
3.1 Synthesis of acetyl intermediates and Heptakis(6-O-methyl-randomly-2,3-sulfopropyl)- $\beta$ -CD.....	51
3.2 Optimization of sulfoalkylation reaction on secondary hydroxyls .....	53
3.3 Characterization of the final products .....	54
3.3.1 NMR integrations .....	55
3.3.2 Inverse Detection CE.....	61
3.3.3 Hydrophilic interaction chromatography.....	64
3.4 Chiral separations of aromatic alcohols .....	78
Chapter 4. Summary and Future Work.....	86
References.....	89

<b>List of Figures</b>	<b>Page</b>
Figure 1.1. A top view of the chemical structure of $\alpha$ -, $\beta$ -, and $\gamma$ - CD (from left to right)	1
Figure 1.2. A side view of the toroidal shape of $\beta$ -CD. One of the $\alpha$ -D-glucose units is shown with the standard numbering .....	3
Figure 1.3. Selective de-benzylation of heptakis(2,3,6-tri-O-benzyl)- $\beta$ -CD [9] .....	5
Figure 1.4. (a.) (R and S) heptakis (mono-6-deoxy-6- $\alpha$ -methoxyformyl)- $\beta$ -CD, (b.) the heptakis(di-6 <sup>A</sup> , 6 <sup>D</sup> -deoxy-6-formyl)- $\beta$ -CD and (c.) the reaction conditions for hydrolysis of glycosides [10, 11].....	6
Figure 1.5. (a.) Heptakis(mono-6-deoxy-6-monourea-permethyated)- $\beta$ -CD (PMMABCD) bond to silica particle and (b.) coumarin- based anticoagulants separated by the PMMABCD silica [12].....	8
Figure 1.6. Series of single isomer, amphiphilic CDs (2,3-di-O-alkyl-6-O-sulfoalkyl CD potassium salts).....	9
Figure 1.7. This depiction of the stationary phase on a Luna HILIC column shows the cross-linked diols on the silica support surface. A rich water layer near the stationary phase has been reported when using a mobile phase with large ACN composition.....	15
Figure 1.8. Separation of “analytes” based on charge to size ratios .....	17
Figure 1.9. Separation of a negatively charged “analytes” as pH is changed without changing the applied field voltage .....	18
Figure 1.10. Secondary interaction with CD and an analyte .....	20
Figure 1.11. Reaction scheme for the synthesis of a single isomer heptakis(6-O-methyl)- $\beta$ -CD .....	22

Figure 1.12. Reaction scheme for the optimization of the synthesis of heptakis(randomly-2,3-O-sulfopropyl)- $\beta$ -CD (KSP <sub>x</sub> $\beta$ -CD) and heptakis(randomly-2,3-O-sulfobutyl)- $\beta$ -CD (KSB <sub>x</sub> $\beta$ -CD).....	24
Figure 2.1. <sup>1</sup> H NMR spectrum (600 MHz, CDCl <sub>3</sub> ) of heptakis(6-O-TBDMS)- $\beta$ -CD ...	32
Figure 2.2. <sup>13</sup> C NMR spectrum (150 MHz, CDCl <sub>3</sub> ) of heptakis(6-O-TBDMS)- $\beta$ -CD ...	33
Figure 2.3. <sup>1</sup> H NMR spectrum (600 MHz, CDCl <sub>3</sub> ) of heptakis(2,3-di-O-acetyl-6-O-TBDMS)- $\beta$ -CD .....	35
Figure 2.4. <sup>13</sup> C NMR spectrum (150 MHz, CDCl <sub>3</sub> ) of heptakis(2,3-di-O-acetyl-6-O-TBDMS)- $\beta$ -CD .....	36
Figure 2.5. <sup>1</sup> H NMR spectrum (600 MHz, acetone-d <sub>6</sub> ) of heptakis(2,3-di-O-acetyl)- $\beta$ -CD .....	38
Figure 2.6. <sup>13</sup> C NMR spectrum (150 MHz, acetone-d <sub>6</sub> ) of heptakis(2,3-di-O-acetyl)- $\beta$ -CD .....	39
Figure 2.7. <sup>1</sup> H NMR spectrum (600 MHz, acetone-d <sub>6</sub> ) of heptakis(2,3-di-O-acetyl-6-O-methyl)- $\beta$ -CD .....	41
Figure 2.8. <sup>13</sup> C NMR spectrum (150 MHz, acetone-d <sub>6</sub> ) of heptakis(2,3-di-O-acetyl-6-O-methyl)- $\beta$ -CD .....	42
Figure 2.9. <sup>1</sup> H NMR spectrum (600 MHz, DMSO-d <sub>6</sub> ) of heptakis(6-O-methyl)- $\beta$ -CD.	43
Figure 2.10. <sup>13</sup> C NMR spectrum (150 MHz, DMSO-d <sub>6</sub> ) of heptakis(6-O-methyl)- $\beta$ -CD .....	44



Figure 2.11. $^1\text{H}$ -NMR spectra of Heptakis(6-O-methyl-randomly-2,3-O-sulfobutyl)- $\beta$ -CDs in $\text{D}_2\text{O}$ .....	46
Figure 2.12. $^1\text{H}$ -NMR spectra of $\text{KSP}_x$ $\beta$ -CDs in $\text{D}_2\text{O}$ .....	49
Figure 2.13. $^1\text{H}$ -NMR spectra of $\text{KSB}_x$ $\beta$ -CDs in $\text{D}_2\text{O}$ .....	50
Figure 3.1. A plot of the expected integration ratios as a function of the DS for the $\text{KSP}_x$ $\beta$ -CDs .....	56
Figure 3.2. A plot of the expected integration ratios as a function of the DS for the $\text{KSP}_x$ $\beta$ -CDs .....	57
Figure 3.3. A plot of the expected integration ratios as a function of the DS for the $\text{KSB}_x$ $\beta$ -CDs .....	59
Figure 3.4. A plot of the expected integration ratios as a function of the DS for the $\text{KSB}_x$ $\beta$ -CDs .....	60
Figure 3.5. Inverse detection CE separations of $\text{KSP}_x$ $\beta$ -CDs .....	62
Figure 3.6. Inverse detection CE separations of $\text{KSB}_x$ $\beta$ -CDs .....	63
Figure 3.7 Effect of water concentration on HILIC separations of $\text{KSP}_{\text{DS } 4.5}\text{DM}$ $\beta$ -CD. 66	
Figure 3.8. HILIC separations of single isomer $\alpha$ -CDs .....	67
Figure 3.9. HILIC separations of single isomer $\beta$ -CDs .....	68
Figure 3.10. Effect of water concentration on HILIC separations of $\text{KSP}_x$ $\beta$ -CD (reaction DMF 4 SP) .....	69
Figure 3.11. HILIC separations of a spiked sample of native $\beta$ -CD, a low DS (reaction THF 0 SP) and high DS (reaction DMF 4 SP) to establish retention times of DS 0-14... 70	

	Page
Figure 3.12. HILIC separations of KSP <sub>x</sub> β- CD .....	71
Figure 3.13. HILIC separations of KSB <sub>x</sub> β- CD .....	73
Figure 3.14. Effect of water concentration on HILIC separations of KSB <sub>x</sub> β- CD (reaction DMF 4 SB).....	74
Figure 3.15. HILIC separations of KSB <sub>x</sub> β- CDs .....	75
Figure 3.16. The chiral aryl alcohols used in the CE separation studies .....	79
Figure 3.17. Chiral CE separations of (+/-) 1-phenyl ethanol .....	80
Figure 3.18. Chiral CE separations of (+/-) 3-phenyl-2-propanol .....	81
Figure 3.19. Chiral CE separations of (+/-) 4-phenyl-2-butanol .....	82
Figure 3.20. Chiral CE separations of (+/-) 1-phenyl-3-buten-2-ol .....	83

<b>List of Tables</b>	<b>Page</b>
Table 2.1. The actual values for the masses used to optimize the sulfoalkylation of heptakis(6-O-TBDMS)- $\beta$ -CD (followed by the deprotection of the primaries).....	48
Table 3.1. The calculated DS from integration ratios are provided for the KSP <sub>x</sub> $\beta$ -CDs from the reaction optimization experiments .....	58
Table 3.2. The calculated DS from integration ratios are provided for the KSB <sub>x</sub> $\beta$ -CDs from the reaction optimization experiments .....	61
Table 3.3. The peak areas were used to determine the DS of Heptakis(randomly-2,3-O-sulfopropyl)- $\beta$ -CD from HILIC LT-ELSD results .....	72
Table 3.4. The peak areas were used to determine the DS of Heptakis(randomly-2,3-O-sulfobutyl)- $\beta$ -CD from HILIC LT-ELSD results.....	76
Table 3.5. The calculated R <sub>s</sub> values for the chiral resolution of the aryl alcohols are provided below.....	84

## **Acknowledgements**

I would like to thank my wife Ashley mainly for always being there for me and for being an amazing person, but also for guidance and assistance with my thesis. I would also like to thank my daughter Ester for making me want to complete this thesis! And of course, I would like to thank ALL my family (especially my parents and siblings) for encouraging me to finish and being there for me whenever I needed them.

There are several individuals that have assisted me in getting through this program. A number of these individuals were members of Dr. Green's research lab. Firstly, I would like to express my gratitude to Dr. Daniel L. Kirschner for all his assistance, guidance, and most importantly, his friendship. If not for Dan, I would never have even come close to finishing! I would also like to thank Zhipeng Dai whom also provided assistance, guidance and friendship though the latter half of my project. Other graduate students that provided assistance include Dr. Collin McGill, Jim Warner, and Jamie McKee. There were also countless undergraduates that sat through a number of lab group meetings and gave me some excellent feedback. I would also like to thank Dr. Sarah Petitto, Dr. Chris Iceman, Dr. Anastasia Ilgen, and Vanessa Ritchie for providing me with moral support from my peers. It is always nice to vent our frustrations with others having similar worries!

I would also like to thank the Department of Chemistry and Biochemistry for all the support they have provided me through the numerous years that I have spent in the lab. They have provided funding, lab space, education, and countless opportunities that made

my experience here so wonderful. A special thanks to Mist D'June- Gussak for all her support and assistance! Thanks to Libby Miles as well for your help.

I would like to thank my committee members, Dr. Thomas P. Trainor and Dr. Brian T. Rasley for their assistance and feedback. I would also like to thank Dr. Thomas P. Clausen for being on my committee at the beginning. Unfortunately, I took forever and he retired before I could finish. I would also like to extend my gratitude to Dr. William Simpson, the Department Chair, for his assistance and feedback over the years as well. Lastly, I would like to thank my Dr. Thomas K. Green for being the advisor to my committee and being patient with me through the years. I have learned a lot from Tom and appreciate all that he has done for me and my family.

## Chapter 1. Introduction and Research Goals

### 1.1 Introduction to cyclodextrins and their chemistry

First discovered in the year 1891 by A. Villiers, naturally occurring cyclodextrins (CDs) are cyclic oligosaccharides composed of  $\alpha$ -D-glucose units connected via a 1,4 glycosidic linkage that are produced enzymatically from starch. The more common CDs are composed of 6, 7 and 8 glucose units and are called  $\alpha$ -,  $\beta$ - and  $\gamma$ -CDs, respectively (Figure 1.1). These CDs have a tubular shape that varies in diameter based on the number of glucose units. The maximum diameters for  $\alpha$ -,  $\beta$ - and  $\gamma$ -CDs are 5.3 Å, 6.5 Å, and 8.3 Å respectively and they all have the same depth of 7.9 Å.

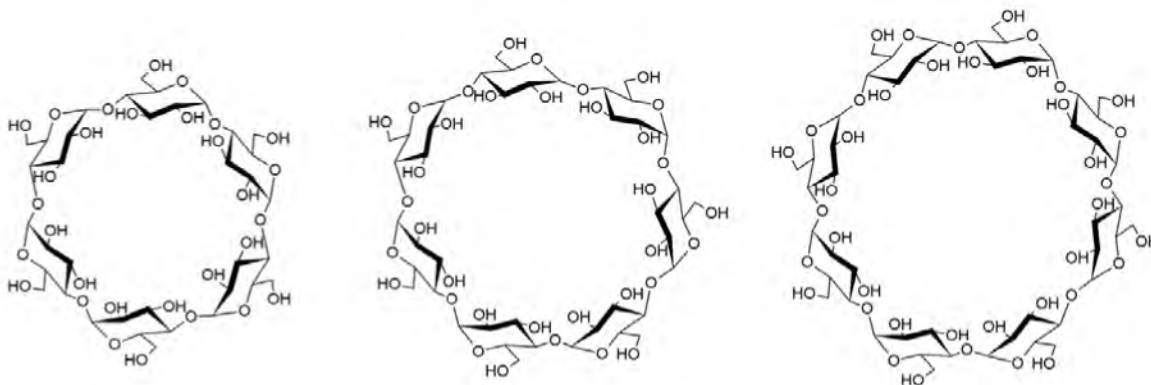


Figure 1.1. A top view of the chemical structure of  $\alpha$ -,  $\beta$ -, and  $\gamma$ -CD (from left to right).

The CDs exterior is composed of 18, 21, or 24 hydroxyls on  $\alpha$ -,  $\beta$ - and  $\gamma$ -CDs, respectively, which make the exterior of the CD hydrophilic. The interior of the CD cavity is composed of the non  $\pi$ -glycosidic linkage and the hydrogen backbone of the

glucose units [1]. As a result, these cavities are hydrophobic in nature and allow for “host/guest” complexes to be formed with hydrophobic molecules in aqueous environments. The CDs ability to interact with other molecules in this way has caused them to alter the chemical and physical properties of the “guest”. This phenomenon has caused them to be the focus of numerous studies and in a variety of fields. CDs have been used in the chemical industry as enzyme mimics, in the medical field as drug delivery agents, in aquatic chemistry to remove contamination, and many other applications and fields [2].

Another fascinating aspect of a CDs hydrophobic cavity is their highly chiral nature. There are 30, 35 and 40 chiral centers in  $\alpha$ -,  $\beta$ - and  $\gamma$ - CD's, respectively. This aspect of the cavity has been utilized as a means to chirally resolve compounds in gas chromatography (GC), liquid chromatography (LC), and capillary electrophoresis (CE) based on differences in the guest interactions between chiral pairs of molecules [3-5]. Research has even shown evidence that CDs can be used as chiral additives to have enzyme mimicking behavior and stereospecific catalytic properties on a range of substrates in numerous types of reactions [6].

Although extremely useful for a number of applications, the native CDs are limited in their selectivity of interactions with guest molecules. However, the CDs exterior hydroxyls allow for the modification of the native CDs. Modifications to the hydroxyls may change the interactions of the CD with a given guest molecule as well as change the solubility of the CDs in different solvents [7]. These hydroxyl groups on the CD exterior can be classified as either secondary or primary hydroxyls. The C(2) and C(3) contain

secondary hydroxyls which are on the same side of the CD while the C(6) contains primary hydroxyls on the opposite side of the CD (Figure 1.2). The CDs are typically classified as having a secondary and a primary face, which can then be modified based on the differences in the reactivity of these hydroxyls [7]. Modifications of these reactive sites have ranged from changing a single hydroxyl on one glucose unit (mono substituted CDs), full modification of all reactive sites (permodification), selective modification of all the C(2), C(3) and/or C(6) hydroxyls, and random modification of the hydroxyls.

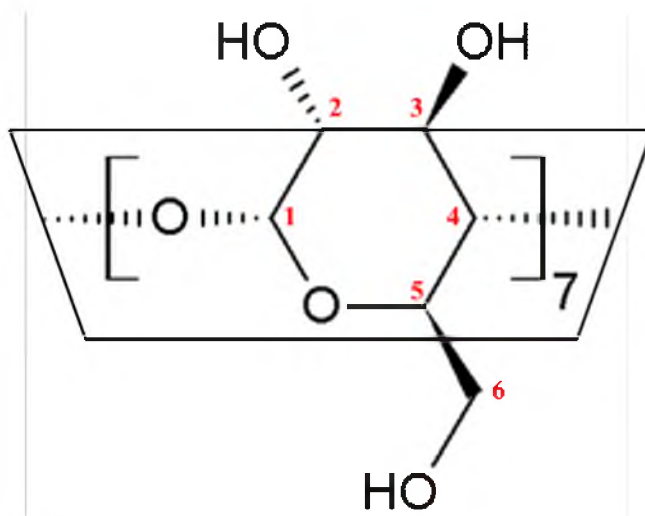


Figure 1.2. A side view of the toroidal shape of  $\beta$ -CD. One of the  $\alpha$ -D-glucose units is shown with the standard numbering.

Regiospecific mono-, di- and tri- substituted CDs have been achieved by taking advantage of the reactivity differences of the hydroxyls or through regioselective reagents. The mono-, di- and tri- substituted CDs usually require purification to isolate them due to the presence of CDs with higher degrees of substitution. Typically, limiting



amounts of the substituent are used to minimize undesired reaction with other hydroxyls. These modified CDs have had large success as enzyme mimics. The hydrophobic cavity of the CD acts as the “receiving pocket” and specific substituents can mimic enzymatic catalytic ability [8].

One such example of this application is the work being done by Bols’ group. Utilizing the novel approach by Sinay and Peirce [9] to selectively debenzylate one or two 6-O-benzyl groups of per-benzylated CDs (Figure 1.3), Bols’ group was able to synthesize a number of mono- and di- substituted 6-O-aldehyde CDs and investigated their enzymatic mimicking abilities [10, 11]. Most recently, the group has produced a pair of diastereomeric mono-6-deoxy-6-formyl  $\beta$ -CDs (Figure 1.4) that show a significant increase in their enzymatic ability to hydrolyze nitrophenyl glycosides at an increased rate of catalysis over previously studied di-6-deoxy-6-aldehyde  $\beta$ -CDs enzyme mimics. The mono-6-deoxy-6-S-formyl  $\beta$ -CD showed a 10 fold increase in catalysis of the nitrophenyl glycosides over the mono-6-deoxy-6-R-formyl  $\beta$ -CD and a 1000 fold increase over uncatalyzed reactions [11]. Further fine tuning of these types of CDs is being done to further understand the effects of functional groups and CD size on the ability of these enzyme mimics.

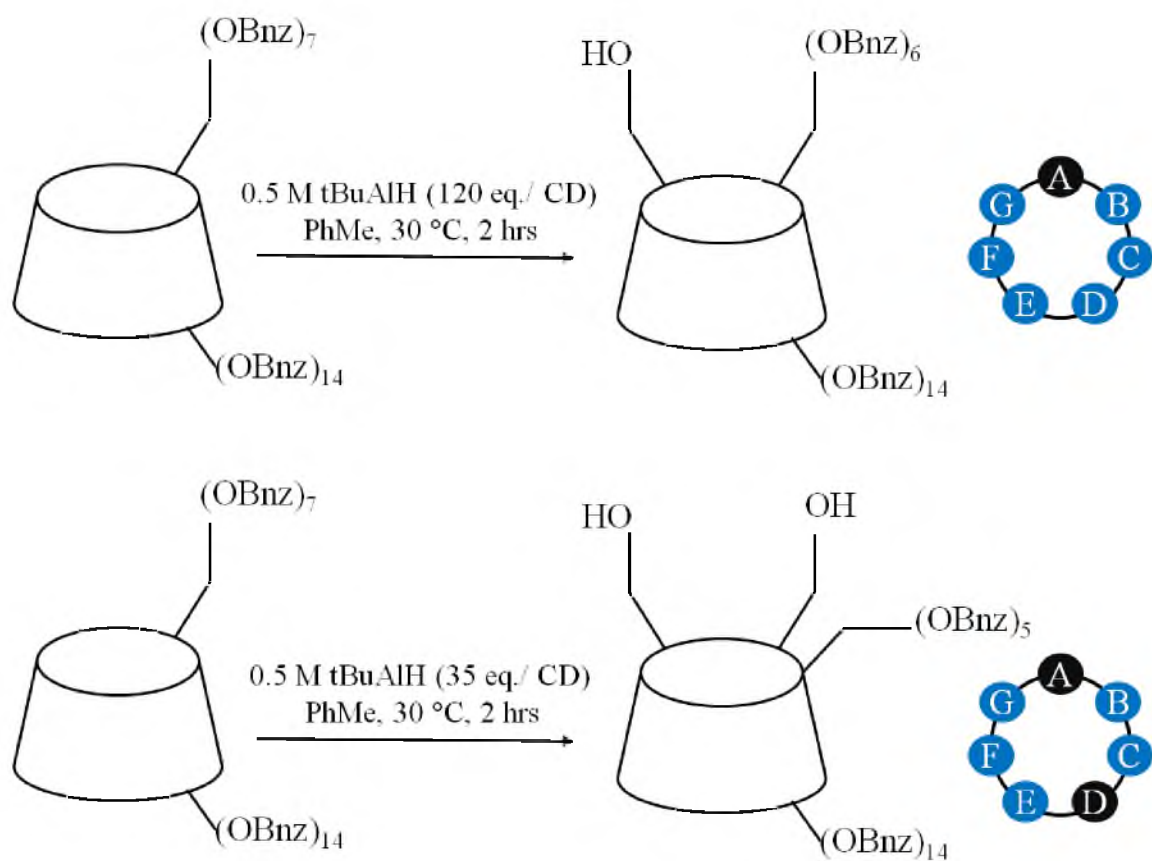


Figure 1.3. Selective de-benzylation of heptakis(2,3,6-tri-O-benzyl)-  $\beta$ -CD [9].

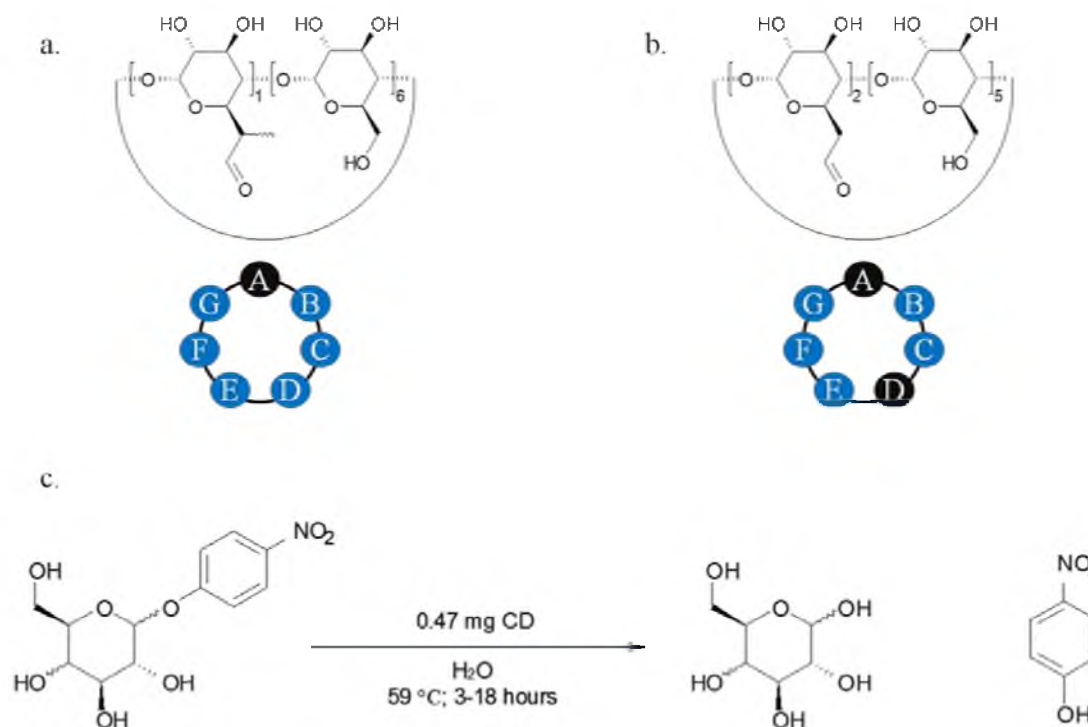


Figure 1.4. (a.) (R and S) heptakis (mono-6-deoxy-6- $\alpha$ -methoxyformyl)-  $\beta$ -CD, (b.) the heptakis(di-6<sup>A</sup>, 6<sup>D</sup>-deoxy-6-formyl)-  $\beta$ -CD and (c.) the reaction conditions for hydrolysis of glycosides [10, 11].

Complete modification of all reactive sites has also been achieved. The problem in this case is a steric issue that depends on the size of the substituent being added to the CD. As the CDs hydroxyls become modified, a crowding effect makes it difficult to continue to add more of the substituents. This is more of a problem for the C(2) and C(3) hydroxyls since they are adjacent to one another on the glucose unit and make up 12, 14, and 16 hydroxyls on one face of the ring for  $\alpha$ -,  $\beta$ -, and  $\gamma$ - CDs, respectively. The C(6)s

are less affected by this because they are facing away from the CD cavity and have some flexibility. For these CDs, it is important to use the correct reaction conditions and reagents to fully alkylate the CD or difficult purification may be necessary to remove under substituted CD's [7].

A current review on the use of CDs as a chiral stationary phase (CD-CSP) has been published [4]. It should be noted that one position is functionalized to attach to the column stationary phase while the other positions are fully reacted with another functional group. The novel CD-CSPs show great versatility in chiral resolution of a range of analytes utilizing LC, GC and capillary electrochromatography (CEC). One example from the review by Simonyi and coworkers physically binds a (6-monodeoxy-6-monourea) permethylated  $\beta$ -CD (PMMABCD) onto a silica support surface (Figure 1.5). Initial investigations of permethylated  $\beta$ -CD showed promise on the chiral separation of coumarin- based anticoagulants using CE. Comparison of the PMMABCD to a commercially available column Nuceodex- $\beta$ -PM column showed enhanced peak shape with lower retention times for similar conditions [12].

Selective modification of CDs usually requires a long reaction scheme involving protection/ deprotection type reactions. Like the mono- substituted type CDs, utilizing differences in reactivity of the hydroxyls and regioselective reagents allow for the successful modification of the given C(2), C(3) and/or C(6) hydroxyl. In these types of reaction schemes, high yields of the intermediates are essential to have a significant mass of the final products. These single isomer CDs have been utilized in a number of fields,

including separation science [4, 5], drug delivery devices [13, 14], and as reaction catalysts [6].

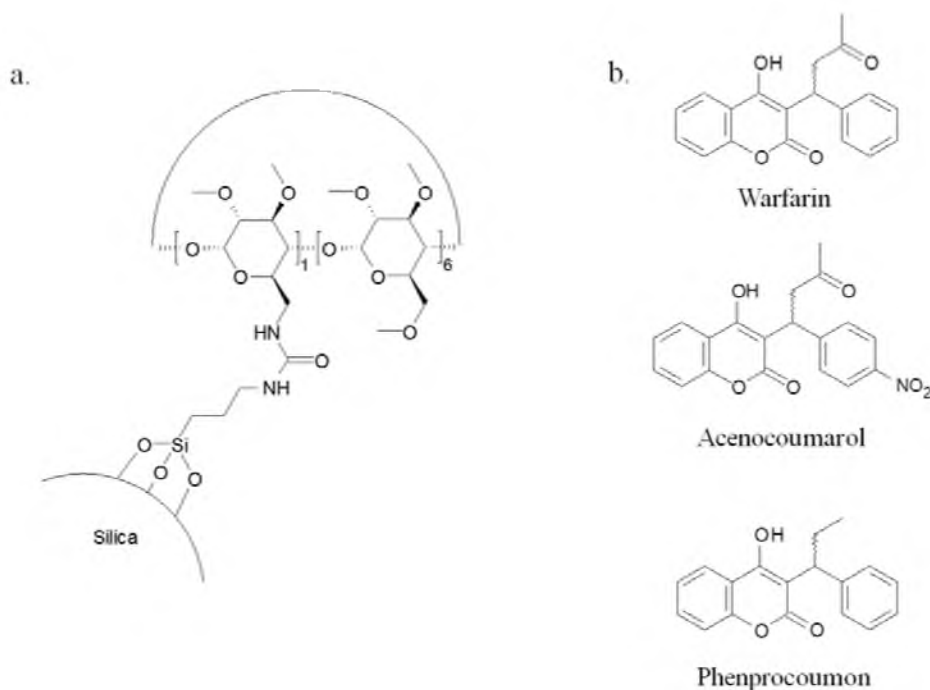


Figure 1.5. (a.) Heptakis(mono-6-deoxy-6-monourea-permethylated)-  $\beta$ -CD (PMMABCD) bond to silica particle and (b.) coumarin- based anticoagulants separated by the PMMABCD silica [12].

The selective modification of the primary face with sulfoalkyl groups and the secondary face with alkyl groups has been achieved to produce a series of amphiphilic CDs. Using the bulky protecting group *tert*-butyldimethylsilyl chloride (TBDMSCl) as opposed to the indiscriminate trimethylsilyl chloride (TMSCl), it is possible to selectively protect the C(6) hydroxyl using only a slight excess of the reagent [15]. Once the C(6) hydroxyls

have been protected, alkylation of the C(2) and C(3) hydroxyls followed by deprotection and sulfoalkylation at the C(6) in the presence of 18-crown-6 ether (18-crown-6) was performed to achieve the final amphiphilic CD products [16]. The series of CDs (Figure 1.6) were evaluated as mass transfer promoters in the hydroformylation of 1-decene [17]. The heptakis (2,3-di-O-methyl-6-O-sulfoalkyl)-  $\beta$ -CDs proved to be more efficient at producing a large increase in the reaction rate while producing the desired linear aldehyde in greater yield.

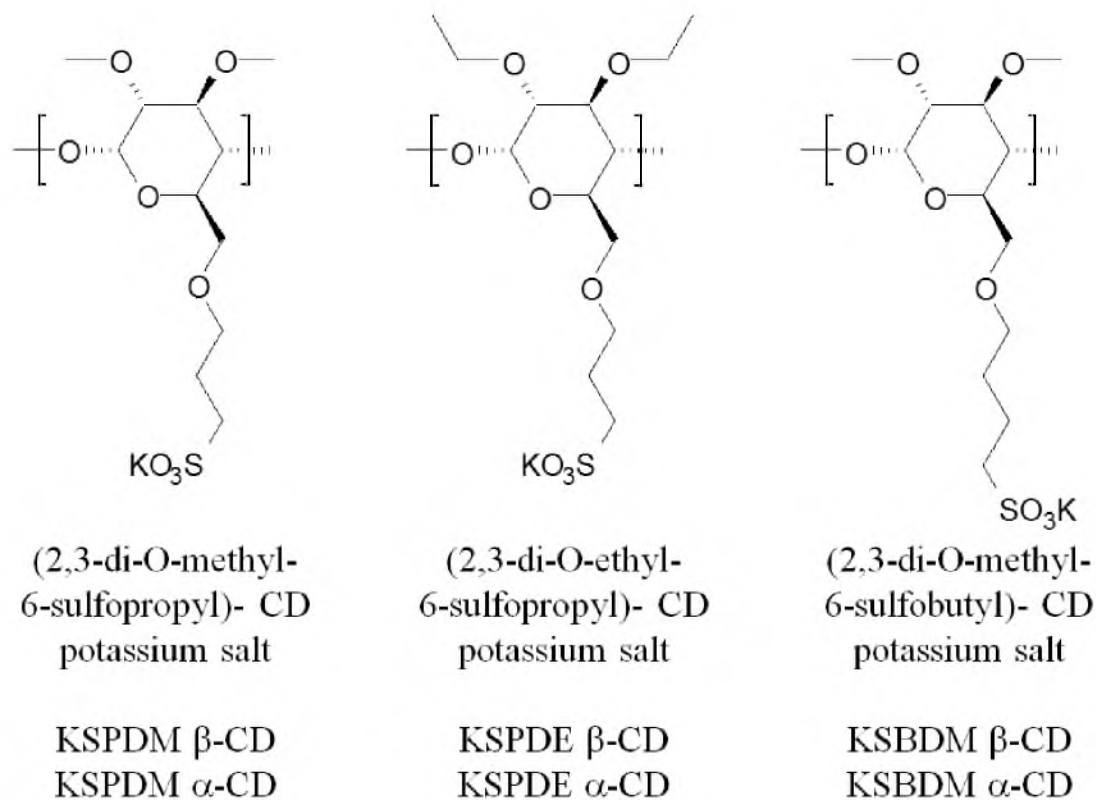


Figure 1.6. Series of single isomer, amphiphilic CDs (2,3-di-O-alkyl-6-O-sulfoalkyl CD potassium salts).

For randomly modified CDs, the reactivity of the different hydroxyls plays a significant role in the localization of the substituent being added to the CD. The most reactive hydroxyls are the primary C(6) hydroxyls due to less steric interference. Of the two secondary hydroxyls, the C(2) hydroxyl has been classified as being more reactive than the C(3) hydroxyls [7]. For these CDs, analysis and characterization of the degree of substitution (DS) of the mixture is crucial due to the fact that differences in batches may exhibit different DS, which can affect the behavior of the mixture for a given process. However, extensive purification is not necessary.

Random sulfobutyl ether CDs (SBE-CD), first introduced by Stella and coworkers [18], have been vastly utilized as a chiral additive in CE separations [5]. Further discussion of the application of these SBE-CDs will follow in Section 1.3. However, it is important to characterize the charge distribution for randomly substituted SBE-CDs and this has been successfully achieved using NMR, CE, LC, MS and elemental analysis (EA) techniques. While all these methods of characterization are relevant, the LC method will be discussed in further detail due to its novel application to this research.

## **1.2 Hydrophilic interaction chromatography analysis of highly polar molecules**

High performance liquid chromatography (HPLC) is a method of separation based on partitioning of a solute between a mobile phase (solvent) and a stationary phase (solid particles) packed in a column. The solute is in equilibrium between the mobile phase and

stationary phase. A simple HPLC system consists of a solvent reservoir/ solvent pump, an injection port, a column and a detector. Before discussing the solvent reservoir/ solvent pump, the column type must be described and the mode of separation. The column is typically packed with microporous silica particles (commonly 3-5  $\mu\text{m}$  particle size) with modified or unmodified surfaces. HPLC can be said to be categorized into two modes of separation based on the type of stationary phase: normal-phase liquid chromatography (NPLC) and reverse-phase liquid chromatography (RPLC). In NPLC, common stationary phases include bare silica ( $\text{SiO}_2$  with surface  $\text{SiOH}$ ), or chemically bonded amino, cyano, and diol groups which are polar. For RPLC, common stationary phases include chemically bonded octadecyl (C18), octyl (C8), propyl (C3), or phenyl groups which are all hydrophobic [19].

For HPLC, solvent systems typically consist of a strong solvent, which has polarity similar to the stationary phase, and a weak solvent, which has polarity opposite to the stationary phase. In NPLC, a polar solvent is considered the strong solvent with a non-polar solvent being the weak solvent. The reverse is observed for RPLC. Changing the solvent composition will affect the retention times of analytes. An increase in the strong solvent will decrease retention time of the solutes. There are two solvent elution systems that are typically applied in HPLC: isocratic elution and gradient elution.

Isocratic elutions utilize a constant solvent system composition where the percentage of the strong solvent and weak solvent are not varied. In gradient elution, the solvent system is varied over time to maximize separation. For gradient elutions, a small percentage of strong solvent is held constant to elute poorly retained solutes. An increase



in the percentage of strong solvent at a set time during the separation will allow more strongly retained solutes to elute. A gradient elution requires the use a dual pump system that allows for the increase in the percentage of the strong solvent [19].

In separating out two solutes or bands in HPLC, the resolution ( $R_s$ ) of these bands can be expressed in Equation 1.1.

$$R_s = (1/4)(\alpha - 1)N^{1/2} \left( \frac{k}{1+k} \right) \quad \text{Equation 1.1}$$

where  $k$  is the average retention factor,  $N$  is the column plate number, and  $\alpha$  is the separation factor of the two bands ( $\alpha = k_1/k_2$ ). This equation is used in method development by breaking experimental parameters into retention ( $k$ ), column efficiency ( $N$ ) and selectivity ( $\alpha$ ). Both  $k$  and  $\alpha$  are influenced by similar parameters, including mobile phase composition, stationary phase composition, and temperature. Mobile phase and temperature are easily manipulated and are routinely varied to modify  $k$  and  $\alpha$ . The parameters that affect  $N$  include the flow rate, column length and particle size. While the flow rate can be varied easily, this parameter has little effect on  $N$ . In order to change the stationary phase, column length or particle size, the column must be changed. Of the three parameters attributed to the column, changing the stationary phase composition is the best parameter to explore for difficult separations due to the cost of the columns and the greatest change in resolution [20].

The use of hydrophilic interaction chromatography (HILIC) was first described in 1990 by Dr. Andrew Alpert [21]. HILIC is a LC technique that is used to separate polar analytes and is said to be analogous to NPLC although the mechanism for HILIC separations are believed to be much more complex than NPLC. HILIC employs similar

stationary phases as those in NPLC and include silica, amino, diol, cyano and other polar functional groups. However, the mobile phase that is utilized is more comparable to RPLC. The mobile phase consists of a water miscible organic solvent in high concentrations and water. Being that HILIC can be used to separate out charge analytes, it is also comparable to ion chromatography (IC).

While HILIC shares similar properties to NPLC, RPLC and IC, this mode of separation provides some advantages over these other methods. Due to the non-polar nature of non-aqueous NPLC, some analytes are poorly soluble in the solvent mixtures of NPLC. The use of much more polar solvent systems allow for the solubility of these analytes when using HILIC. For RPLC, highly polar compounds are weakly retained on the column and eluted quickly and typically with poor resolution. HILIC separations allow for the interaction of these more polar analytes with the column and to achieve resolution. Finally, IC typically requires the use of costly ion pairing agents which are not necessary in HILIC separations [22, 23].

The mechanism for the separation of analytes is still under debate but is believed to be a partitioning of the analytes between the mobile phase and the water layer(s) adsorbed onto the polar stationary phase [24]. The type of stationary phase is also very important in the mechanism of interaction with the analytes as well. The stationary phase may introduce other factors like hydrogen bonding, dipole interactions, Van der Waals forces and even electrostatic interactions that may largely influence the separation mechanism. Other factors that will influence the separation mechanism are the solvent conditions which include organic solvent type and concentrations, salt additives, and pH [23].

The organic solvent choice for HILIC separations is typically acetonitrile (ACN). However, any water miscible aprotic solvent can be used (dioxane, tetrahydrofuran, dimethylformamide). The amount of organic solvent is typically high for isocratic separations to ensure analyte retention to the column. Gradient systems are employed to start with high amounts of organic solvent which are decreased gradually to elute more polar analytes. The use of protic solvents can also be employed but much higher concentration of the organic solvent are usually required to ensure sufficient retention on the column.

Salt additives are employed to control both the pH and ionic strength of the mobile phase. The pH is especially important when separating ionizable analytes and a buffer will ensure that analytes will be in a single ionic form. For neutral analytes, no buffer is necessary. However, the use of these additives helps to provide a robust mobile phase for reproducible results.

A novel application by Vigh's group [25] utilizes HILIC to characterize some commercially available, highly charged, single isomer and randomly substituted sulfated CDs. A evaporative light scattering detector (ELSD) was chosen as the detector due to the lack of a chromophore on the CDs being analyzed and was shown by Lucy and coworkers to have similar sensitivity to mass spectroscopy (MS) detectors for cyclodextrins [26]. The HILIC column (Luna) that is employed by Vigh's group has the surface of the silica chemically modified with cross-linked diol groups (Figure 1.7). Excellent separation is obtained and can be used to determine the DS of the sulfated CD being analyzed and compared with other methods of characterization. Upon comparing

the lot-to-lot variation of commercially available highly sulfated  $\beta$ -CD from Beckman-Coulter, they found a significant difference was observed between the two lots that may have significant impacts on application these CDs.

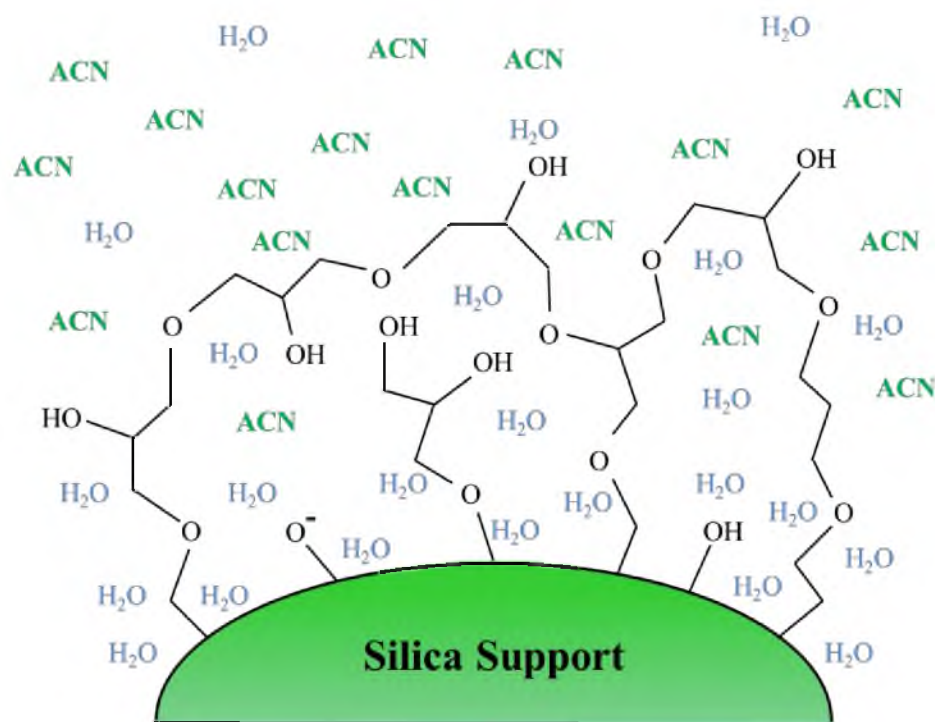


Figure 1.7. This depiction of the stationary phase on a Luna HILIC column shows the cross-linked diols on the silica support surface. A rich water layer near the stationary phase has been reported when using a mobile phase with large ACN composition.

### **1.3 Application of highly charged cyclodextrins in chiral capillary electrophoresis separations**

Modern CE was first developed by Hjertén in 1967 and used capillaries with internal diameters (id) of 3 mm, which were rotated to diffuse heat [27]. The use of 75  $\mu\text{m}$  id capillaries were applied in 1981 [28]. The addition of micelles in 1984 by Terabe allowed for the separation of charged and neutral analytes using micelles as pseudo-stationary phases, and was termed micellar electrokinetic capillary electrophoresis (MECC) [29]. Introduction of CDs as chiral additives in CE have been termed cyclodextrin capillary electrokinetic chromatography (CD-cEKC) [30].

A simple (and typical) CE system consists of a high voltage power supply, a buffer containing a background electrolyte (BGE), a bare fused silica capillary, a detector and a non-conducting compartment. Analytes are injected via siphoning, pressure (hydrodynamic injection) or through application of a voltage (electrokinetic injection). Typically, CE is used to separate charged analytes based on their mobility through the capillary. CE separations are highly advantageous for a variety of reasons including small sample volumes (on the order of nL), high separation efficiencies (on the order of a hundred thousand theoretical plates), and ease of modification to a given buffer system to optimize separations [31].

Electrophoresis is defined as the process of separating charged analytes through a given media as an electric field is applied. In CE, the analytes are separated out by their electrophoretic mobilities ( $\mu_{\text{ep}}$ ), which is usually based on the charge to size ratio. The  $\mu_{\text{ep}}$  ( $\text{cm}^2/\text{V} \cdot \text{sec}$ ) is defined as follows:

$$\mu_{ep} = \frac{v_{ep}}{E} = \frac{q}{6\pi\eta r} \quad \text{Equation 1.2}$$

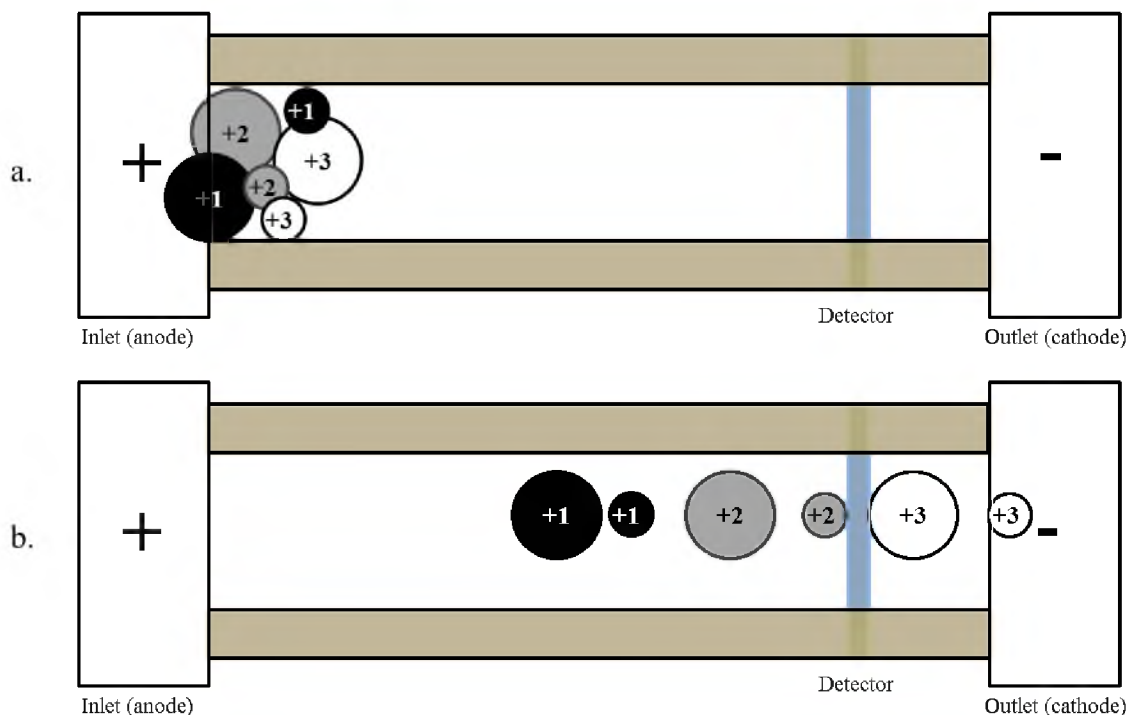


Figure 1.8. Separation of “analytes” based on charge to size ratios. (a) At injection, all analytes are at the capillary inlet. (b) As the voltage is applied, the analytes begin to separate based on charge to size ratio.

where  $v_{ep}$  is the electrophoretic velocity (cm/sec) and  $E$  is the field strength (V/cm). The  $v_{ep}$  is a function of the viscosity of the solution ( $\eta$ ) and the hydrated radius of the analyte ( $r$ ) and  $q$  is the charge of the analyte. The effect of charge and size are illustrated in Figure 1.8.

One of the major factors not in Equation 1.2 that affects mobility is the electroosmotic flow (EOF). EOF is the pumping mechanism in CE that is a result of the negatively ionized silanol groups on the capillary wall after “conditioning” the capillary with 1 N

sodium hydroxide. This causes an electrical double layer to form near the capillary wall that causes an effective pumping of the bulk solution in the capillary. The  $\mu_{ep}$  can be expressed by the following equation:

$$\mu_{ep} = \mu_{obs} \pm \mu_{EOF} \quad \text{Equation 1.3}$$

Where  $\mu_{obs}$  is the observed mobility of an analyte and  $\mu_{EOF}$  is the electroosmotic mobility. The  $\mu_{EOF}$  is typically measured using a neutral analyte. At high pH, EOF is high and has a large effect on the mobility of the analyte, and at low pH, EOF is less influential (Figure 1.9).

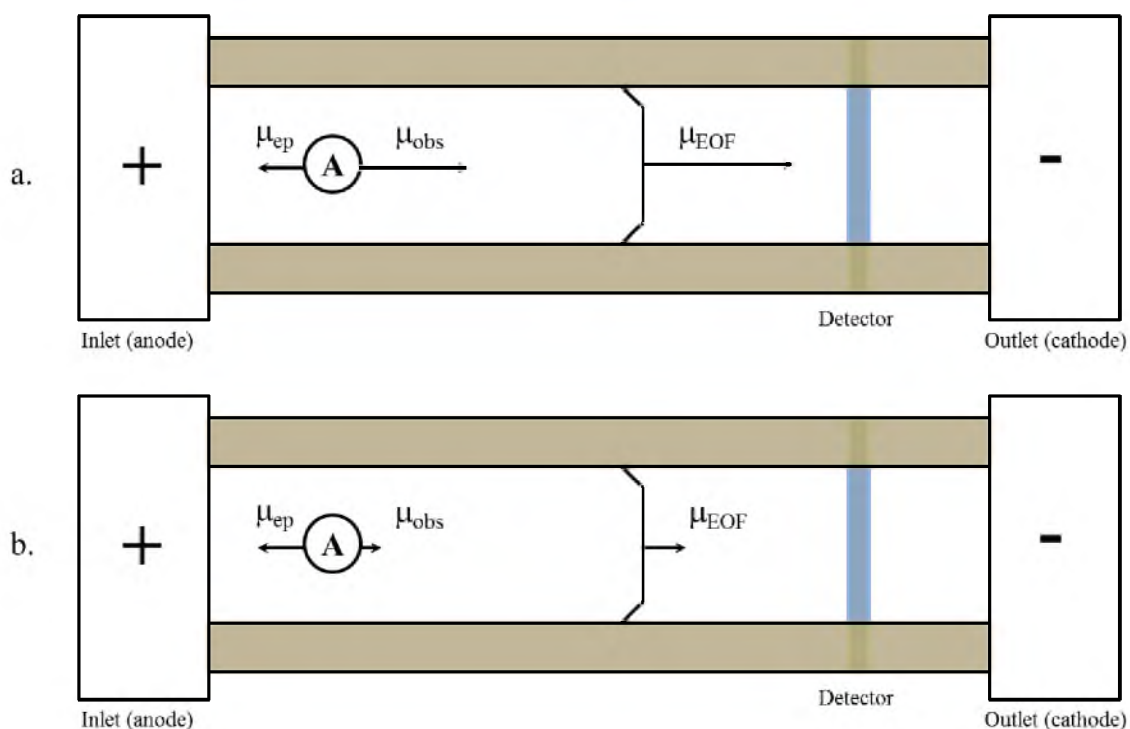


Figure 1.9. Separation of a negatively charged “analytes” as pH is changed without changing the applied field voltage. (a) The  $\mu_{obs}$  of the analyte at high pH is

overwhelmingly toward the cathode. (b) At lower pH, the  $\mu_{\text{obs}}$  may still be toward the cathode but the migration time will be much lower compared to higher pH.

Addition of a buffer additive can cause secondary equilibrium effects that also influence  $\mu_{\text{ep}}$ . The most common additives include micelles and CDs but other additives such as chelating agents can also be employed. These additives act as a pseudophase that interacts with the analyte in competition with the bulk aqueous solution. The partitioning between these two phases can cause an effective differentiation between analytes with similar  $\mu_{\text{obs}}$ . CDs have the advantage of being highly chiral in nature and have been found to chirally resolve a large number of enantiomeric pairs.



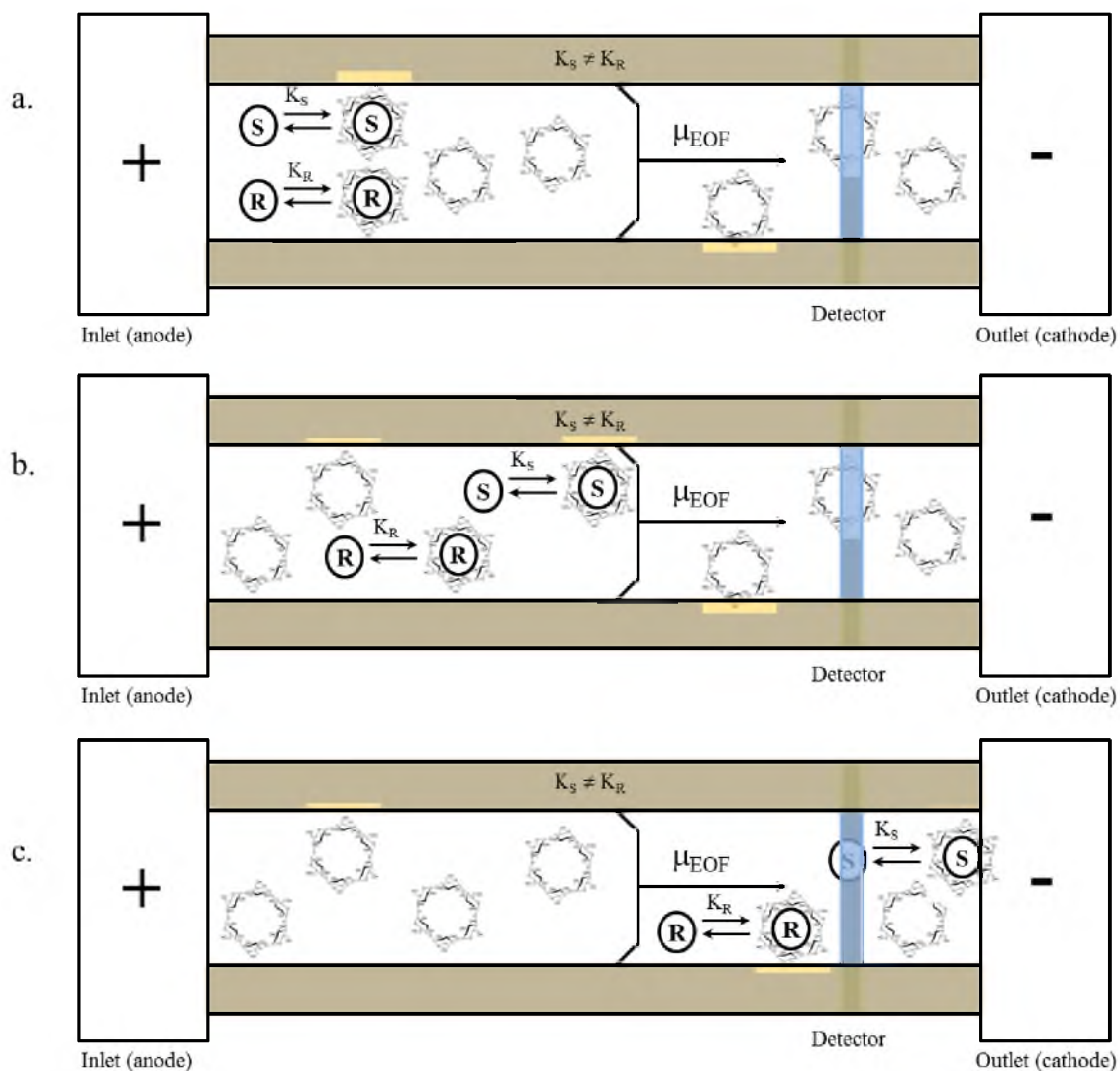


Figure 1.10. Secondary interaction with CD and an analyte.

The versatility of CDs as chiral selectors has caused them to become the most commonly used chiral additive for CE, especially charged cyclodextrins [32]. They have been utilized in the separation of acidic, basic and zwitterionic compounds as chiral additives and as stationary phases in CE [4]. Formation of an inclusion complex between the CD and the analyte changes the  $\mu_{obs}$  of the analyte based on the strength of the interaction,

mobility of the analyte, and mobility of the complex. This mode of separation is illustrated in Figure 1.10.

As previously mentioned, CDs have a chiral cavity that allow for differences in the  $K_{eq}$  between enantiomeric pairs. In the absence of CDs (or another chiral additive or modification), chiral separations for enantiomeric pairs are not achieved. If there is a large enough difference in the  $K_{eq}$  to cause a significant difference in the  $\mu_{obs}$  of the enantiomeric pairs, resolution of the two can be achieved. If the desired resolution is not achieved, slight changes in the concentration of CD or modifications can be studied to see if the desired resolution is achieved. Also, studies that include the application of different types of CDs are highly useful in understanding what factors affect the separation of a given type of analyte.

#### 1.4 Summary of research goals

There were several goals for this research which are outlined below:

1. The synthesis of heptakis(6-O-methyl-randomly-2,3-O-sulfobutyl)-  $\beta$ -CD (KSB<sub>x</sub>M  $\beta$ -CD) was the primary goal of this research. These would be the inverse of those produced by Kirschner (Figure 1.6) which showed promise in hydroformylation studies [17]. Those produced by Kirschner were single isomers with the secondary hydroxyls being alkylated and the primary hydroxyls being sulfoalkylated. The CDs produced here would likely have a range of substitution

of sulfobutylation on the secondary hydroxyls while being alkylated at the primary face.

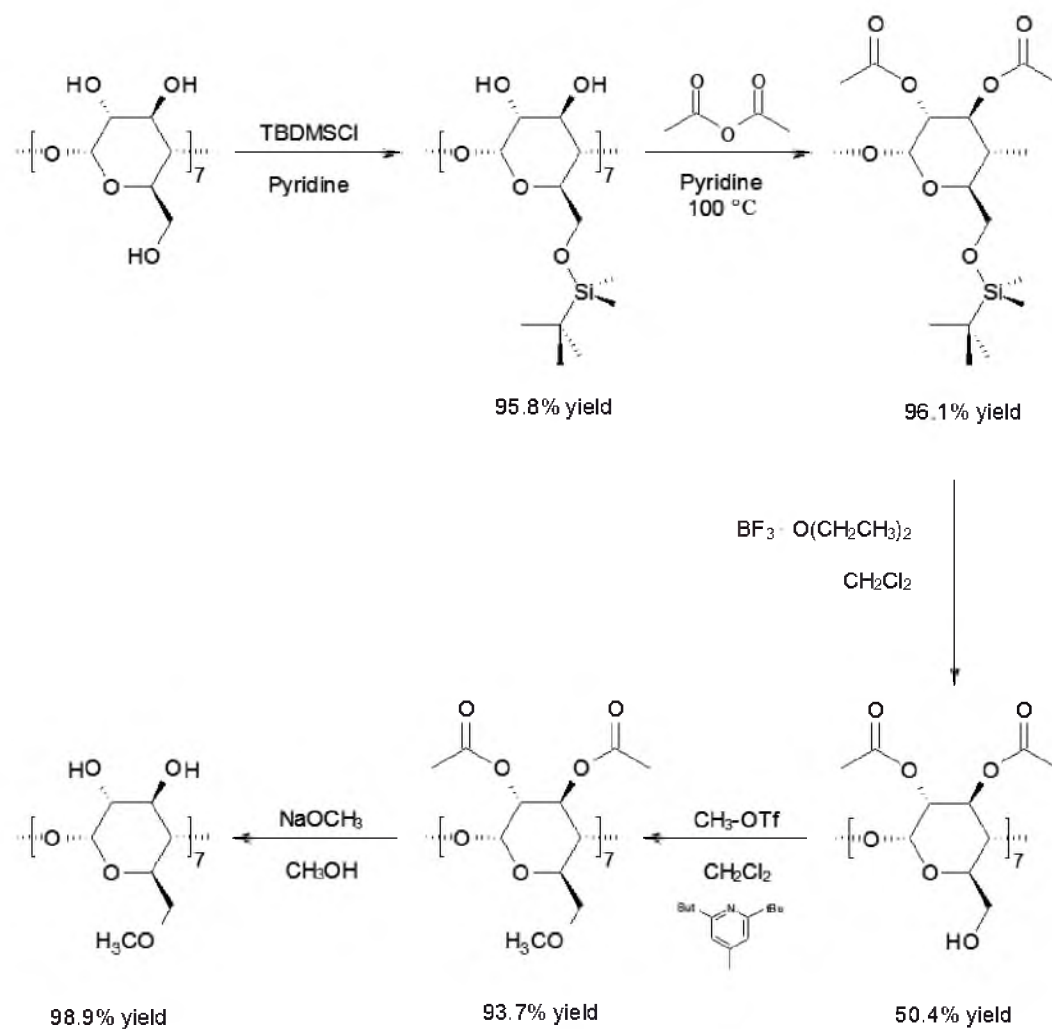


Figure 1.11. Reaction scheme for the synthesis of a single isomer heptakis(6-O-methyl)- $\beta$ -CD.

The initial step of this research was to obtain an efficient reaction scheme to produce single isomer heptakis(6-O-methyl)-  $\beta$ -CD for sulfobutylation (Figure 1.11). The use of acetyl intermediates was chosen over other methods due to minimal purification required at each intermediate, mild reaction conditions, and high yields for most steps. Other synthetic schemes were tried but proved difficult to purify and had poor yields for multiple steps. For this research, heptakis(6-O-methyl)-  $\beta$ -CD was the target starting material but other alkyl groups can be obtained using the same reaction scheme. Alterations to the alkyl triflate would be the only modification to the reaction scheme and these can be obtained by following Baum's procedure [33].

2. A series of sulfoalkylations experiments were performed to optimize the reaction conditions and achieve the highest possible DS at the secondary hydroxyls. This optimization would assist in obtaining the highest degree of sulfobutylation for the secondary hydroxyls for heptakis(6-O-methyl)-  $\beta$ -CD. Heptakis(6-O-TBDMS)-  $\beta$ -CD was chosen as the starting material for these optimization experiments due to the ease of synthesis and purification. Also, the product would yield another set of CDs to compare to Kirschner's CDs described above. The outline for the optimization of sulfoalkylation is provided in Figure 1.12. The sulfoalkylations were performed using 1,3-propane sultone or 1,4-butane sultone to observe differences in reactivity. The amount of sultone and potassium hydride were held constant at 4 equivalents per hydroxyl, respectively, while

varying the amount of 18-crown-6 (potassium complexing agent) to optimize the sulfoalkylation.

It is hypothesized that the degree of sulfoalkylation on the secondary hydroxyls will increase as the amount of 18-crown-6 is increased as was seen by Kirschner for the primary hydroxyls in THF [16]. This is due to the fact that 18-crown-6 forms a coordination complex with  $K^+$  that has shown to increase the nucleophilic behavior of the deprotonated hydroxyl and aid in dissolution of the charged products [34]. The use of KH instead of NaH was chosen due to the higher complexing ability of the 18-crown-6 over with  $K^+$  over  $Na^+$  [35].

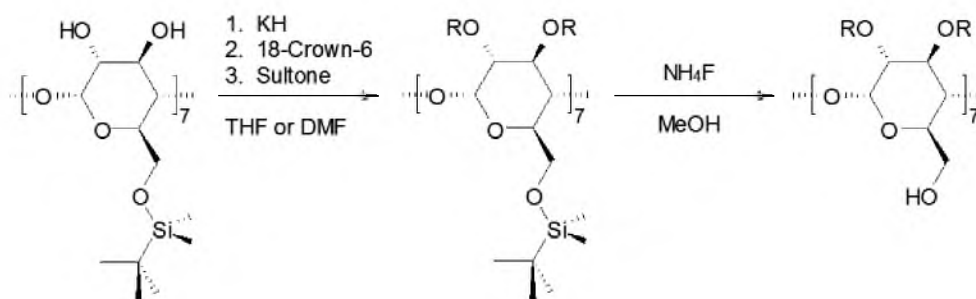


Figure 1.12. Reaction scheme for the optimization of the synthesis of heptakis(randomly-2,3-O-sulfoalkyl)- $\beta$ -CD ( $KSP_x$   $\beta$ -CD) and heptakis(randomly-2,3-O-sulfoalkyl)- $\beta$ -CD ( $KSB_x$   $\beta$ -CD). (The subscript “x” indicates the DS has not been defined).

The effect of solvent on the sulfoalkylation was also explored. Given that the sulfoalkylation is a  $S_N2$  type ring opening reaction using a strong base to produce an alkoxide, the use of a highly polar, aprotic solvent was needed. This would

maximize the solubility of the anionic intermediates and products while not reacting with the strong base. The most commonly used solvents for these types of reactions are THF and DMF. While dimethylsulfoxide (DMSO) would be ideal due to its high polarity, it was unsuccessful due to the reaction of the solvent with the base to form the dimethyl sulfide ion [36, 37].

3. The series of CDs produced for this research were characterized by HILIC LT-ELSD to determine the DS and to evaluate the optimal conditions for achieving the highest possible DS. While other methods were used to determine the DS of the final products, HILIC LT-ELSD provided the most reproducible and reliable means to characterize the CDs. As mentioned previously, the use of HILIC LT-ELSD was first introduced by Vigh [25]. This new method for analysis of highly charged CDs will be applied to the single isomers produced by Kirschner as well as the final products synthesized here.
4. Finally, the CDs produced here will be applied to chiral CE separation studies and compared with the single isomer CDs produced by Kirschner et al [17]. A number of reviews in chiral CE separations focus on the analysis of pharmaceutical final products [38]. However, it is also important to investigate synthetically relevant intermediates for these pharmaceutical products, such as chiral aryl alcohols. Chiral alcohols are the products of reductions of ketones, and a number of synthetic applications employ chiral catalysts in order to achieve enantiomeric

selectivity. Chiral CE methods offer a means of establishing the selectivity of the reaction, defined as enantiomeric excess. Although chiral HPLC with CD stationary phases have been used to resolve racemic aryl  $\alpha$ -alcohols [4] these separations are not particularly challenging using chiral CE with charged cyclodextrins. Choi's group [39] studies the separation of a series of aryl propyl alcohols using heptakis(6-O-sulfato)-  $\beta$ -CD. However, they cannot achieve baseline resolution without the presence of silver colloids. This research attempts to apply the CDs produced in our lab to a series of chiral,  $\alpha$ -,  $\beta$ - and  $\gamma$ -aryl alcohols in which the distance of the chiral center from the aromatic group varies. This investigation will also provide insight into the effect of the substituent on the secondary hydroxyls (hydrophobic or hydrophilic) on chiral separations.

## Chapter 2. Materials and Methods

### 2.1 Materials

Deuterated solvents were of 99.98% isotopic purity. Deuterium oxide ( $D_2O$ ) was purchased from Sigma Aldrich (St. Louis, MO). Deuterated chloroform ( $CDCl_3$ ), acetone- $d_6$ , and dimethylsulfoxide-  $d_6$  ( $DMSO-d_6$ ) were purchased from Alfa Aesar (Ward Hill, MA). Flash silica gel (40-63  $\mu m$ ) was purchased from Silicycle (Quebec, Canada) and Dowex 50W-X8 cation exchange resin was purchased from Dow Chemical (Midland, MI). Amicon ultrafiltration system and regenerated cellulose ultrafiltration membranes (500 NMWL) were purchased from Millipore (Billerica, MA). Water was prepared from a Millipore (Billerica, MA) Milli-Q ultrapure water purification system with 18 M $\Omega$ -cm resistivity. All other chemicals were analytical reagent grade unless otherwise stated.

Denatured ethanol was purchased from AAPER Alcohol and Chemical Co. (Toronto, Canada). Methanol and 2-propanol were purchased from Fisher Scientific (Hampton, NH). Anhydrous pyridine, tetrahydrofuran (THF), and N,N-dimethylformamide (DMF) were purchased from Alfa Aesar (Ward Hill, MA). THF was freshly distilled from potassium metal in the presence of benzophenone. DMF was stirred over  $CaH_2$ , filtered, and distilled under reduced pressure (20 torr) at 57 °C onto activated 4 Å 8-12 mesh sieves. Toluene, hydrochloric acid (HCl), phosphoric acid ( $H_3PO_4$ ) and hexane were purchased from BDH Chemical (Poole Dorset, UK). Dichloromethane ( $CH_2Cl_2$ ) and



chloroform ( $\text{CHCl}_3$ ) were purchased from Sigma Aldrich (St. Louis, MO). HPLC grade acetonitrile was purchased from EMD Chemical (Darmstadt, Germany).

Native  $\beta$ -CD was purchased from Calbiochem (Billerica, MA). Sodium bicarbonate ( $\text{NaHCO}_3$ ), benzoic acid (BA) and tris(hydroxymethyl)aminomethane (TRIS base) were purchased from Sigma Aldrich (St. Louis, MO). Potassium bicarbonate ( $\text{KHCO}_3$ ) and sodium hydroxide ( $\text{NaOH}$ ) were purchased from J.T. Baker (Phillipsburg, NJ). The *tert*-butyldimethylsilyl chloride (TBDMSCl) was purchased from Oakwood Products, Inc (West Columbia, SC). The 2,6-di-*tert*-butyl-4-methyl pyridine was purchased from Acros Organics (Geel, Belgium). The 1,3-propane sultone was purchased from TCI (Tokyo, Japan). Ammonium formate ( $\text{NH}_4\text{CO}_2\text{H}$ ), methyl iodide, silver triflate, acetic anhydride, 47% borontrifluoride etherate, sodium methoxide ( $\text{NaOCH}_3$ ), 1,4-butane sultone, 1,4,7,10,13,16-hexaoxacyclooctadecane (18-Crown-6), potassium hydride (KH), and ammonium fluoride ( $\text{NH}_4\text{F}$ ) were purchased from Alfa Aesar (Ward Hill, MA).

## 2.2 NMR analysis

The crude intermediates were analyzed by  $^1\text{H}$  NMR spectra with a Varian (Santa Clara, CA) Mercury 300 MHz FT-NMR instrument. Characterization of the intermediates and final products were done by obtaining  $^1\text{H}$ ,  $^{13}\text{C}$ , gCOSY, gHSQC, gHMBC and DEPT spectra with a Bruker (Billerica, MA) Avance<sup>III</sup> 600 MHz FT-NMR instrument. All assignments were made by gCOSY, gHSQC and gHMBC techniques.

## **2.3 CE analysis**

CE electropherograms were obtained with an Agilent (Santa Clara, CA) 3D Electrophoresis instrument equipped with a diode array detector.

### **2.3.1 Characterization of final products with inverse detection CE**

Indirect detection (at 214 nm) of sulfoalkylated cyclodextrins was performed using a 20 mM benzoic acid adjusted to pH 6.0 with 0.1 M Tris base, filtered through a 0.22  $\mu\text{m}$  filter and degassed for 10 minutes. Samples were prepared by adding 1 mg of CD/ mL of Milli-Q water, filtered through a 0.22  $\mu\text{m}$  filter, degassed for 10 minutes and injected for 2.0 seconds at 50 mbar. The separation voltage was 10 kV on a 32.5 cm (24.0 cm eff.) x 50  $\mu\text{m}$  (id) bare fused silica capillary. The capillary was conditioned with 0.1 M NaOH (1.0 minutes), then with Milli-Q water (1.0 minutes), and finally with buffer (2.0 minutes) between each run.

### **2.3.2 Chiral analysis of aromatic alcohols**

Chiral analysis was performed on a series of chiral aromatic alcohols (detected at 214 nm) using a 20 mM borate run buffer at pH 9.0 and containing 15 mM CD. Samples were prepared by adding 1.0  $\mu\text{L}$  of aryl alcohol/ 0.990 mL of 10% methanol in water and injected for 1.0 seconds at 50 mbar. The separation voltage was 8.0 kV on a 32.5 cm (24.0 cm eff.) x 50  $\mu\text{m}$  (id) bare fused silica capillary. The capillary was conditioned with 0.1 M NaOH (1.0 minutes), then with Milli-Q water (1.0 minutes), and finally with buffer (2.0 minutes) between each run.

## 2.4 HILIC/ LT-ELSD analysis

HPLC characterization of the sulfopropylated and sulfobutylated CDs were performed using an Agilent Technologies (Santa Clara, CA) 1100 series HPLC equipped with a degasser, binary gradient pump, thermostat, and a diode array detector coupled to a Sedere (Alfortville Cedex, France) Sedex 85 low temperature evaporative light scattering detector (LT-ELSD). The stationary phase was a Phenomenex (Torrance, CA) Luna HILIC column (3  $\mu\text{m}$ , 200Å, 150 mm x 4.6 mm). Mobile phase conditions consisted of 10-30 mM ammonium formate in varying amounts of water/ acetonitrile. The flow rate was set at 1.5 mL/ minute with injection volumes of 10  $\mu\text{L}$  of sample. The column was equilibrated at 25 °C and the LT-ELSD maintained a  $\text{N}_2$  (g) pressure of 3.5 bar, a temperature of 60 °C, and a gain of 6. The peak areas are used to determine the DS.

## 2.5 Synthetic procedures

This section contains the synthetic procedures used to achieve the sulfoalkylated CDs. The reagent, methyl triflate, was synthesized rather than purchased due to the fact that the shipping of the reagent was difficult and the reagents required to synthesize the methyl triflate were cheap and readily available. Some of the procedures found in the literature were modified due to either a lack of availability of a given chemical/reagent or the inability to obtain similar results.

### 2.5.1 Synthesis of Methyl triflate

This procedure was replicated from Baum's procedure [33].

All glassware and material were predried and the reaction was performed under inert gas.

In a 100 mL round bottom flask covered with aluminum foil, 3.8 mL ( $6.1 \times 10^{-2}$  moles) of  $\text{CH}_3\text{I}$  was added to 50 mL of  $\text{CH}_2\text{Cl}_2$  and stirred. A mass of 14.388 g ( $5.600 \times 10^{-2}$  moles) of silver triflate was slowly added to the reaction vessel and stirred for 20 hours. The insoluble silver iodide was vacuum filtered and a  $^1\text{H}$ -NMR spectrum was obtained to ensure the reaction was completed.

The solution was found to have trace amounts of unreacted  $\text{CH}_3\text{I}$  but an overall concentration of 1.22 M of methyl triflate was calculated from the  $^1\text{H}$ -NMR integration values. The solution was stored under Ar gas and refrigerated in an amber vial until the reagent was needed.

### 2.5.2 Synthesis of Heptakis (6-O-methyl)- $\beta$ -CD by acetyl intermediates

Heptakis (6- O- tert-Butyldimethylsilyl)-  $\beta$ - CD ( $\beta 2$ ).

This procedure is a modification of Fugedi's procedure [15].

All glassware and material were predried and the reaction was performed under inert gas.

A mass of 6.395 g ( $5.634 \times 10^{-3}$  moles) of  $\beta$ -CD was added to 150 mL of anhydrous pyridine in a 500 mL three neck round bottom flask under  $\text{N}_2$  gas. The solution was stirred until the solid dissolved. While purging with  $\text{N}_2$  gas, 6.892 g ( $4.572 \times 10^{-3}$ ) of TBDMSCl was slowly added to the solution. The reaction was allowed to run overnight.

A small amount of the reaction solution was checked to verify that the reaction was complete.

The product was poured over ice water and vacuum filtered.  $^1\text{H}$ - NMR analysis indicated that the product needed no further purification. A dried mass of 10.446 g ( $5.398 \times 10^{-3}$  moles) was obtained which gave a yield of 95.81% yield.  $^1\text{H}$  NMR (600 MHz,  $\text{CDCl}_3$ ):  $\delta$  6.71 (3-OH), 5.26 (2-OH), 4.87 (H-1), 4.01 (H-3), 3.87, 3.69 (H-6), 3.62 (H-2), 3.59 (H-5), 3.54 (H-4), 0.85 (H-9), 0.02, 0.01 (H-7).  $^{13}\text{C}$  NMR (150 MHz,  $\text{CDCl}_3$ ):  $\delta$  102.18 (C-1), 81.93 (C-4), 73.78 (C-2), 73.60 (C-3), 72.72 (C-5), 61.82 (C-6), 26.11 (C-9), 18.49 (C-8), -4.86, -4.98 (C-7).

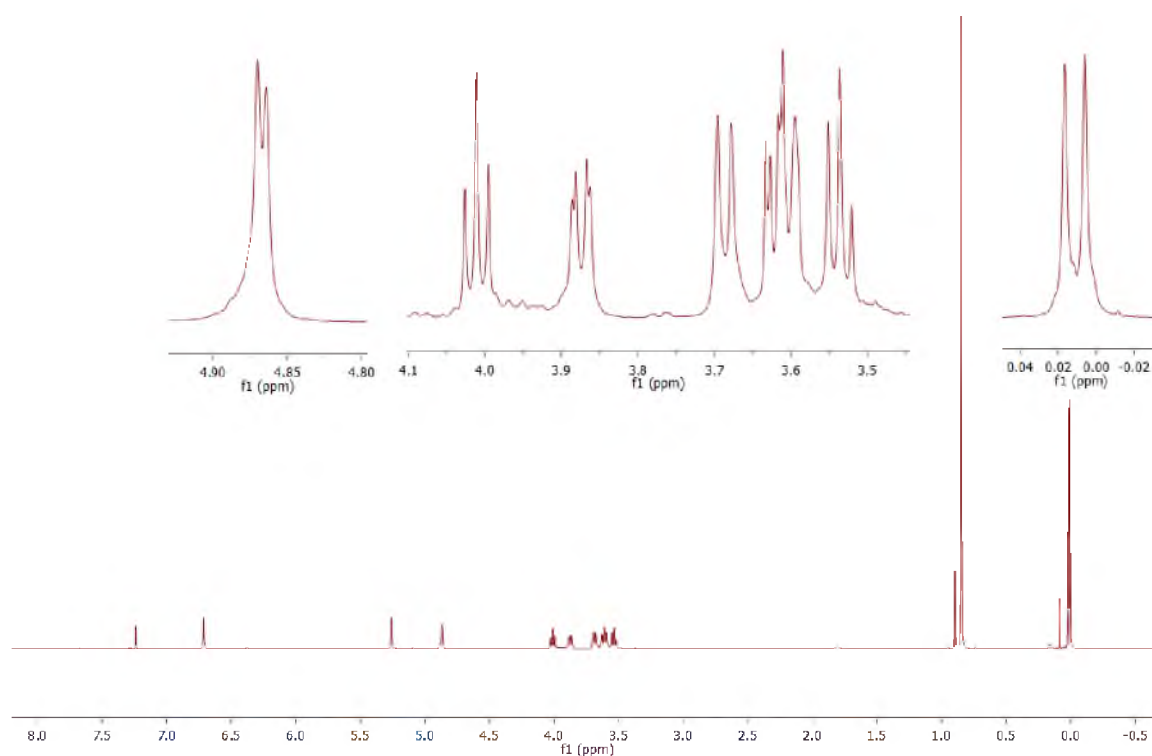


Figure 2.1.  $^1\text{H}$  NMR spectrum (600 MHz,  $\text{CDCl}_3$ ) of heptakis(6-O-TBDMS)-  $\beta$ -CD.

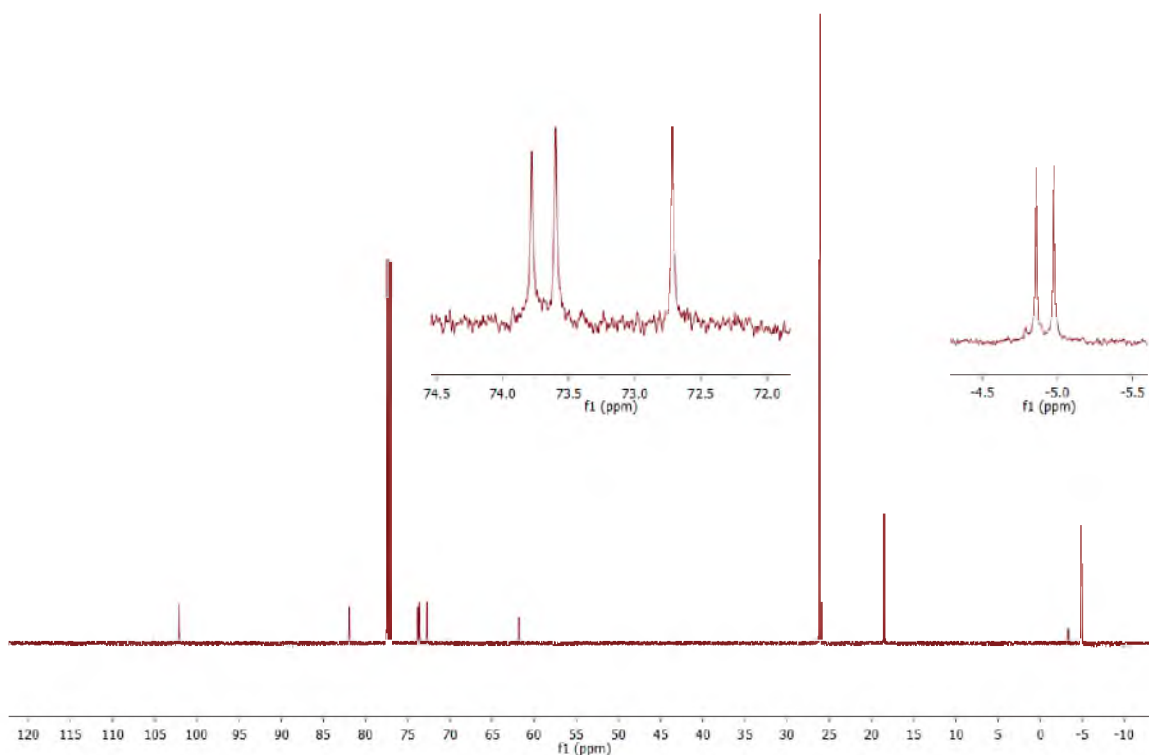


Figure 2.2.  $^{13}\text{C}$  NMR spectrum (150 MHz,  $\text{CDCl}_3$ ) of heptakis(6-O-TBDMS)- $\beta$ -CD.

Heptakis (2,3-O-Acetyl-6-O-tert-Butyldimethylsilyl)-  $\beta$ -CD ( $\beta$ 3).

This procedure is a modification of Takeo's procedure [40].

A predried mass of 6.414 g ( $3.314 \times 10^{-3}$  moles) of  **$\beta$ 2** was dissolved in 140 mL of a (1:1) acetic anhydride/ pyridine solution in a 500 mL round bottom flask. The solution was heated to 100  $^{\circ}\text{C}$  and stirred for approximately 4 hours. The final solution was red/orange in color. A small sample was worked up and a  $^1\text{H}$ -NMR spectrum was obtained to ensure the reaction was complete.

The solution was rotary evaporated under reduced pressure until most of the liquid was removed. A 10 mL portion of toluene was added to co-evaporate the remaining liquid. This was repeated three more times until a reddish solid was obtained. The solid was then extracted with  $\text{CHCl}_3$  and  $\text{NaHCO}_3$  (aq). The  $\text{CHCl}_3$  was washed twice with water and rotary evaporated.

The solid was then dissolved in hot 2- propanol and poured over ice water. The precipitate was vacuum filtered and dried to obtain a white solid with a mass of 8.041 g ( $3.186 \times 10^{-3}$  moles) and a yield of 96.14%.  $^1\text{H}$  NMR (600 MHz,  $\text{CDCl}_3$ ):  $\delta$  5.32 (H-3), 5.13 (H-1), 4.68 (H-2), 4.01, 3.70 (H-6), 3.84 (H-5), 3.83 (H-4), 2.04, 2.03 (H-11, H-13), 0.86 (H-9), 0.02 (H-7).  $^{13}\text{C}$  NMR (150 MHz,  $\text{CDCl}_3$ ):  $\delta$  171.00 (C-10), 169.68 (C-12), 96.61 (C-1), 75.40 (C-4), 71.99 (C-5), 71.70 (C-3), 71.40 (C-2), 62.01 (C-6), 26.05 (C-9), 21.13, 20.99 (C-11 and C-13), 18.45 (C-8), -4.80, -5.09 (C-7).

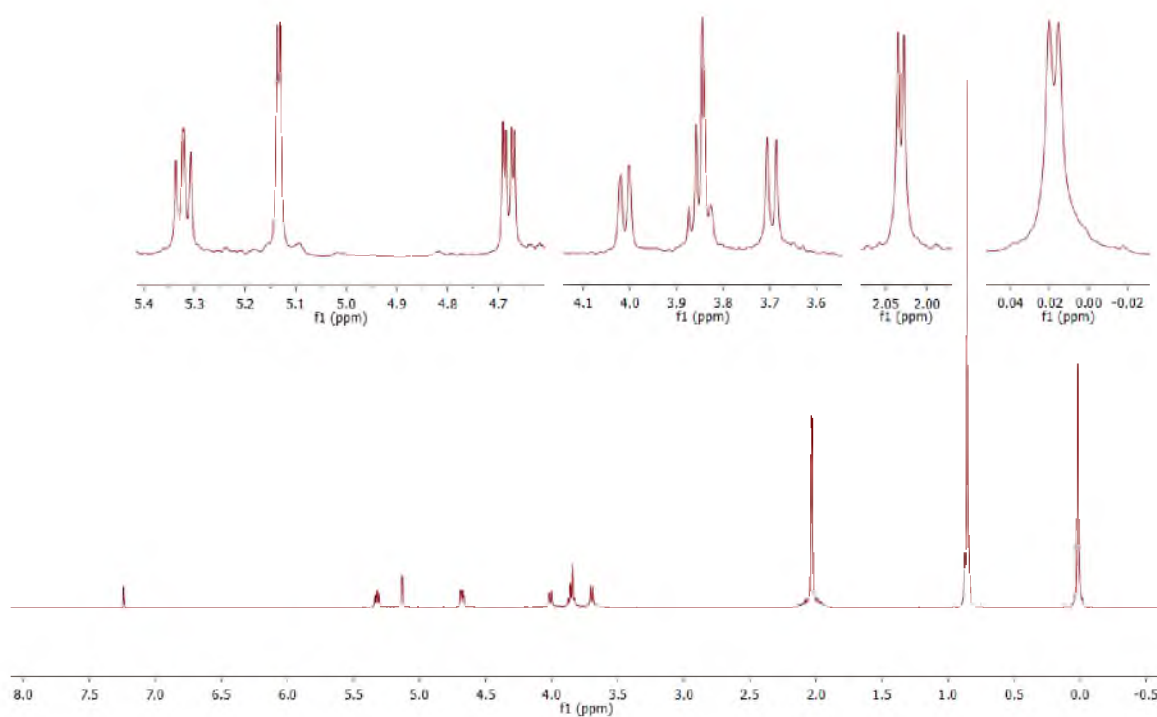


Figure 2.3.  $^1\text{H}$  NMR spectrum (600 MHz,  $\text{CDCl}_3$ ) of heptakis(2,3-di-O-acetyl-6-O-TBDMS)- $\beta$ -CD.



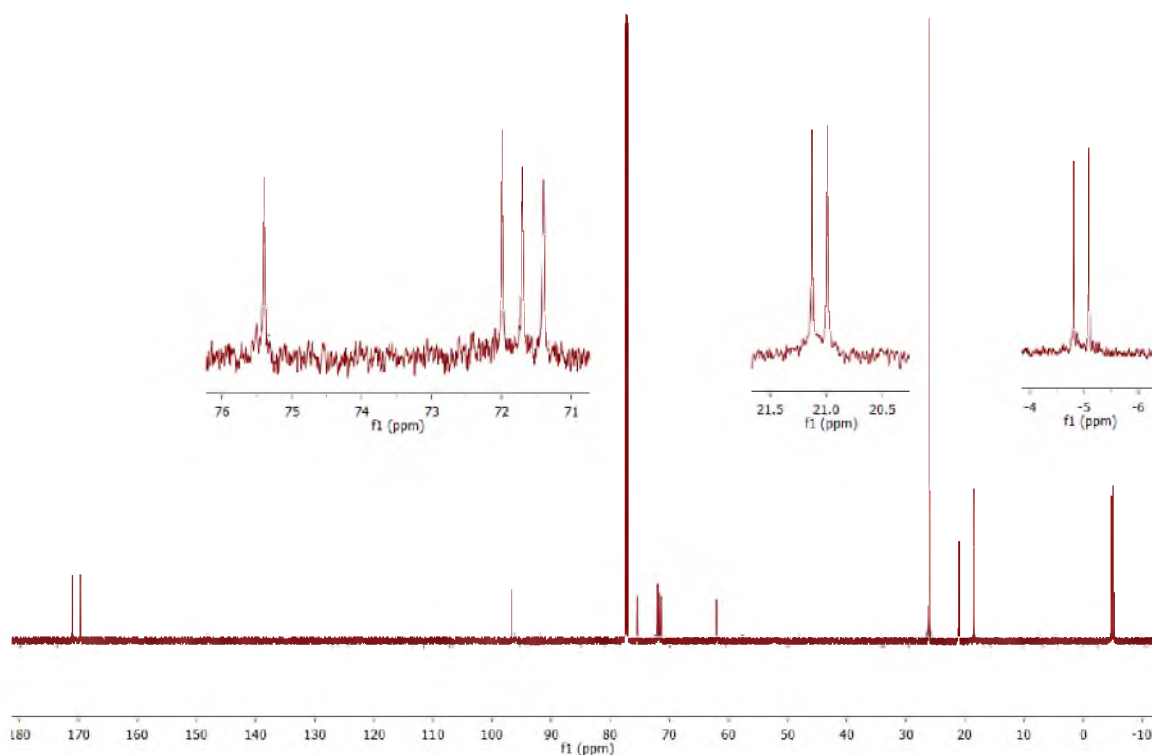


Figure 2.4.  $^{13}\text{C}$  NMR spectrum (150 MHz,  $\text{CDCl}_3$ ) of heptakis(2,3-di-O-acetyl-6-O-TBDMS)- $\beta$ -CD.

Heptakis (2,3- Di- O- Acetyl)-  $\beta$ - CD ( $\beta$ 4).

This procedure is a modification of Takeo's procedure [40].

A predried mass of 7.250 g ( $2.873 \times 10^{-3}$  moles) of  $\beta$ 3 was dissolved in 90 mL of a  $\text{CH}_2\text{Cl}_2$  in a 250 mL round bottom flask. The solution was stirred and 12.0 mL ( $9.7 \times 10^{-2}$  moles) of  $\text{BF}_3 \cdot \text{O}(\text{CH}_2\text{CH}_3)_2$  was added. The solution was allowed to react at room temperature for approximately 24 hours. The solution was poured over ice water and the

organic layer was washed with a saturated  $\text{NaHCO}_3$  (aq) solution. The  $\text{CHCl}_3$  was rotary evaporated and NMR indicated that ~12% silyl groups remained.

The solid was dissolved in 100 mL of  $\text{CHCl}_3$  and mixed with 6.0 mL ( $4.9 \times 10^{-2}$ ) of  $\text{BF}_3 \cdot \text{O}(\text{CH}_2\text{CH}_3)_2$ . The solution was stirred at room temperature for approximately 24 hours, then poured over ice water and washed with a saturated  $\text{NaHCO}_3$  (aq) solution.

Normal phase column chromatography was used to separate out unreacted CD using (3:1)  $\text{CHCl}_3$ : ethanol ( $R_f$  0.36) and a dried mass of 2.496 g ( $1.448 \times 10^{-3}$  moles) was recovered with high purity at a yield of 50.40%.  $^1\text{H}$  NMR (600 MHz, acetone- $d_6$ ):  $\delta$  5.39 (H-3), 5.18 (H-1), 4.70 (H-2), 3.96, 3.86 (H-6), 3.95 (H-4), 3.94 (H-5), 2.05 (H-8 and H-10).  $^{13}\text{C}$  NMR (150 MHz, acetone- $d_6$ ):  $\delta$  171.13 (C-7), 170.20 (C-9), 97.34 (C-1), 76.50 (C-4), 73.31 (C-5), 71.98 (C-2), 71.72 (C-3), 61.50 (C-6), 21.15, 21.01 (C-8 and C-10).

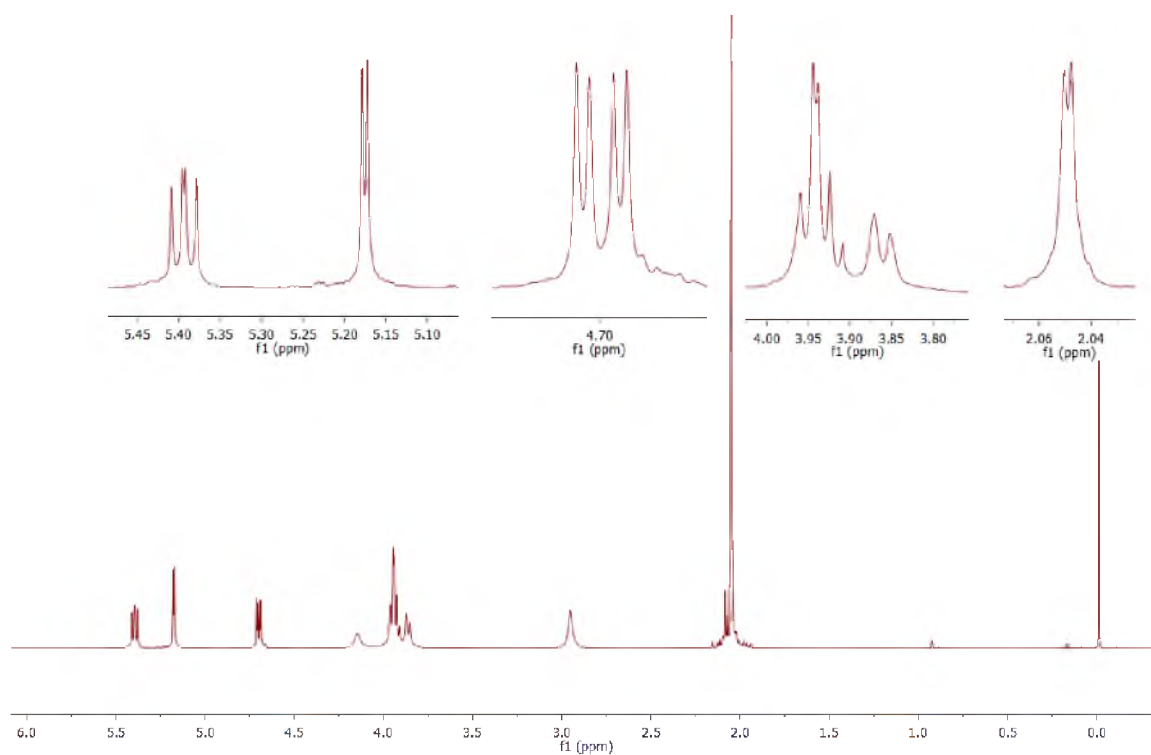


Figure 2.5.  $^1\text{H}$  NMR spectrum (600 MHz,  $\text{acetone-d}_6$ ) of heptakis(2,3-di-O-acetyl)-  $\beta$ -CD.

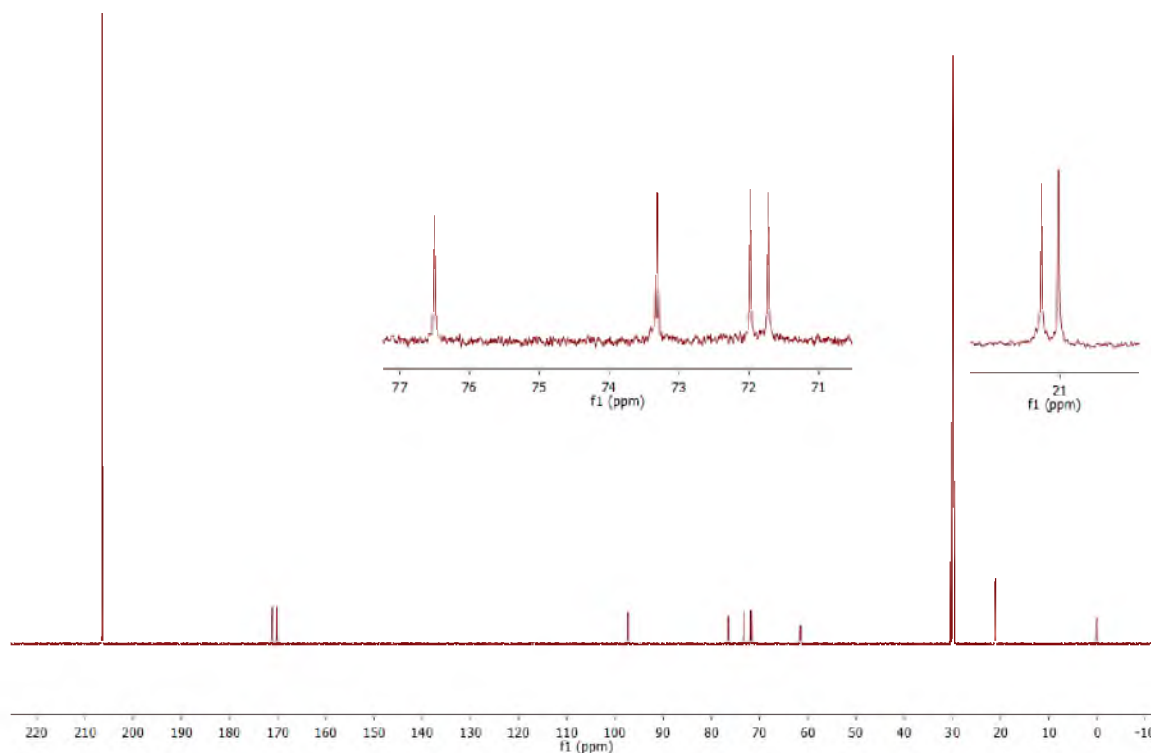


Figure 2.6.  $^{13}\text{C}$  NMR spectrum (150 MHz, acetone- $\text{d}_6$ ) of heptakis(2,3-di-O-acetyl)-  $\beta$ -CD.

Heptakis (2,3- Di- O- Acetyl- 6- O- Methyl)-  $\beta$ - CD ( $\beta 5$ ).

This procedure is a modification of Takeo's procedure [40].

A predried mass of 1.113 g ( $6.457 \times 10^{-4}$  moles) of  **$\beta 4$**  was dissolved using 14.1 mL of a 1.6 M methyl triflate ( $2.3 \times 10^{-2}$  moles) solution of  $\text{CH}_2\text{Cl}_2$  in a 50 mL sealable test tube. A mass of 4.708 g ( $2.293 \times 10^{-2}$  moles) of 2,6-di-tert-butyl-4-methyl pyridine was dissolved in 15 mL of  $\text{CH}_2\text{Cl}_2$  and added to the reaction vessel and sealed with a Teflon lined cap. The reaction vessel was stirred at  $80^\circ\text{C}$  for approximately 4.5 hours. The

reaction vessel was slowly cooled to room temperature and 10 mL of methanol was stirred into the mixture for 15 minutes.

The cloudy mixture was filtered and the organic layer was washed twice with 1.0 M  $\text{HCl}_{(\text{aq})}$ ,  $\text{NaHCO}_{3(\text{aq})}$  and concentrated. The resulting solid was dissolved in a small amount of  $\text{CH}_2\text{Cl}_2$  and poured over 200 mL of hexanes, filtered and dried. A dried mass of 1.102 g ( $6.049 \times 10^{-4}$  moles) was obtained in a yield of 93.68%.  $^1\text{H}$  NMR (600 MHz, acetone- $\text{d}_6$ ):  $\delta$  5.38 (H-3), 5.15 (H-1), 4.70 (H-2), 4.04 (H-5), 3.96, 3.57 (H-6), 3.86 (H-4), 3.36 (H-7), 2.06 (H-9 and H-11).  $^{13}\text{C}$  NMR (150 MHz, acetone- $\text{d}_6$ ):  $\delta$  171.00 (C-8), 170.09 (C-10), 97.30 (C-1), 76.84 (C-4), 71.93 (C-2), 71.82 (C-6), 71.76 (C-5), 71.64 (C-3), 59.19 (C-7), 21.08, 20.93 (C-9 and C-11).

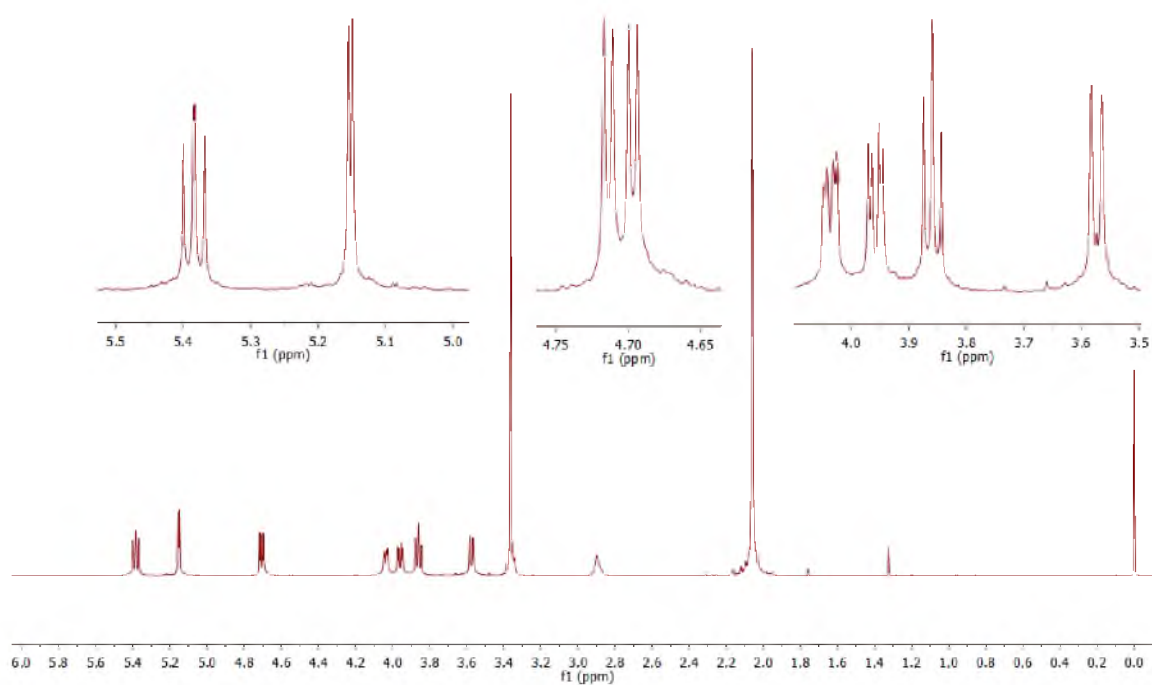


Figure 2.7.  $^1\text{H}$  NMR spectrum (600 MHz, acetone- $\text{d}_6$ ) of heptakis(2,3-di-O-acetyl-6-O-methyl)- $\beta$ -CD.

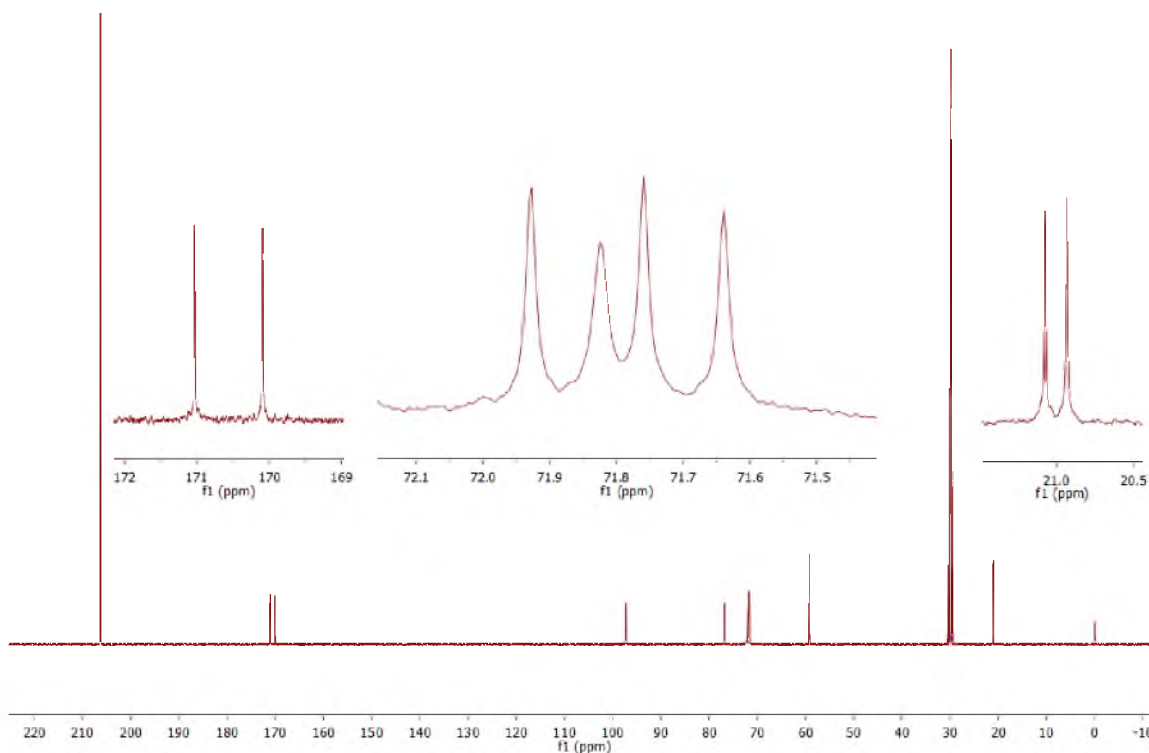


Figure 2.8.  $^{13}\text{C}$  NMR spectrum (150 MHz, acetone- $\text{d}_6$ ) of heptakis(2,3-di-O-acetyl-6-O-methyl)-  $\beta$ -CD.

Heptakis (6- O- Methyl)-  $\beta$ - CD ( $\beta 6$ ).

This procedure is a modification of Takeo's procedure [40].

A predried mass of 1.083 g ( $5.944 \times 10^{-4}$  moles) of  $\beta 5$  was dissolved in 10 mL of methanol in a 50 mL round bottom flask. A mass of 0.899 g ( $1.66 \times 10^{-2}$  moles) of  $\text{NaOCH}_3$  in 20 mL of methanol was added and the solution was stirred for approximately 2.5 hours. A 16.9 mL volume of 1.0 M  $\text{HCl}_{(\text{aq})}$  was added to quench the reaction. Solid  $\text{NaHCO}_3$  was used to neutralize the solution, filtered and concentrated.

Crystallization from hot acetone was utilized to obtain a highly pure product with a dried mass of 0.725 g ( $5.88 \times 10^{-4}$  moles) at a yield of 98.9%.  $^1\text{H}$  NMR (600 MHz,  $\text{DMSO-d}_6$ ):  $\delta$  5.83 (2-OH), 5.75 (3-OH), 4.78 (H-1), 3.71 (H-5), 3.60 (H-3), 3.57 (H-6), 3.32 (H-2), 3.27 (H-4), 3.24 (H-7).  $^{13}\text{C}$  NMR (150 MHz,  $\text{DMSO-d}_6$ ):  $\delta$  102.30 (C-1), 82.35 (C-4), 73.06 (C-3), 72.35 (C-2), 70.98 (C-6), 70.34 (C-5), 58.09 (C-7).

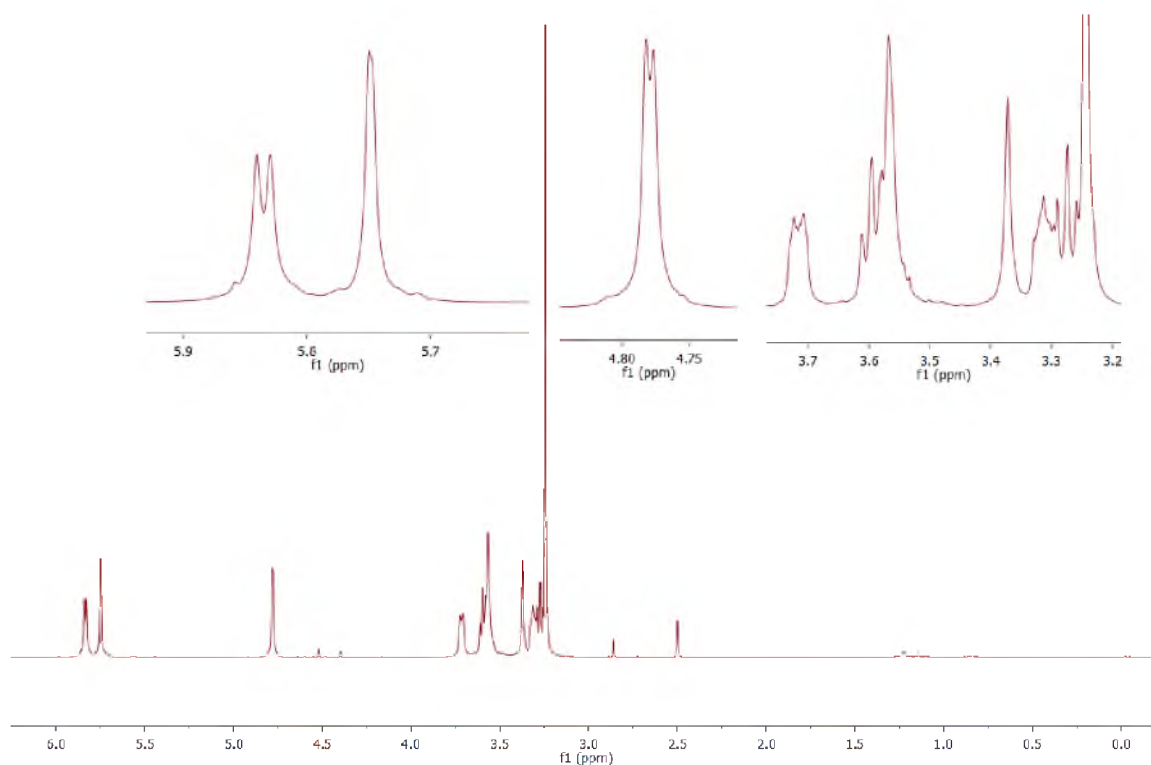


Figure 2.9.  $^1\text{H}$  NMR spectrum (600 MHz,  $\text{DMSO-d}_6$ ) of heptakis(6-O-methyl)- $\beta$ -CD.



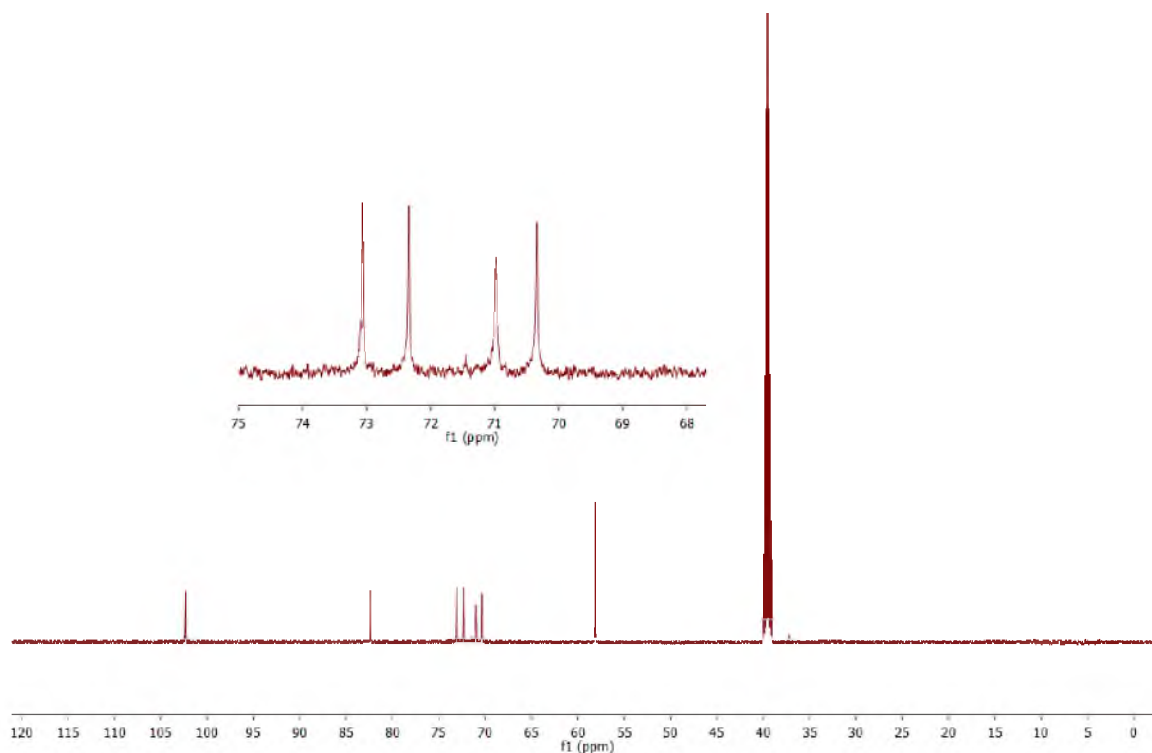


Figure 2.10.  $^{13}\text{C}$  NMR spectrum (150 MHz, DMSO- $d_6$ ) of heptakis(6-O-methyl)-  $\beta$ -CD.

### 2.5.3 Sulfobutylation of Heptakis (6-O-Methyl)- $\beta$ -CD ( $\beta$ 6).

This procedure is a modification of Kirschner's procedure [16].

All glassware and material were predried and the reaction was performed under inert gas. Addition of 0.2430 g ( $1.970 \times 10^{-4}$  moles) of  $\beta$ 6 was dissolved in 50 mL of anhydrous DMF and purged with  $\text{N}_2$  gas. The solution was stirred until the solid was dissolved and the reaction vessel was cooled to  $0^\circ\text{C}$ . A mass of 0.876 g ( $2.18 \times 10^{-2}$  moles) of KH (washed 4 times with hexanes and dried under Argon) was added slowly over 30 minutes

to prevent excessive foaming. The reaction vessel was then warmed to room temperature and 3.0477 g ( $8.2288 \times 10^{-2}$  moles) of 18-crown-6 was added while purging with  $N_2$  gas. A volume of 1.129 mL ( $1.103 \times 10^{-2}$  moles) of 1,4-butane sultone (dissolved in 10 mL of anhydrous DMF) was slowly added to the reaction vessel over 1 hour while purging with  $N_2$  gas. The reaction vessel was stirred at room temperature for 24 hours.

Addition of 20.0 mL of methanol was used to quench the reaction. The cloudy mixture was stirred for 10 minutes. The resulting solution was concentrated, dissolved in 25 mL of water and vacuum filtered. Ion exchange was used to convert to the acid form, followed by extraction (3 times) with  $CH_2Cl_2$  and neutralized with  $\sim 1.5$  g of  $KHCO_3$ . The product was purified by ultrafiltration using an Amicon Model 8400 Stirred Cell Ultrafiltration Unit with a regenerated cellulose 500 MW cutoff membrane, concentrated and dried in a vacuum oven to a constant mass.

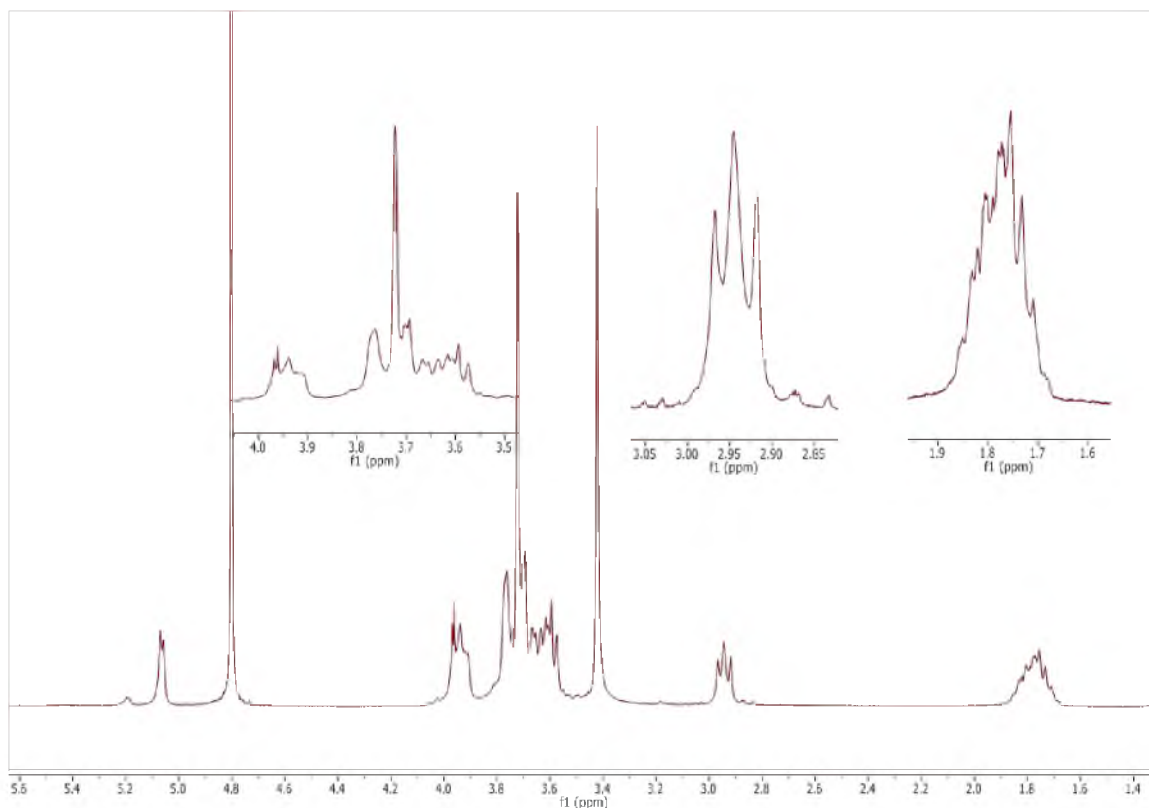


Figure 2.11.  $^1\text{H}$ -NMR spectra of Heptakis(6-O-methyl-randomly-2,3-O-sulfobutyl)-  $\beta$ -CDs in  $\text{D}_2\text{O}$ .

#### 2.5.4 Optimization of Sulfoalkylation at the secondary face.

A series of sulfoalkylation experiments were performed to determine the optimal conditions for reacting the secondary hydroxyls. Changes in solvent choice, amount of 18-crown-6 ether, and sultone were varied and analyzed. A sample procedure for the sulfopropylation of 6-O-TBDMSi  $\beta$ -CD is provided below and is a modification of Kirschner's procedure [16].

**Heptakis(Randomly-2,3-O-Sulfopropyl)-  $\beta$ -CD with 4 equivalent of 18-crown-6 per hydroxyl in THF (THF 4 SP)**

All glassware and material were predried and the reaction was performed under inert gas. Addition of 0.208 g ( $1.07 \times 10^{-4}$  moles) of  $\beta$ 2 was dissolved in 25 mL of anhydrous THF and purged with N<sub>2</sub> gas. The solution was stirred until the solid was dissolved and the reaction vessel was cooled to 0 °C. A mass of 0.414 g ( $1.03 \times 10^{-2}$  moles) of KH (washed 4 times with hexanes and dried under Argon) was added slowly over 30 minutes to prevent excessive foaming. The reaction vessel was then warmed to room temperature and 1.5403 g ( $5.83 \times 10^{-3}$  moles) of 18-crown-6 was added while purging with N<sub>2</sub> gas. A mass of 0.7155 g ( $5.86 \times 10^{-3}$  moles) of 1,3-propane sultone (dissolved in 5 mL of anhydrous THF) was slowly added to the reaction vessel over 10 minutes while purging with N<sub>2</sub> gas. The reaction vessel was stirred at room temperature for 24 hours.

Addition of 10.0 mL of methanol was used to quench the reaction. The cloudy mixture was stirred for 10 minutes and 0.208 g ( $5.61 \times 10^{-3}$  moles) of ammonium fluoride was added. The reaction mixture was then refluxed for 3 days.

The resulting grey mixture was concentrated, dissolved in 25 mL of water and vacuum filtered. Ion exchange was used to convert the CD to the acidic form, followed by extraction (3 times) with CH<sub>2</sub>Cl<sub>2</sub> and neutralized with ~1.5 g of KHCO<sub>3</sub>. The product was purified by ultrafiltration using an Amicon Model 8400 Stirred Cell Ultrafiltration Unit with a regenerated cellulose 500 MW cutoff membrane, concentrated and dried in a vacuum oven to a constant mass.

The other reactions were run using the same reaction conditions. The actual values used are provided in Table 2.1. It is important to note that significant foaming was observed when KH was added to reactions utilizing DMF the solvent. Minimal foaming was seen for reactions utilizing THF as a solvent until the reaction was quenched with methanol. Also, the DMF reactions were orange and cloudy after 24 hours while the THF reactions were grey and cloudy.  $^1\text{H}$  NMR spectra for the KSP<sub>x</sub>  $\beta$ -CD and KSB<sub>x</sub>  $\beta$ -CD series are shown in Figures 2.11 and Figure 2.12, respectively.

Table 2.1. The actual values for the masses used to optimize the sulfoalkylation of heptakis(6-O-TBDMS)-  $\beta$ -CD (followed by the deprotection of the primaries). A general procedure for these reactions is provided above.

Reaction Name	Solvent	Mass of CD (g)	Mass of KH (g)	Mass of 18-C-6 (g)	Mass of Sultone (g)	Mass of NH <sub>4</sub> F (g)
THF 0 SP	THF	0.499	1.009	0.000	1.7560	0.5034
THF 1 SP	THF	0.479	1.003	0.8773	1.7260	0.4571
THF 4 SP	THF	0.208	0.414	1.5403	0.7155	0.2077
DMF 4 SP	DMF	0.207	0.448	1.5105	0.7151	0.2067
DMF 0 SB	DMF	0.206	0.429	0.000	0.8088	0.1925
DMF 1 SB	DMF	0.201	0.406	0.379	0.7892	0.1878
DMF 4 SB	DMF	0.196	0.398	1.472	0.7696	0.2174
DMF 8 SB	DMF	0.201	0.422	3.220	0.7892	0.2013

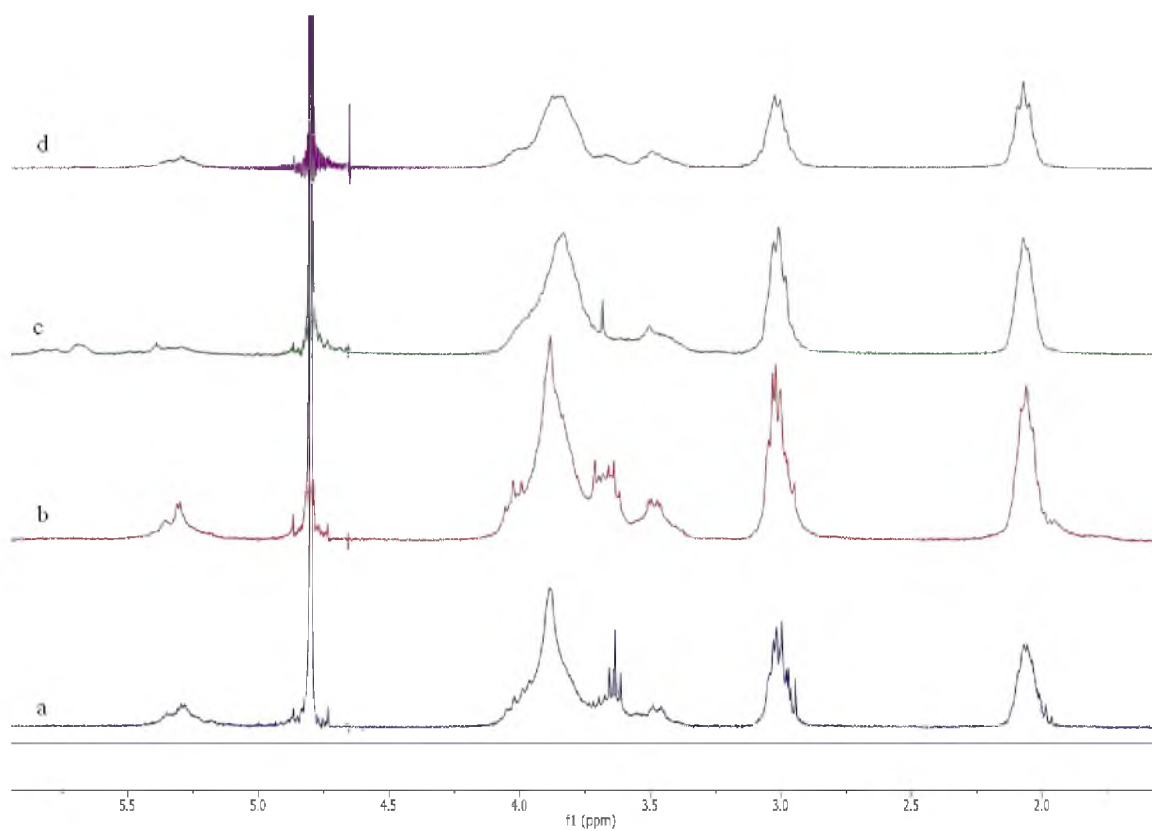


Figure 2.12.  $^1\text{H}$ -NMR spectra of  $\text{KSP}_x$   $\beta$ -CDs in  $\text{D}_2\text{O}$ : a) reaction THF 0 SP; b) reaction THF 1 SP; c) reaction THF 4 SP; and d) reaction DMF 4 SP.

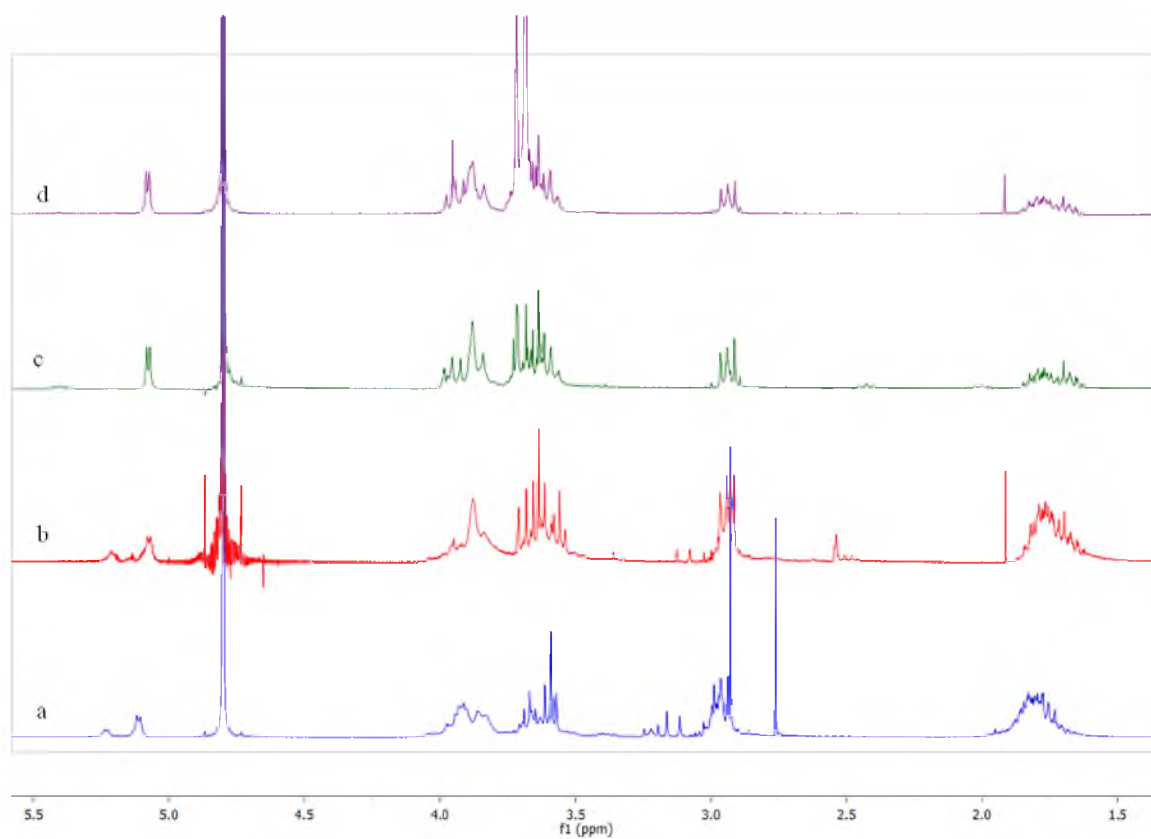


Figure 2.13.  $^1\text{H}$ -NMR spectra of  $\text{KSB}_x$   $\beta$ -CDs in  $\text{D}_2\text{O}$ : a) reaction DMF 0 SB; b) reaction DMF 1 SB; c) reaction DMF 4 SB; and d) reaction DMF 8 SB.

## Chapter 3. Results

### 3.1 Synthesis of acetyl intermediates and Heptakis(6-O-methyl-randomly-2,3-sulfopropyl)- $\beta$ -CD

The synthetic scheme chosen for the synthesis of single isomer heptakis(6-O-methyl)-  $\beta$ -CD was through the acetyl intermediates used to protect the secondary hydroxyls. While a number of reaction schemes were explored (benzyl intermediates and direct alkylation schemes), the use of acetyls as the intermediates proved to have the highest yields with mild reaction conditions and minimal purification which was first accomplished by Takeo in 1989 [41]. The only step that has a poor yield is the purification of heptakis(2,3-di-O-acetyl)-  $\beta$ -CD ( **$\beta$ 4**) which has a 50% yield after purification. This is due to inefficient deprotection of the primary hydroxyls even with a large excess of  $\text{BF}_3$ .

Another drawback of this reaction scheme is the use of the expensive hindered organic base 2,6-di-tert-butyl-4-methyl pyridine for the synthesis of heptakis(2,3-di-O-acetyl-6-O-methyl)-  $\beta$ -CD ( **$\beta$ 5**). This hindered organic base is meant to selectively deprotonate the 6-OH while leaving the acetyl protecting groups attached to the secondary face. While it can be recovered, purified and reused in subsequent reactions, it is a costly base that causes some purification issues at this step. Alternatively, two possible substitutes that should be explored are 2,6-di-methyl pyridine (2,6-lutidine) and pyridine. These two reagents are much less expensive and are liquids that can be removed under reduced pressure. However, it should be done on a small scale due to the possible deacetylation of the secondary face of the CD.



The overall yield for this reaction scheme is 43%. This is due to the low yield for **β4**. Attempts to increase this yield to 85% by further deacetylation of unreacted starting material would provide an overall yield of 73%. This should be attempted in order to provide a larger starting material for alkylation of the primaries. As mentioned before, this reaction scheme can be used to produce a series of 6-O-alkyl CDs using the same reaction conditions with the exception of the synthesis of **β5**. Changing the alkyl triflate here is all that is necessary to produce a series of 6-O-alkyl CDs.

Preliminary sulfobutylation experiments with heptakis(6-O-methyl)-  $\beta$ -CD (**β6**) showed poor reactivity with 1,4-butane sultone when using THF as a solvent, which was attributed solubility issues of the CD in the solvent. Also, the use of DMSO was ineffective due to the reaction of the solvent with strong base (KH) to form the dimsyl anion which then reacted with the sultone. Work by Stella et. al. [42] to produce a sulfobutylated CD with an average DS as high as 9.1 has been achieved in aqueous conditions. However, limited solubility of **β6** in aqueous environments would have likely limit reactivity. As a result, the solvent of choice for the sulfobutylation was DMF. However, it was later determined that the sulfobutylation produced low DS in this solvent. Results are similar to those found by Qu et. al. [43] using dioxane as a solvent without 18-crown-6 and with a sodium hydroxide solution (as opposed to the KH used in these experiments).

### 3.2 Optimization of sulfoalkylation reaction on secondary hydroxyls

To optimize the reaction conditions for the sulfoalkylation of the secondary rim of the CD, heptakis(6-O-TBDMS)- $\beta$ -CD was chosen as the starting material due to the fact that it is readily synthesized with little purification. The excess KH and sultone were held constant at 4 equivalents per hydroxyl. The type of sultone, the solvent and amount of 18-crown-6 (a potassium complexing agent) were varied. This would provide insight into the differences in reactivity of 1,3-propane sultone vs. 1,4-butane sultone while also observing solvent effect. Also, the effects of 18-crown-6 on the electrophilic behavior of the secondary hydroxyls was also investigated to compare with the results obtained by Kirschner [16].

For the synthesis of KSP<sub>x</sub>  $\beta$ -CDs in THF, the average DS (from HILIC) was 3.3, 4.6 and 6.1 when going from 0, 1 and 4 equivalents of 18-crown-6, respectively. This shows a direct increase in DS as the amount of 18-crown-6 was added, which followed Kirschner's observations [16]. This effect is likely due to the increase in solubility of the alkoxide and the final product. It is also hypothesized that the ion pairing between potassium and 18-crown-6 causes an increase in the nucleophilic ability of the alkoxide formed, and thus increasing reactivity [34]. It is hypothesized that the C(2) hydroxyl is being preferentially reacted and the quick drop in yield of the DS 8 and 9 are attributed to the poor reactivity of the C(3) in THF. This is based on evidence from other studies that shows that the C(2) is more acidic and accessible for reaction than the C(3) [7]. However, further investigation is necessary to confirm this hypothesis.

When changing the solvent to DMF using 4 equivalents of 18-crown-6, a much more Gaussian distribution of DS was observed. This indicates that there is a solvent effect that is increasing the reactivity of the C(3) and allowing for better reactivity. An average DS was 8.4 for this reaction and the existence of higher DS of substitution are detected up to the fully sulfopropylated charged state. Being that the higher DS obtained for KSP<sub>DS 8.4</sub>  $\beta$ -CD was observed in DMF, sulfobutylated studies were focused on using DMF as solvent as opposed to THF.

Interestingly, the same pattern was not seen for the KSB<sub>x</sub>  $\beta$ -CD when analyzed with NMR and HILIC. It is also important to note that an increase in the amount of 18-crown-6 to 4 and 8 equivalents afforded extremely poor reactivity and afforded both with a DS of 0.2 (from HILIC). It is possible that the reactions with 0 and 1 equivalents of 18-crown-6 afforded higher DS than the 0.7 and 0.8, respectively (from HILIC), but the results are being investigated further to determine the extent of the reaction.

### **3.3 Characterization of the final products**

The series of CDs produced for this research were characterized to determine the DS using a number of methods, including <sup>1</sup>H-NMR integration analysis, inverse CE, and HILIC LT-ELSD. Another method for determination of the DS is to use elemental analysis, but the analysis is performed by another lab and the products must be of high purity in order to have the results be useful. One of the main issues with the KSP<sub>x</sub>  $\beta$ -

CDs, KSB<sub>x</sub> β-CDs and the KSB<sub>x</sub>M β-CD was the inability to remove impurities from the samples. This rendered some of the methods used for DS analysis as unreliable.

This issue of unreliability was observed when characterizing the CDs using NMR analysis. Overly high predictions of DS were seen for multiple CDs even when integrating different regions. As a result, the NMR analysis was used primarily to determine that impurities were present and not removed during Ultrafiltration even after flushing with a total volume of roughly 1.5 L of Milli-Q water per sample. This also led to the decision to not send out the samples for elemental analysis at this time.

### 3.3.1 NMR integrations

The use of integration values to determine the DS of a sample by <sup>1</sup>H NMR spectroscopy is a quick means of obtaining this information. However, the samples must be highly pure in order to obtain an accurate value. This method of analysis is also limited in the fact that it cannot provide information on the variation of charge states, only an average of the DS can be obtained. There are a number of ways in which to obtain DS values and allow one to double check the obtained values.

For the analysis of the highly charged KSP<sub>x</sub> β-CDs, integration of the anomeric hydrogens (O<sub>2</sub>CH: 5.4 – 5.2 ppm), the glycosidic hydrogens (OCH: 4.0 – 3.4 ppm), and sulfopropyl hydrogens (OCH<sub>2</sub>: 3.6 ppm; -CH<sub>2</sub>–: 2.1 – 1.9 ppm; CH<sub>2</sub>SO<sub>3</sub><sup>–</sup>: 3.1 – 2.9 ppm) provide a set ratios that can be used to approximate the DS. The graphs used to

determine the DS are shown below (Figures 3.1 and 3.2) and the calculated DS values are listed in Table 3.1.

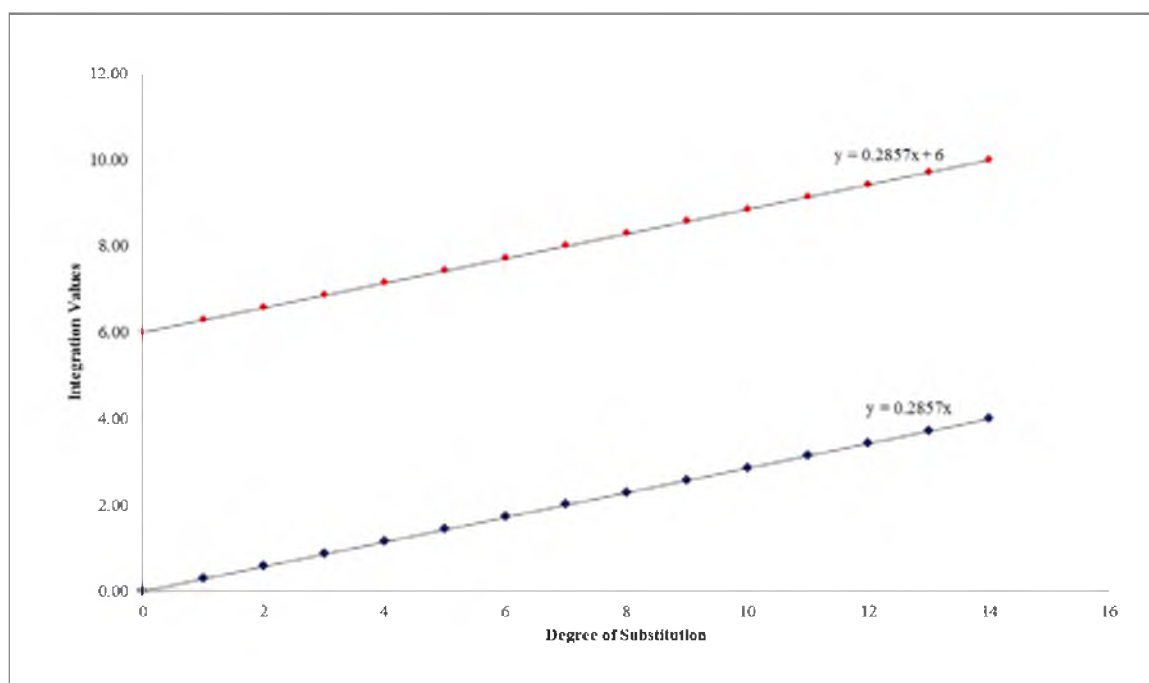


Figure 3.1. A plot of the expected integration ratios as a function of the DS for the KSP<sub>X</sub>  $\beta$ -CDs. The expected integration ratios (relative to the anomeric integration value set to 1.00) for the  $-\text{CH}_2-$  and  $\text{CH}_2\text{SO}_3^-$  sulfopropyl hydrogens (blue) and the glycosidic hydrogens and the  $\text{OCH}_2$  sulfopropyl hydrogens (red).

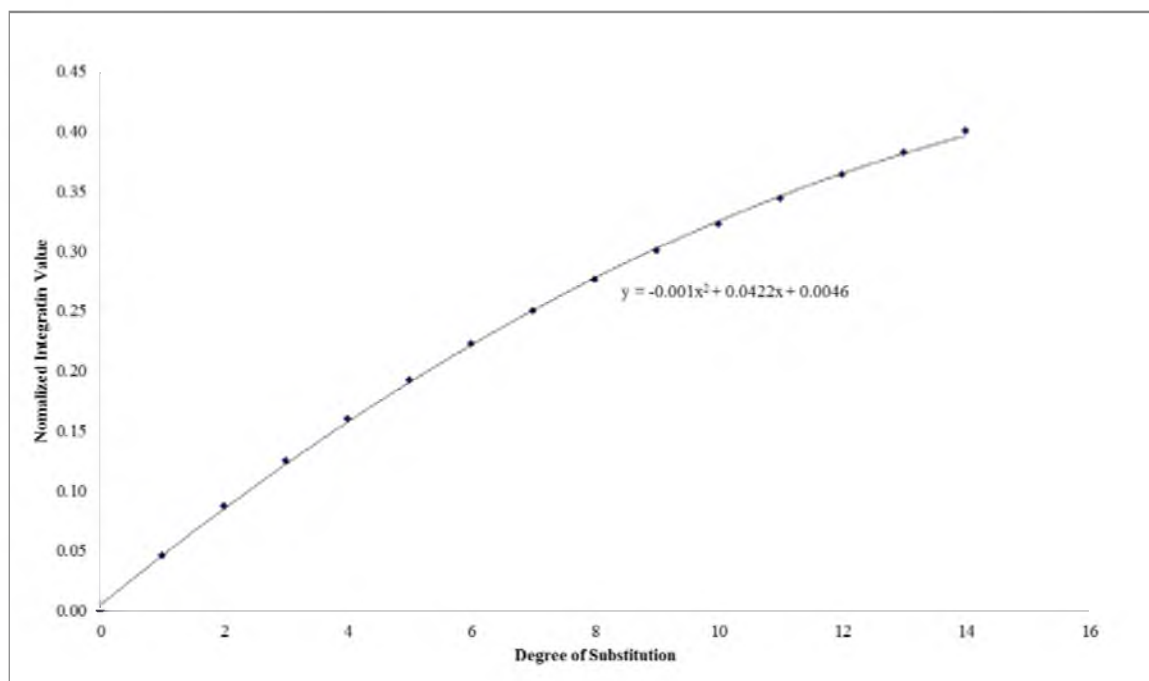


Figure 3.2. A plot of the expected integration ratios as a function of the DS for the KSP<sub>X</sub> β-CDs. The expected integration ratios (relative to the glycosidic integration value set to 1.00) for the -CH<sub>2</sub>- and CH<sub>2</sub>SO<sub>3</sub><sup>-</sup> sulfopropyl hydrogens.

Table 3.1. The calculated DS from integration ratios are provided for the KSP<sub>x</sub> β-CDs from the reaction optimization experiments. The integration ratios are from: a) the glycosidic region (containing the sulfopropyl OCH<sub>2</sub>) relative to the anomeric region; b) the -CH<sub>2</sub>- sulfopropyl hydrogens relative to the anomeric region; c) the CH<sub>2</sub>SO<sub>3</sub><sup>-</sup> sulfopropyl hydrogens relative to the anomeric region; d) the -CH<sub>2</sub>- sulfopropyl hydrogens relative to the glycosidic region; and e) the CH<sub>2</sub>SO<sub>3</sub><sup>-</sup> sulfopropyl hydrogens relative to the glycosidic region. Values noted with an asterisk were omitted from the average DS because they are outliers.

Reaction Name	DS 1 <sup>a</sup>	DS 2 <sup>b</sup>	DS 3 <sup>c</sup>	DS 4 <sup>d</sup>	DS 5 <sup>e</sup>	Average DS (STD)
THF 0 SP	6.86	8.37	8.05	9.10	8.62	8.20 (0.75)
THF 1 SP	16.63*	12.22	12.22	10.18	10.18	11.20 (1.02)
THF 4 SP	15.05*	13.27	12.53	12.23	11.25	12.32 (0.72)
DMF 4 SP	28.18*	18.94*	17.75*	13.08	11.88	12.48 (0.60)

For the analysis of the highly charged KSB<sub>x</sub> β-CDs, integration of the anomeric hydrogens (O<sub>2</sub>CH: 5.3– 5.0 ppm), the glycosidic hydrogens (OCH: 4.1 – 3.4 ppm), and sulfobutyl hydrogens (OCH<sub>2</sub>: around 3.6 ppm; -CH<sub>2</sub>CH<sub>2</sub>–: 2.0 – 1.6 ppm; CH<sub>2</sub>SO<sub>3</sub><sup>-</sup>: 3.1 – 2.9 ppm) provide a set ratios that can be used to approximate the DS. The graphs used

to determine the DS are shown below (Figures 3.3 and 3.4) and the calculated DS values are listed in Table 3.2.

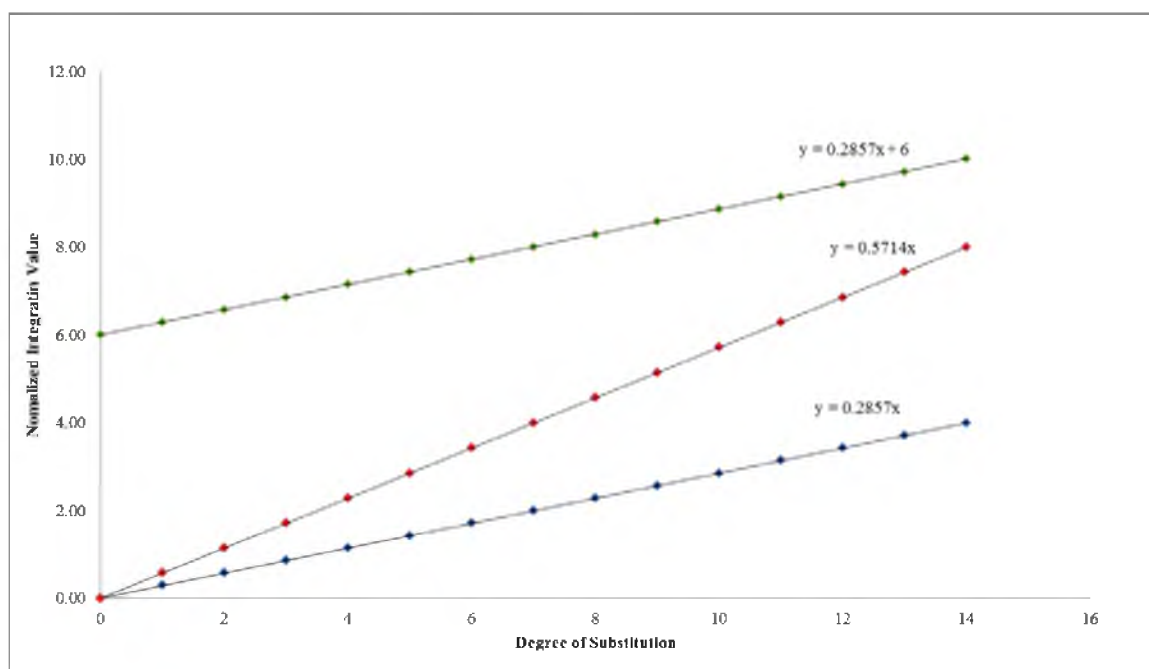


Figure 3.3. A plot of the expected integration ratios as a function of the DS for the  $\text{KSB}_X$   $\beta$ -CDs. The expected integration ratios (relative to the anomeric integration value set to 1.00) for the  $\text{CH}_2\text{SO}_3^-$  sulfobutyl hydrogens (blue), the  $-\text{CH}_2\text{CH}_2-$  sulfobutyl hydrogens (red), and the glycosidic hydrogens and the  $\text{OCH}_2$  sulfobutyl hydrogens (green).



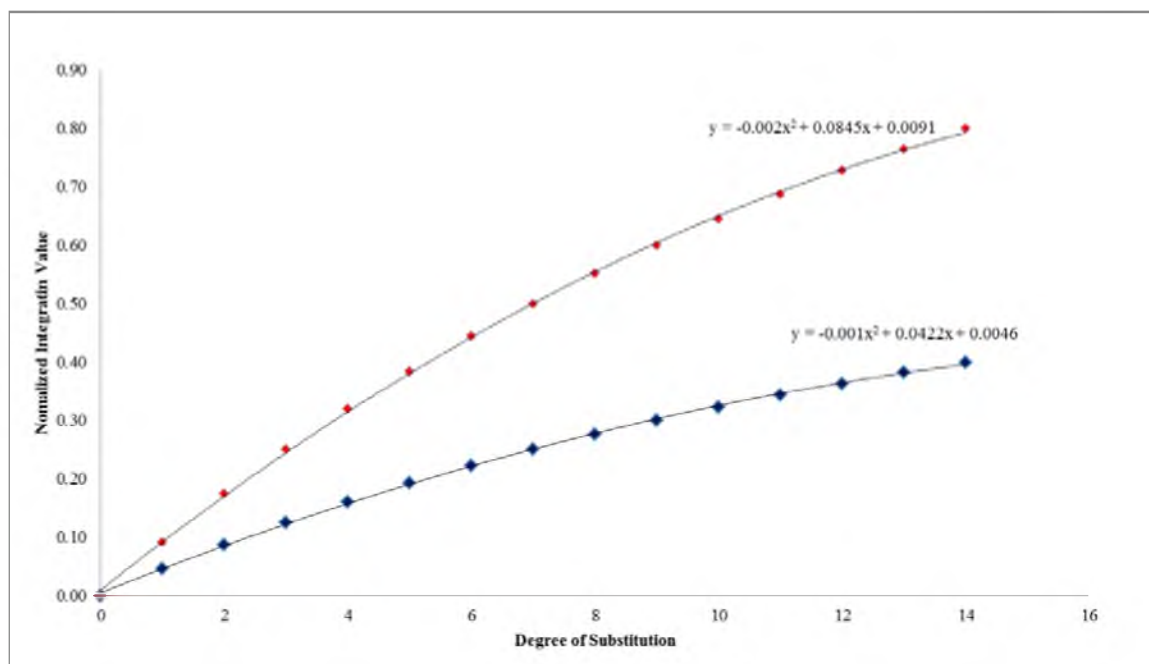


Figure 3.4. A plot of the expected integration ratios as a function of the DS for the KSB<sub>X</sub> β-CDs. The expected integration ratios (relative to the glycosidic integration value set to 1.00) for the  $\text{CH}_2\text{SO}_3^-$  sulfobutyl hydrogens (blue) and the  $-\text{CH}_2\text{CH}_2-$  sulfobutyl hydrogens (red).

Table 3.2. The calculated DS from integration ratios are provided for the KSB<sub>x</sub> β-CDs from the reaction optimization experiments. The integration ratios are from: a) the glycosidic region (containing the sulfobutyl OCH<sub>2</sub>) relative to the anomeric region; b) the -CH<sub>2</sub>CH<sub>2</sub>- sulfobutyl hydrogens relative to the anomeric region; c) the CH<sub>2</sub>SO<sub>3</sub><sup>-</sup> sulfobutyl hydrogens relative to the anomeric region; d) the -CH<sub>2</sub> CH<sub>2</sub>- sulfobutyl hydrogens relative to the glycosidic region; and e) the CH<sub>2</sub>SO<sub>3</sub><sup>-</sup> sulfobutyl hydrogens relative to the glycosidic region. Values noted with an asterisk were omitted from the average DS because they are outliers.

Reaction Name	DS 1 <sup>a</sup>	DS 2 <sup>b</sup>	DS 3 <sup>c</sup>	DS 4 <sup>d</sup>	DS 5 <sup>e</sup>	Average DS (STD)
DMF 0 SB	7.74	13.48	10.45	17.65*	12.02	10.92 (2.13)
DMF 1 SB	6.72	8.30	8.09	9.06	8.74	8.18 (0.80)
DMF 4 SB	12.60*	4.80	3.47	3.40	2.31	3.50 (0.88)
DMF 8 SB	42.14*	3.82	2.98	1.30	1.01	2.28 (1.16)

### 3.3.2 Inverse Detection CE

Analysis of the single isomers CDs samples with inverse detection CE has been successfully reported in by previous works and shows good agreement with other techniques. Stella reports the characterization of randomly sulfated CDs using 30 mM Benzoic Acid adjusted to pH 6.0 with 0.1 M TRIS base [18, 44] and Kirschner reported the use of similar separation conditions to characterize the series of 2,3-di-alkyl-6-O-

sulfoalkyl CDs [16]. However, attempts to analyze the  $\text{KSP}_x$   $\beta$ -CDs using the same separation conditions produced incomprehensible results, which is elaborated in Figure 3.5.

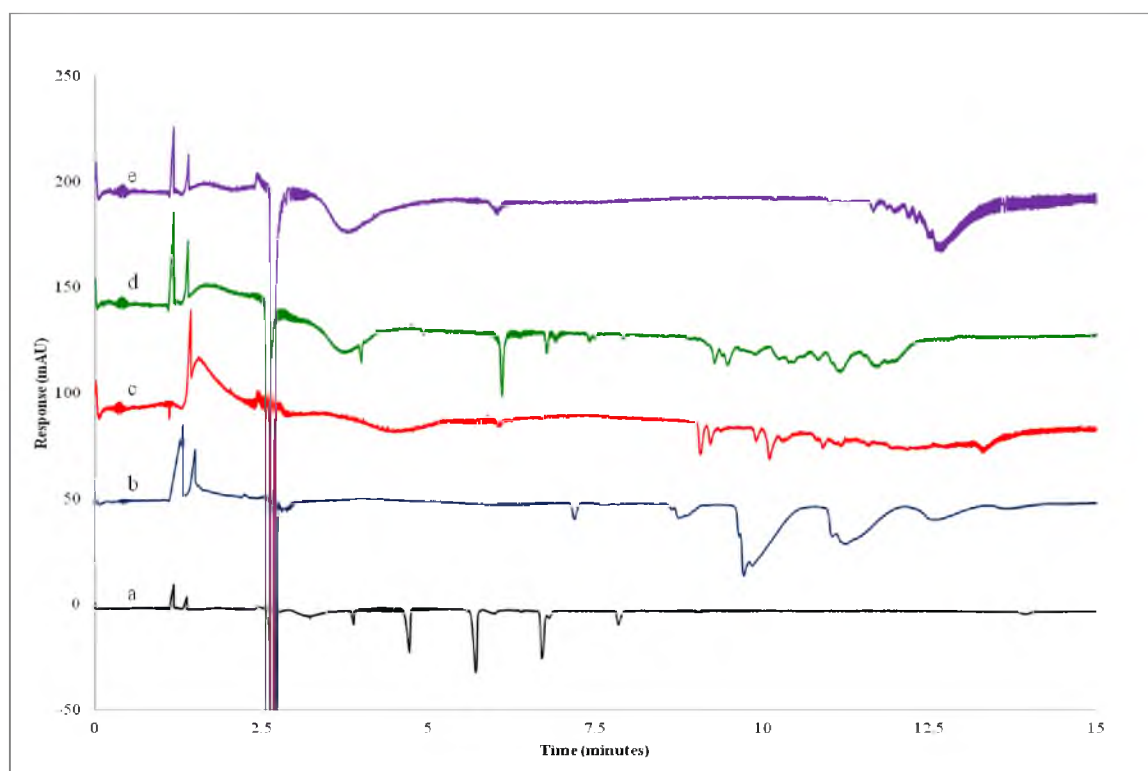


Figure 3.5. Inverse detection CE separations of  $\text{KSP}_x$   $\beta$ -CDs: a)  $\text{KSP}_{4.5}\text{DM}$   $\beta$ -CD; b) reaction THF 0 SP; c) reaction THF 1 SP; d) reaction THF 4 SP; and e) reaction DMF 4 SP. Separations were carried out 2 sec. injection at 50 mbar; 10 kV separation on a 32.5 cm (24.0 cm eff.)  $\times$  50  $\mu\text{m}$  (i.d.). Buffer: 30 mM Benzoic Acid at pH 6.0.

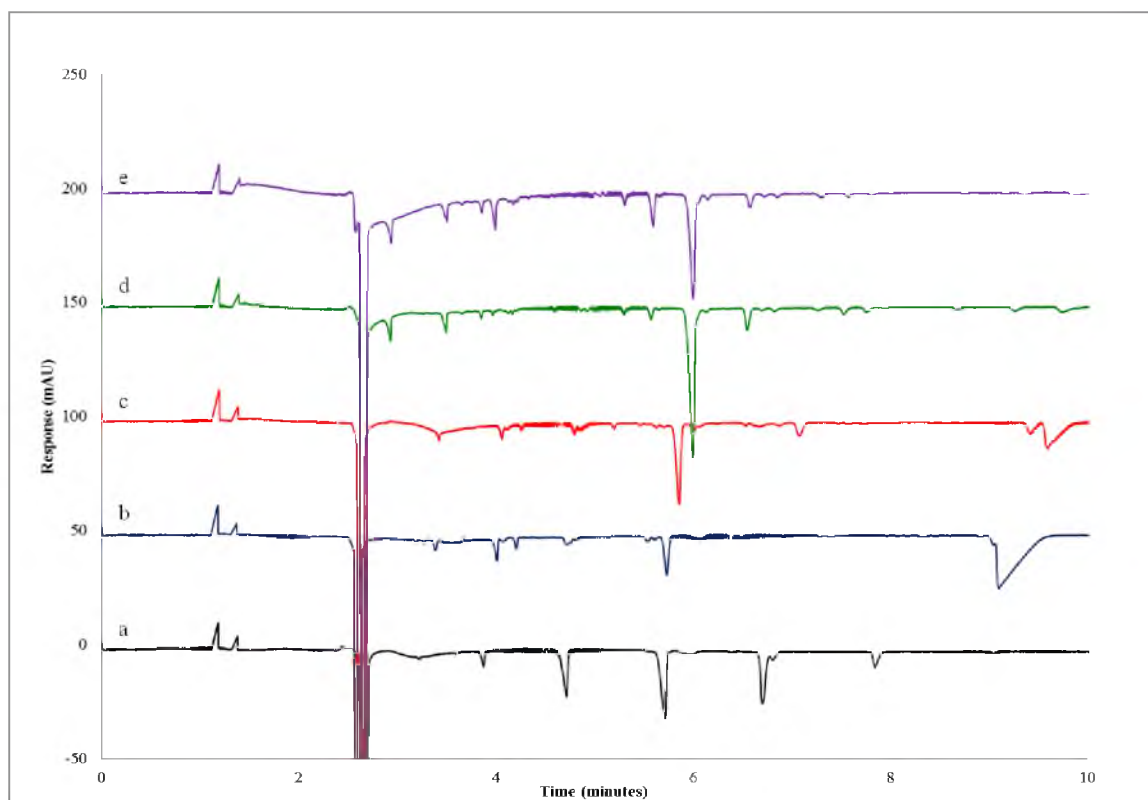


Figure 3.6. Inverse detection CE separations of  $\text{KSB}_x \beta\text{-CDs}$ : a)  $\text{KSP}_{4.5}\text{DM} \beta\text{-CD}$ ; b) reaction DMF 0 SB; c) reaction DMF 1 SB; d) reaction DMF 4 SB; and e) reaction DMF 8 SB. Separations were carried out 2 sec. injection at 50 mbar; 10 kV separation on a 32.5 cm (24.0 cm eff.) x 50  $\mu\text{m}$  (i.d.). Buffer: 30 mM Benzoic Acid at pH 6.0.

When using inverse CE to determine the DS for the  $\text{KSP}_{\text{DS } 4.5}\text{DM} \beta\text{-CD}$  synthesized by Kirschner (Figure 1.6), a simple electropherogram was observed and a range from 1-7 was detectable. Utilizing the same separation conditions for  $\text{KSP}_x \beta\text{-CDs}$  and  $\text{KSB}_x \beta\text{-CDs}$  proved ineffective. The migration of the individual charged states did not line up with those for the  $\text{KSP}_{4.5}\text{DM} \beta\text{-CD}$  as predicted. Although it appears that some

regioisomers with the same low DS are being separated for KSP<sub>x</sub> β-CD, higher charge states appear to coelute due to the high ionic strength causing dispersion of the charges [45].

Application of this separation method to the KSB<sub>x</sub> β-CDs using the same separation conditions appeared to provide a major peak near DS of 4. However, when compared to the HILIC results, we believe this to be the DS of 1, indicating that there is also a significant difference in the migration times of these analytes compared to the KSP<sub>4.5</sub>DM β-CD.

### 3.3.3 Hydrophilic interaction chromatography

The use of HILIC to obtain DS on SBE- CDs has recently been reported by Vigh [25]. This method allows for the analysis of the range of charged states present in the sample and the use of LT-ELSD detection allows for the application of HILIC to UV inactive compounds. The DS can then be calculated by taking the total area of the charged species to obtain an average DS assuming a linear response of the detector to a change in DS. However, it was quickly determined that the use of a single elution protocol to analyze the different products was not feasible. However, a simple method development procedure can be applied by varying the concentration of total % water in the mobile phase.

Initial separations to characterize the charged states of KSP<sub>4.5</sub>DM β-CD produced by Kirschner were carried out using Vigh's procedure. In an effort to explore the effects of

water on separations, a series of isocratic separations were performed using 30 mM ammonium formate and varying the amount of water by 30%, 25% and 20% (v/v) in ACN (Figure 3.5). It was found that the separation of the eight possible charge states (DS of 0-7 possible) of KSP<sub>4.5</sub>DM  $\beta$ -CD was largely influenced by the concentration of water. At 30% (v/v) water, the isomers all eluted less than 3 minutes and were thus weakly retained by the column. Decreasing the amount to 20% (v/v) water caused the CDs to be strongly retained by the column. While resolution of the charged states from the fast eluting salts was not achieved at 25% (v/v) water, an intermittent 28% (v/v) water was chosen to analyze the purity of the single isomer CDs synthesized by Kirschner (Figure 1.6).

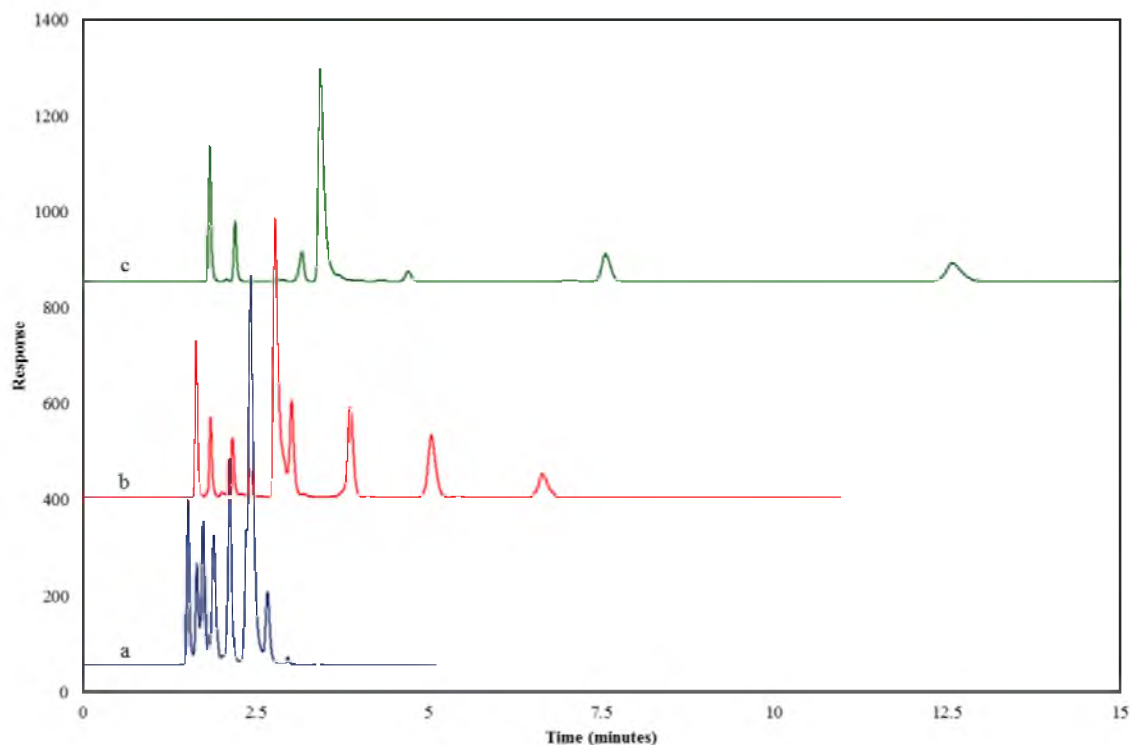


Figure 3.7 Effect of water concentration on HILIC separations of KSP<sub>DS 4.5DM</sub>  $\beta$ -CD. Separations were carried out isocratically at 1.5 mL/ min flow rate using 30 mM ammonium formate in: a) 30% (v/v) water: 70 % (v/v) acetonitrile; b) 25% (v/v) water: 75% (v/v) acetonitrile; and c) 20% (v/v) water: 80% (v/v) acetonitrile.

Analysis of these single isomer CDs using the isocratic 30 mM ammonium formate; 23% (v/v) water: 77% (v/v) ACN separation conditions provided interesting results (Figure 3.6 and Figure 3.7). The single isomer KSPDM  $\alpha$ -CD and KSBDM  $\alpha$ -CD showed some minor impurities but corresponded well to the DS 6 stereoisomer of the standard KSP<sub>DS 4.5DM</sub>  $\beta$ -CD. However, the KSPDE- $\alpha$ -CD showed less retention of the single isomer

compared to single isomer KSPDM  $\alpha$ -CD. Similar results were observed when comparing KSP<sub>DS 4.5</sub>DM  $\beta$ -CD to the KSPDE- $\beta$ -CD and KSBDM-  $\beta$ -CD. This indicates that although a change in the sulfoalkyl chain length on the primary face does not have a large impact on the retention of the CD, a change in the alkyl group on the secondary face was found to be very significant.

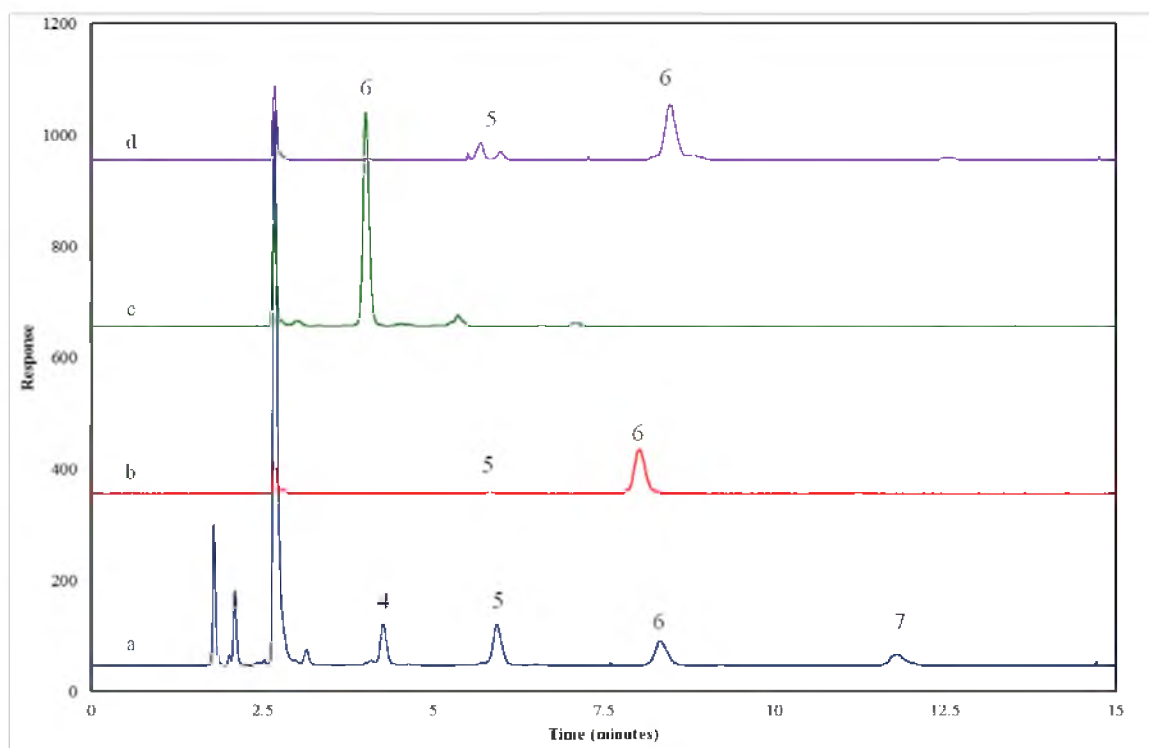


Figure 3.8. HILIC separations of single isomer  $\alpha$ -CDs: a) standard, KSPDM  $\beta$ -CD (DS 4.5); b) KSPDM  $\alpha$ -CD; c) KSPDE  $\alpha$ -CD; and d) KSBDM  $\alpha$ -CD. Separations were carried out isocratically at 1.5 mL/ min flow rate using 30 mM ammonium formate in 23% (v/v) water: 77 % (v/v) acetonitrile.



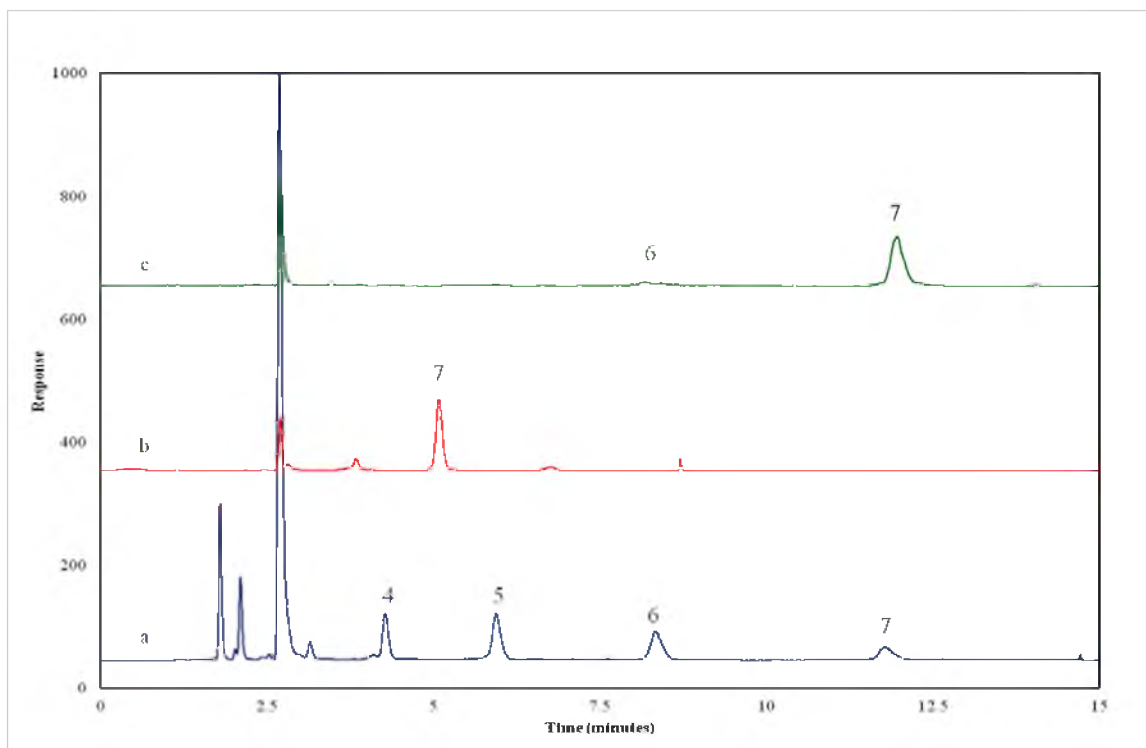


Figure 3.9. HILIC separations of single isomer  $\beta$ -CDs: a) standard, KSP<sub>DS 4.5DM</sub>  $\beta$ -CD; b) KSPDE  $\beta$ -CD; and c) KSBDM  $\beta$ -CD. Separations were carried out isocratically at 1.5 mL/ min flow rate using 30 mM ammonium formate in 23% (v/v) water: 77 % (v/v) acetonitrile.

Attempts to utilize the above separation conditions for the highly charged CDs (DS 0-14) proved ineffective due to strong retention of the mixture. Initial isocratic separations using a highly charged KSP<sub>x</sub>  $\beta$ -CD (reaction DMF 4 SP) are illustrated in Figure 3.10. Small increases in the water content in the mobile phases results in dramatically reduced retention. Optimization of a gradient separation system was eventually used to effectively separate the weakly retained salts and minor impurities and provide nearly

baseline resolution of the fourteen charged species of KSP<sub>x</sub>  $\beta$ -CD. Analysis of a spiked sample containing  $\beta$ -CD, a low DS (Reaction THF 0 SP) and a high DS (Reaction DMF 4 SP) sample provided the full range of DS 0-14 (Figure 3.11). This was then used to analyze all the KSP  $\beta$ -CDs obtained under varying reaction conditions (Figure 3.12).

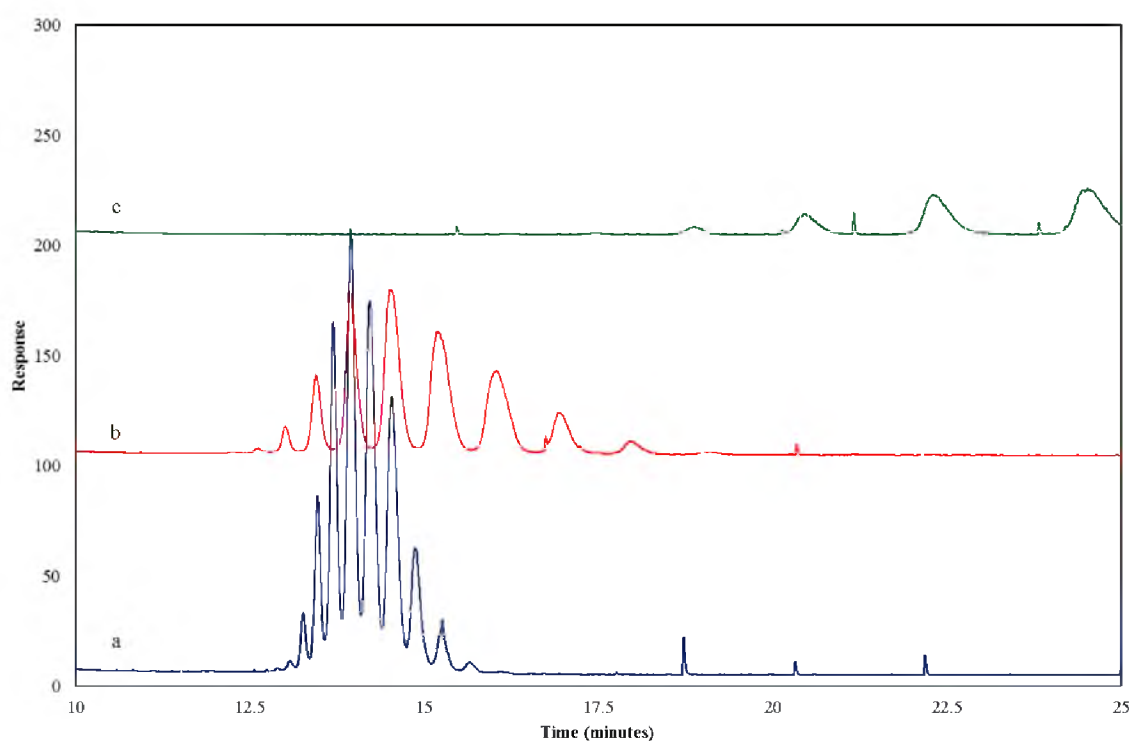


Figure 3.10. Effect of water concentration on HILIC separations of KSP<sub>x</sub>  $\beta$ -CD reaction DMF 4 SP, Table 2.1. Separations were carried out isocratically at 1.5 mL/ min flow rate using 10 mM ammonium formate in a) 32.0 % (v/v) water: 68.0 % (v/v) acetonitrile; b) 30.2 % (v/v) water: 69.8 % (v/v) acetonitrile; and c) 27.2 % (v/v) water: 72.8 % (v/v) acetonitrile.

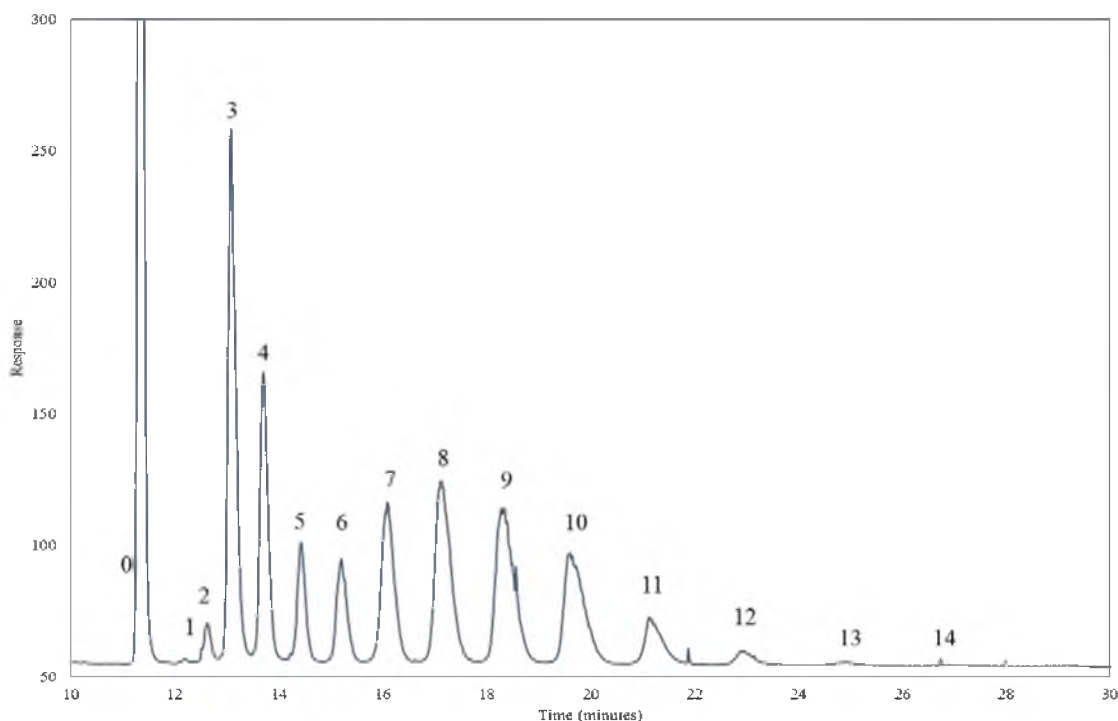


Figure 3.11. HILIC separations of a spiked sample of native  $\beta$ -CD, a low DS (reaction THF 0 SP) and high DS (reaction DMF 4 SP) to establish retention times of DS 0-14. Separations were carried out at 1.5 mL/ min using a binary gradient. (A: 10 mM ammonium formate in water; B: 10 mM ammonium formate in 15% (v/v) water: 85% (v/v) acetonitrile). Solvent mixtures were set up to maintain 0% A for 5 minutes and increase to 16.5% A (total of 29 % (v/v) water) at 8 minutes and held. (Peak at 27.0 minutes corresponds to DS 14 and is detectable but not abundant.)

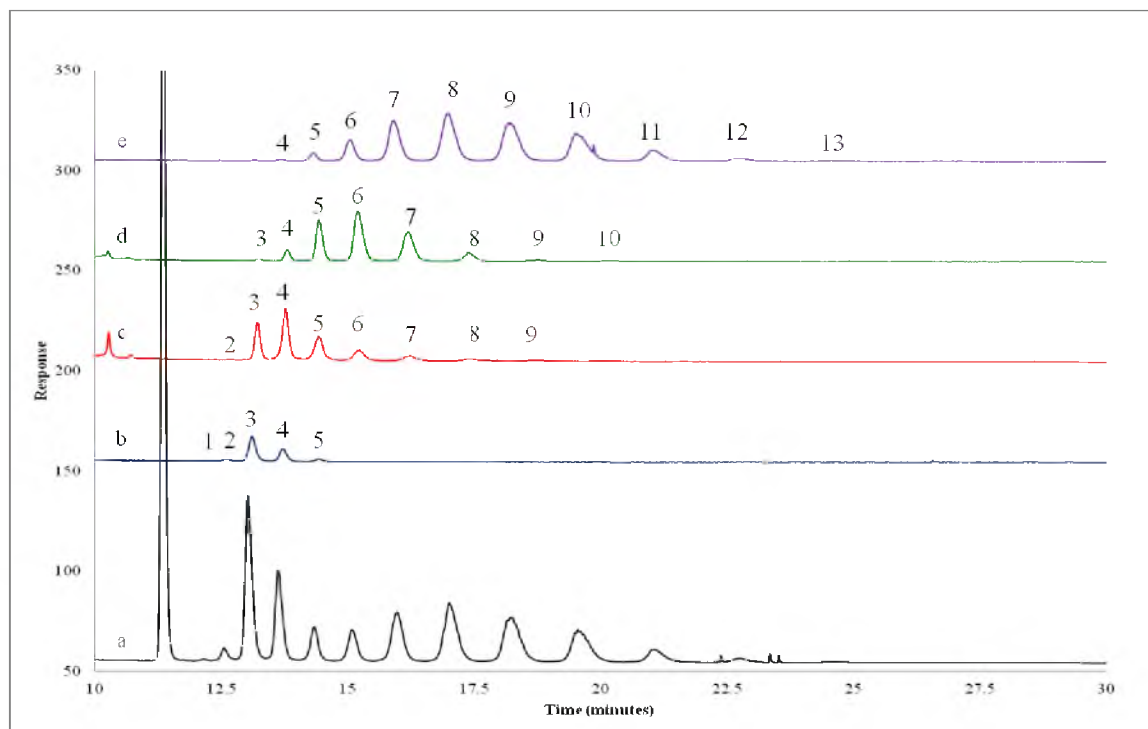


Figure 3.12. HILIC separations of  $\text{KSP}_x \beta\text{-CD}$ : a) a spiked sample of native  $\beta\text{-CD}$ , a low DS and high DS  $\text{KSP}_x \beta\text{-CD}$ ; b) reaction THF 0 SP; c) reaction THF 1 SP; d) reaction THF 4 SP; e) reaction DMF 4 SP. Separations were carried out at 1.5 mL/ min using a binary gradient. (A: 10 mM ammonium formate in water; B: 10 mM ammonium formate in 15% (v/v) water: 85% (v/v) acetonitrile). Solvent mixtures were set up to maintain 0% A for 5 minutes and increase to 16.5% A (total of 29 % (v/v) water) at 8 minutes and held.

The HILIC results have two clear effects from the optimization experiments for  $\text{KSP}_x \beta\text{-CD}$ . The first is the clear increase in the average DS observed when increasing the amount of 18-crown-6 in THF. In addition, there is a significant increase in the average

DS when changing from THF to DMF. The calculated DS from peak area percentages is provided in Table 3.3.

Table 3.3. The peak areas (normalized by the molecular weight of the individual charged states) were used to determine the DS of Heptakis(randomly-2,3-O-sulfopropyl)-  $\beta$ -CD from HILIC LT-ELSD results.

Reaction Name	DS
THF 0 SP	3.3
THF 1 SP	4.6
THF 4 SP	6.1
DMF 4 SP	8.4

It was then hypothesized that the KSB<sub>x</sub>  $\beta$ -CDs would exhibit retention behavior similar to the KSP<sub>x</sub>  $\beta$ -CDs. The same elution protocol was then used to analyze the DS of the series of KSB<sub>x</sub>  $\beta$ -CDs synthesized under various reaction conditions (Figure 3.13). However, it was realized that the retention characteristics were not the same when going from sulfopropyl to sulfobutyl groups. Optimization of an isocratic separation was chosen because of the fact that lower percentages of water were necessary to elute the CDs (Figure 3.14). Interestingly, a systematic decrease in the percentage of water in the

mobile phase results in a reversal of the major and minor KSB<sub>x</sub> β- CD peaks (Figure 3.12).

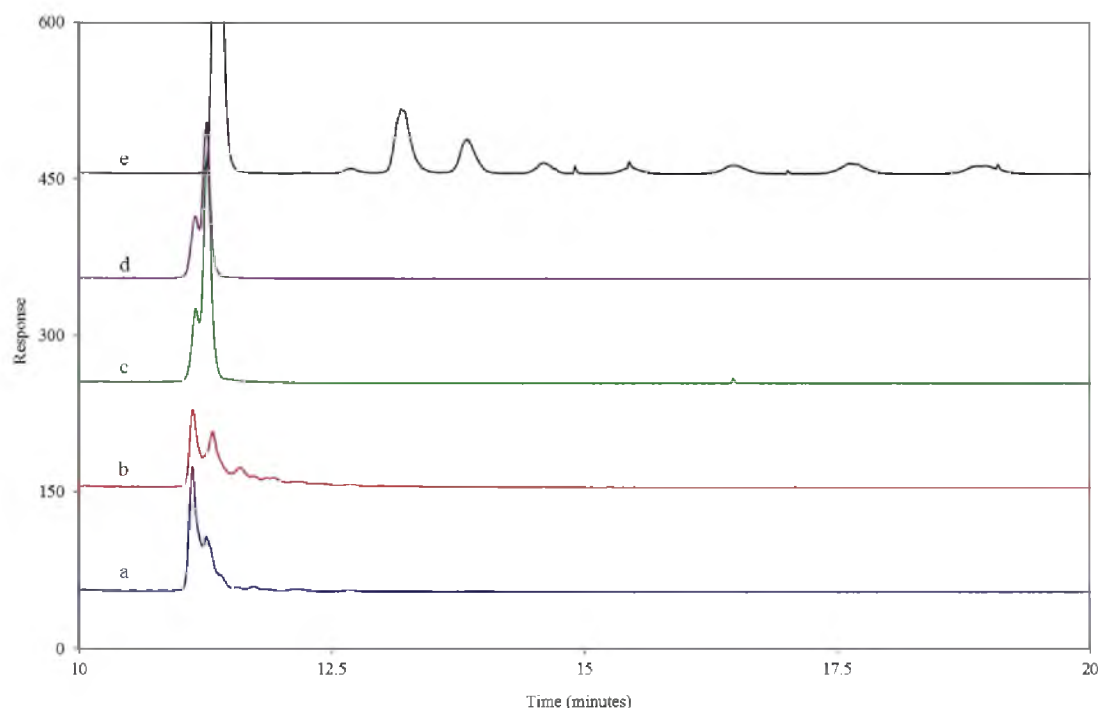


Figure 3.13. HILIC separations of KSB<sub>x</sub> β- CDs: a) reaction DMF 0 SB; b) reaction DMF 1 SB; c) reaction DMF 4 SB; d) reaction DMF 8 SB; and e) a spiked sample of native β- CD, a low DS (reaction THF 0 SP) and high DS (DMF 4 SP) KSP<sub>x</sub> β- CD . Separations were carried out at 1.5 mL/ min using a binary gradient. (A: 10 mM ammonium formate in water; B: 10 mM ammonium formate in 15% (v/v) water: 85% (v/v) acetonitrile). Solvent mixtures were set up to maintain 0% A for 5 minutes and increase to 16.5% A at 8 minutes.

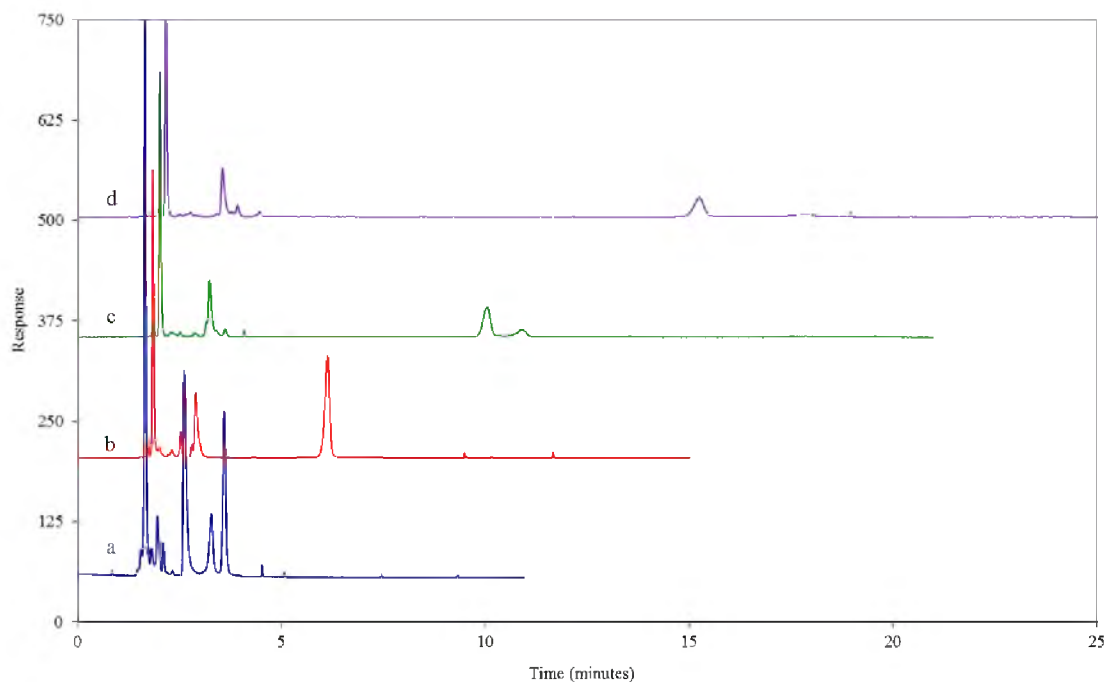


Figure 3.14. Effect of water concentration on HILIC separations of KSB<sub>x</sub> β- CD (reaction DMF 4 SB). Separations were carried out at 1.5 mL/ min under isocratic conditions with 10 mM ammonium formate in: a) 30% (v/v) water: 70% (v/v) ACN; b) 25% (v/v) water: 75% (v/v) ACN; c) 22% (v/v) water: 78% (v/v) ACN; d) 20% (v/v) water: 80% (v/v) ACN.

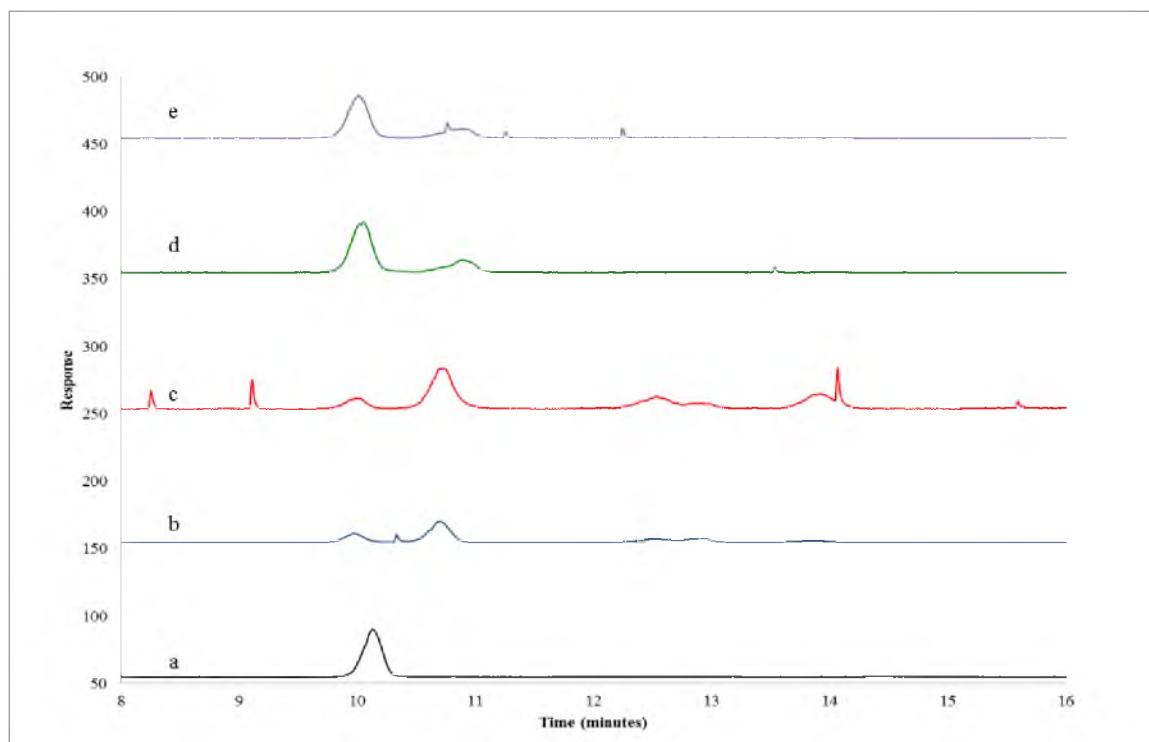


Figure 3.15. HILIC separations of KSB<sub>x</sub> β- CD: a) native β- CD; b) reaction in DMF without 18-C-6; c) reaction in DMF with 1 equiv. of 18-C-6; d) reaction in DMF with 4 equiv. of 18-C-6; and e) reaction in DMF with 8 equiv. of 18-C-6. Separations were carried out isocratically at 1.5 mL/ min using 10 mM ammonium formate in 22% (v/v) water: 78% (v/v) acetonitrile).



Table 3.4. The peak areas (normalized by the molecular weight of the individual charged states) were used to determine the DS of Heptakis(randomly-2,3-O-sulfobutyl)-  $\beta$ -CD from HILIC LT-ELSD results. (\*It is possible that higher DS are present in DMF0SB and DMF1SB. However, further investigation is needed to verify that later peaks are in fact higher DS.)

Reaction Name	DS
DMF 0 SB*	0.68
DMF 1 SB*	0.79
DMF 4 SB	0.23
DMF 8 SB	0.23

The HILIC results for optimizing KSB<sub>x</sub>  $\beta$ -CD were opposite to the results observed for KSP<sub>x</sub>  $\beta$ -CD (Table 3.4). An increase in the amount of 18-crown-6 produced a decrease in the overall DS. This indicates that 1,4-butane sultone is dramatically less reactive under the same reaction conditions. It is also important to note that it is possible that higher DS (a DS of 2 and 3) are present for DMF 0 SB and DMF 1 SB. However, the results are inconclusive and require further investigation to verify.

The use of HILIC LT-ELSD afforded the most reliable results. This is attributed to the ability of the Luna HILIC column to weakly retain the salts and impurities while allowing for stronger retention of the CDs. Analysis of a number of analytes was performed using this method, including the single isomers produced by Kirschner in previous works by this lab. While a single separation mobile phase was not utilized for the single isomers,

KSP<sub>x</sub>  $\beta$ -CDs and the KSB<sub>x</sub>  $\beta$ -CDs, all were successfully characterized using this method.

It is important to note some of the interesting interactions observed during this study.

Initial separations using the separation method defined by Vigh [25] were not effective in isolating the single isomers CDs in Figure 1.6. Using KSP<sub>DS 4.5</sub>DM  $\beta$ -CD as a standard, it was found that an isocratic separation was sufficient enough to separate and resolve DS of 3-7. If the separation of all the charged states from 0-7 is needed, it is recommended to use a gradient elution starting at 15% (v/v) water for the first 5 minutes, increasing to 25% (v/v) at 8 minutes, and held constant. However, for the analysis of the single isomers, the isocratic separation at 25% (v/v) water was sufficient.

Analysis of the single isomer  $\alpha$ -CDs showed that the KSPDM  $\alpha$ -CD and KSBDM  $\alpha$ -CD corresponded to the DS of 6 of the KSP<sub>DS 4.5</sub>DM  $\beta$ -CD standard. However, the KSPDE  $\alpha$ -CD was much more weakly retained. Similar results were observed with  $\beta$ -CDs, where the KSBDM  $\beta$ -CD lined up with DS of 7 and KSPDE  $\beta$ -CD lined up between 4 and 5.

This indicates that the length of the sulfoalkyl chain on the primary hydroxyls (increased from propyl to butyl) was did not significantly affect the retention times. However, a greater affect was observed when changing the alkyl group (increased from methyl to ethyl). From the theory of behind HILIC separations, the increase in the hydrophobicity When analyzing the KSP<sub>DS 8.4</sub>  $\beta$ -CD as a standard, it was found that the weakly retained cation peaks overlapped with the charged states of low DS for most isocratic separations that afforded reasonable retention times. As a result, a gradient elution was chosen to elute the poorly retained cations peaks using 15% (v/v) water in first 5 minutes, followed

by an increase in the % water content in 15 minutes or less, to elute and separate the charged CDs. The water study showed near baseline resolution of all the charged states when using a total of 30% (v/v) water content at 13 minutes. A final analysis using a gradient of 15% (v/v) water for 5 minutes, increased to 29% (v/v) water at 8 minutes, and held for 30 minutes, was used to analyze a mixed standard containing native  $\beta$ -CD, low and high DS of KSP<sub>x</sub>  $\beta$ -CDs.

From the analysis of the single isomer CDs, it was hypothesized that the charged states of KSP<sub>x</sub>  $\beta$ -CDs and KSB<sub>x</sub>  $\beta$ -CDs would have similar retention behavior. However, it was found that the charged states for the KSB<sub>x</sub>  $\beta$ -CDs were retained less on the column than KSP<sub>x</sub>  $\beta$ -CDs. An isocratic water study was performed and it was found that an ideal separation with 22% (v/v) water afforded sufficient separation under 15 minutes and was used to determine the DS of the KSB<sub>x</sub>  $\beta$ -CD reaction series. Interestingly, the elution order of native  $\beta$ -CD (DS of 0) and the charged state DS of 1 reversed when changing from 30% (v/v) water to 22% (v/v) water.

### 3.4 Chiral separations of aromatic alcohols

A chiral separation study was carried out using a series of racemic aryl alcohols that vary the distance of the chiral center from the phenyl group (Figure 3.16). The racemic aryl alcohols are separated using the KSB<sub>DS 6.9</sub>DM  $\beta$ -CD, KSP<sub>DS 4.5</sub>DM  $\beta$ -CD, and KSP<sub>DS 8.4</sub>  $\beta$ -CD to assist in determining the effect of substituent at the secondary rim (Figure 3.17-

3.20). Due to the poor DS observed for KSB<sub>x</sub>M  $\beta$ -CDs and the lack of purity of the samples, these CDs were not used in the study.

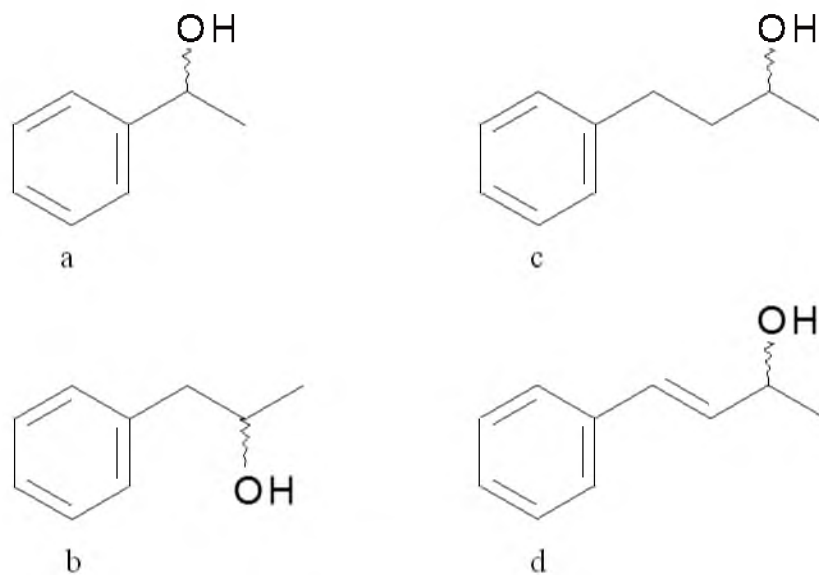


Figure 3.16. The above alcohols are the chiral aryl alcohols used in the CE separation studies: a) (+/-) 1-phenyl ethanol; b) (+/-) 3-phenyl-2-propanol; c) (+/-) 4-phenyl-2-butanol; and d) (+/-) 4-phenyl-3-buten-2-ol.

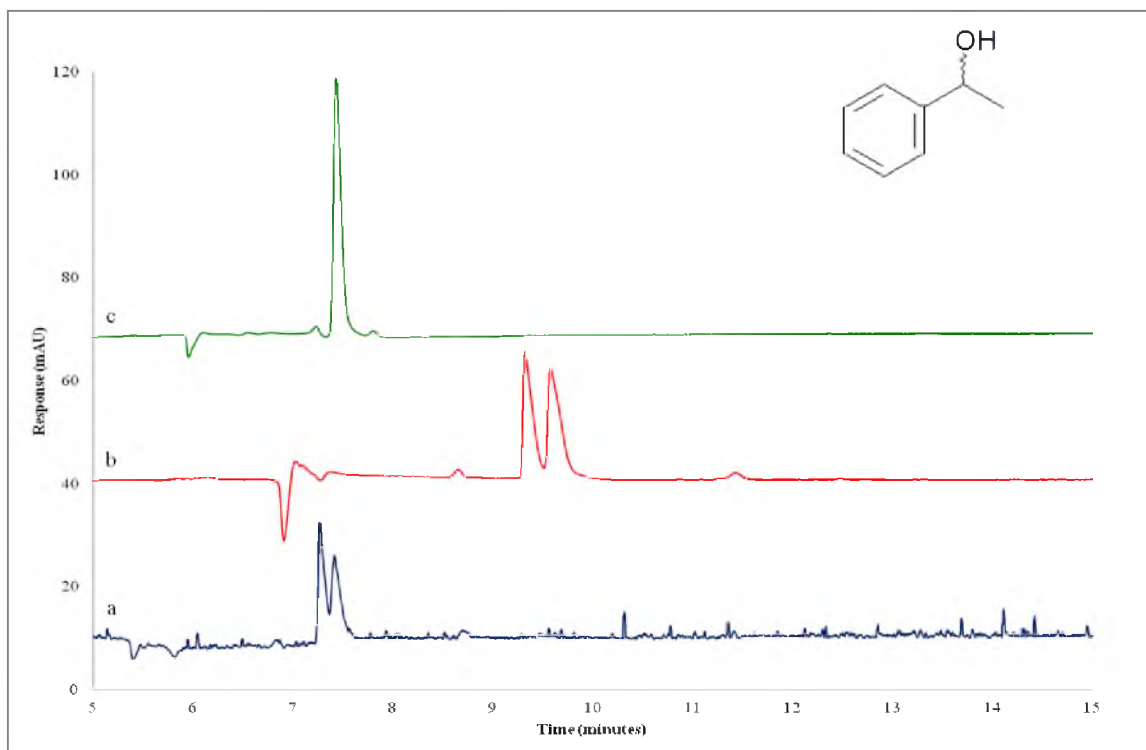


Figure 3.17. Chiral CE separations of (+/-) 1-phenyl ethanol. Buffer additive contains: a) 15 mM KSBDM  $\beta$ -CD; b) 15 mM KSP<sub>4,5</sub>DM  $\beta$ -CD; and c) 15 mM KSP<sub>8,3</sub>  $\beta$ -CD. The buffer contained 20 mM borate at pH 9.0. Separations were carried at 8.0 kV on a 32.5 cm (24.0 cm eff.) x 50  $\mu$ m (i.d.) bare fused silica capillary. A 1.0 sec. injection at 50 mbar was used and analytes were detected at 214 nm.

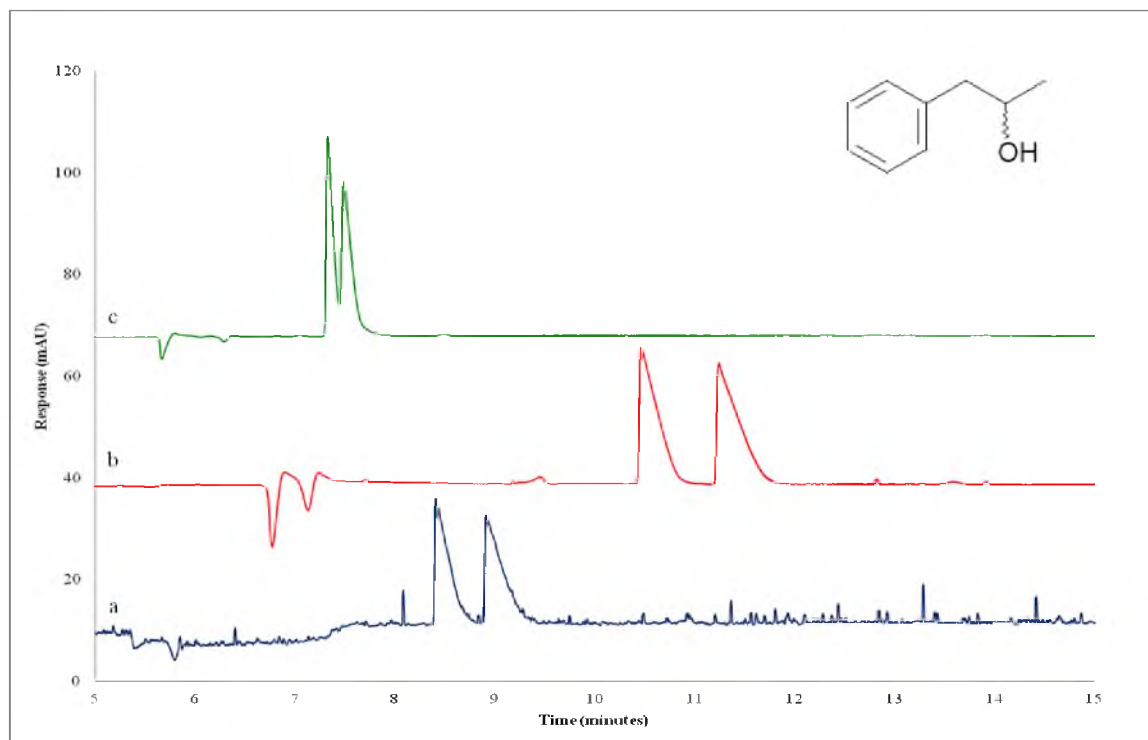


Figure 3.18. Chiral CE separations of (+/-) 3-phenyl-2-propanol. Buffer additive contains: a) 15 mM KSBDM  $\beta$ -CD; b) 15 mM KSP<sub>4.5</sub>DM  $\beta$ -CD; and c) 15 mM KSP<sub>8.3</sub>  $\beta$ -CD. The buffer contained 20 mM borate at pH 9.0. Separations were carried at 8.0 kV on a 32.5 cm (24.0 cm eff.) x 50  $\mu$ m (i.d.) bare fused silica capillary. A 1.0 sec. injection at 50 mbar was used and analytes were detected at 214 nm.

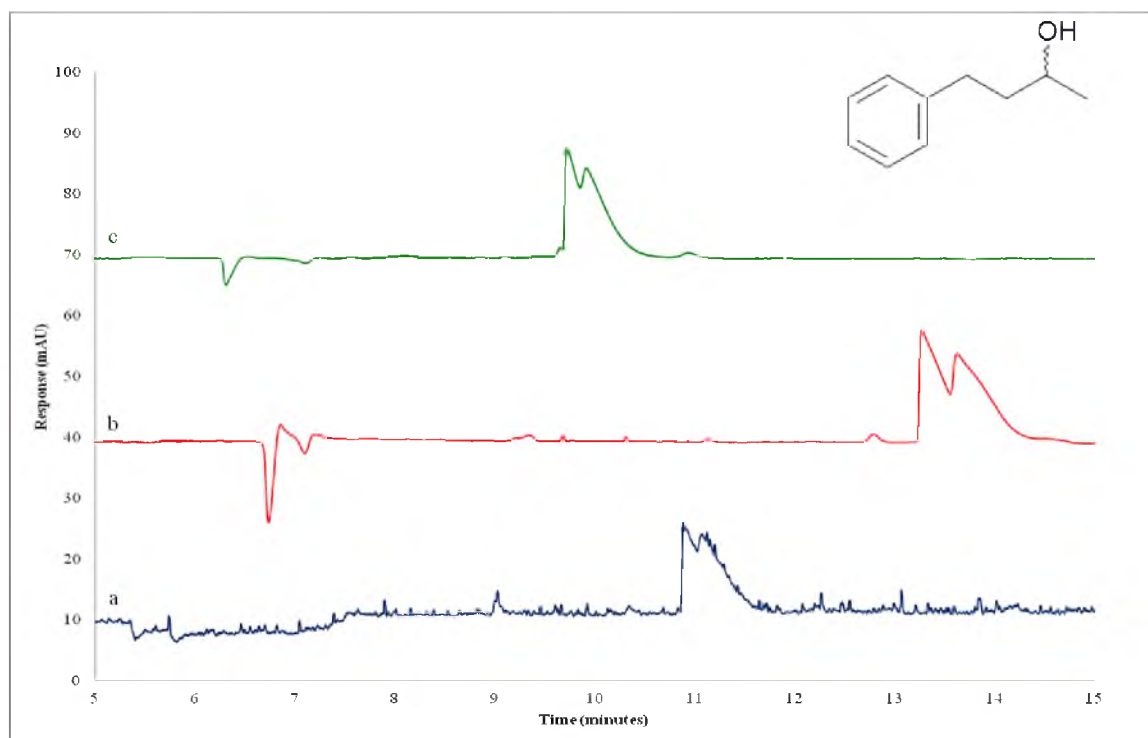


Figure 3.19. Chiral CE separations of (+/-) 4-phenyl-2-butanol. Buffer additive contains: a) 15 mM KSBDM  $\beta$ -CD; b) 15 mM KSP<sub>4.5</sub>DM  $\beta$ -CD; and c) 15 mM KSP<sub>8.3</sub>  $\beta$ -CD. The buffer contained 20 mM borate at pH 9.0. Separations were carried at 8.0 kV on a 32.5 cm (24.0 cm eff.) x 50  $\mu$ m (i.d.) bare fused silica capillary. A 1.0 sec. injection at 50 mbar was used and analytes were detected at 214 nm.

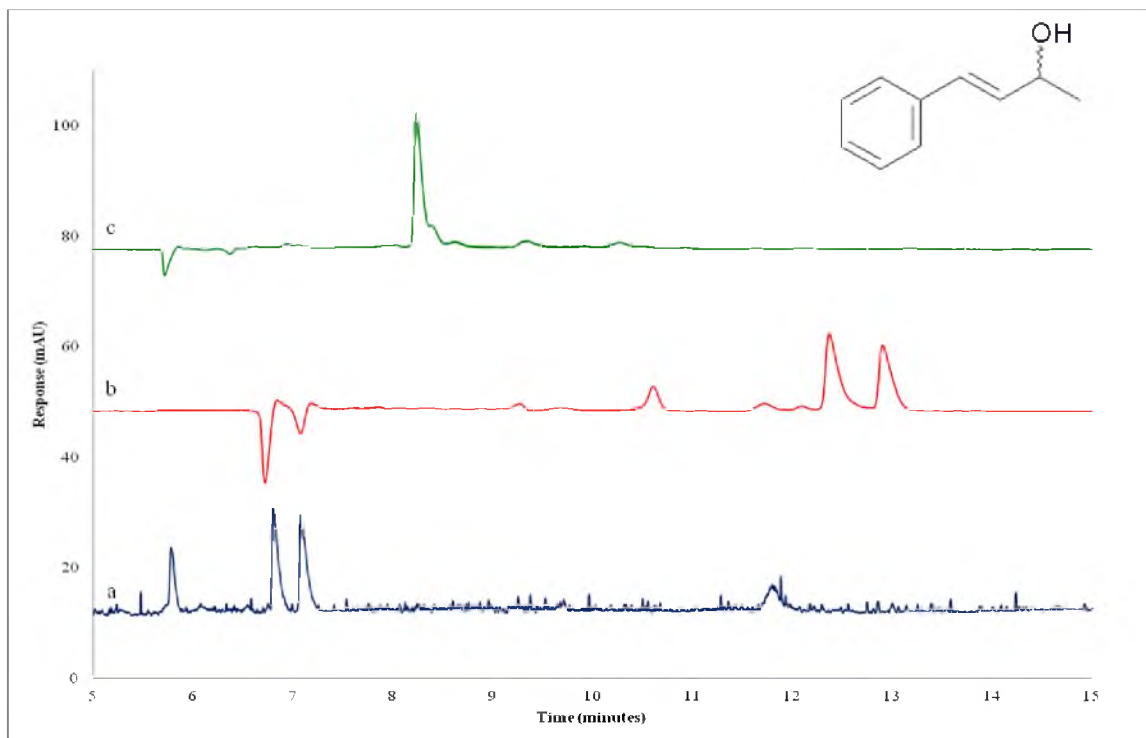


Figure 3.20. Chiral CE separations of (+/-) 1-phenyl-3-buten-2-ol. Buffer additive contains: a) 15 mM KSBDM  $\beta$ -CD; b) 15 mM KSP<sub>4,5</sub>DM  $\beta$ -CD; and c) 15 mM KSP<sub>8,3</sub>  $\beta$ -CD. The buffer contained 20 mM borate at pH 9.0. Separations were carried at 8.0 kV on a 32.5 cm (24.0 cm eff.) x 50  $\mu$ m (i.d.) bare fused silica capillary. A 1.0 sec. injection at 50 mbar was used and analytes were detected at 214 nm.

When analyzing the results of the chiral CE separations of these aryl alcohols, it is important to discuss certain aspects of the CE system and interactions. The separation was carried out using normal polarity (the negative pole is at the detector). This would mean that the negatively charged CDs would migrate toward the inlet of the CE system. If the analyte was to interact strongly with the CD, it would have a longer migration



times. Also, if chiral resolution is to be achieved, a difference in the  $K_{eq}$  between the enantiomers is required. The calculated  $R_s$  values are provided in Table 3.4.

Table 3.5. The calculated  $R_s$  values for the chiral resolution of the aryl alcohols are provided below.

	KSBDM $\beta$ -CD	KSP <sub>4.5</sub> DM $\beta$ -CD	KSP <sub>8.3</sub> $\beta$ -CD
(+/-) 1-phenyl ethanol	1.0	1.2	---
(+/-) 3-phenyl-2-propanol	1.6	2.2	1.1
(+/-) 4-phenyl-2-butanol	0.5	0.8	0.6
(+/-) 4-phenyl-3-buten-2-ol	2.2	3.2	---

While the study was limited to KSP<sub>4.5</sub>DM  $\beta$ -CD, KSBDM  $\beta$ -CD, and KSP<sub>8.3</sub>  $\beta$ -CD, there were some general trends that were observed. It appears that the lower charge afforded the largest interaction (longer migration times) and better resolution. Also, all the CDs showed a general increase in the interaction as the chiral center was moved farther from the aromatic group (excluding the alkenyl derivative), but a maximum resolution is obtained when the chiral center is two bonds away from the aromatic group. Additionally, poor resolution was observed for the (+/-) 4-phenyl-2-butanol with all the CDs, but chiral resolution was observed for (+/-) 4-phenyl-3-buten-2-ol with the KSP<sub>4.5</sub>DM  $\beta$ -CD and KSBDM  $\beta$ -CD, but not for KSP<sub>8.3</sub>  $\beta$ -CD.

These results show better resolution and lower migration times than those obtained by Choi et. al. [39] and without the addition of silver colloids. In order to solidify these results, it is important to apply this study to other CDs and to vary the concentration of the CDs. Also, it would be beneficial to run the analytes in the absence of CD to determine how strongly the CD impacts migration times.

## Chapter 4. Summary and Future Work

For this research, there were four goals: 1) The synthesis of  $\text{KSB}_x\text{M}$   $\beta$ -CD through a protection/ deprotection reaction scheme, 2) The optimization of sulfoalkylation of the secondary rim using heptakis(6-O-TBDMS)-  $\beta$ -CD ( **$\beta$ 2**) by varying solvent choice and amounts of 18-crown-6, 3) characterization of the sulfoalkyl CDs using HILIC LT-ELSD and establishing method development for the analysis of similar CDs, and 4) application of the CDs in chiral CE analysis of aryl alcohols with varying distances of the chiral center from the aromatic group.

The synthesis of heptakis(6-O-methyl)-  $\beta$ -CD was performed by modifications to Fugedi's [15] and Takeo's [41] procedures. This route afforded high yields using moderate reaction conditions while affording minimal purification for majority of the reaction scheme (Figure 1.1). The overall yield for this synthetic scheme is 43%. The sulfobutylation of heptakis(6-O-methyl)-  $\beta$ -CD ( **$\beta$ 6**) showed poor reactivity with 1,4-butane sultone, regardless of the solvent choice.

When optimizing the synthesis of  $\text{KSP}_x$   $\beta$ -CD, it was found that the increase in the amount of 18-crown-6 provided an increase in the DS when the reaction was performed in THF. Also, a higher DS was observed when changing the solvent from THF to DMF. Similar results were not observed when optimizing the synthesis of  $\text{KSB}_x$   $\beta$ -CD. When using 1,4-butane sultone, poor DS was observed for all reaction conditions.

The characterization of the  $\text{KSB}_x\text{M}$   $\beta$ -CD,  $\text{KSP}_x$   $\beta$ -CD and  $\text{KSB}_x$   $\beta$ -CD was reproducibly achieved using HILIC LT-ELSD. The presences of impurities caused NMR and

elemental analysis to be unreliable, and inverse CE was unable to separate the various charged states. While the characterization of KSB<sub>x</sub>M β-CD, KSP<sub>x</sub> β-CD and KSB<sub>x</sub> β-CD were carried out using different conditions, it was found that a study that varies the amount of water could afford baseline separation of the various charged states for these final products.

The initial chiral separation studies here showed a number of effects on resolution that need to be investigated further. First, it appears that the lower DS CDs allow for the highest resolution. Also, a maximum resolution is observed when the chiral center is two bonds away from the aromatic group. Finally, the resolution of the enantiomers is highly dependent on the substituent at the secondary rim of the CD. The CDs with the secondary rim methylated show better resolution than those having sulfopropyl groups.

In an effort to produce a series of CDs with alkyl groups on the primary hydroxyls and randomly sulfoalkyl groups on the secondary hydroxyls, synthesis of a series of hexakis(6-O-alkyl)- α-CDs and heptakis(6-O-alkyl)- β-CDs (alkyls being methyl, ethyl and propyl groups) using the acetyl reaction scheme should be produced. Since poor reactivity was observed for the sulfobutylation of heptakis(6-O-methyl)- β-CD, these CDs should be sulfopropylated with 1,3-propane sultone in DMF with 4 equivalents of 18-crown-6. These 6-O-alkyl-randomly-2,3-O-sulfopropyl potassium salt CDs (KSP<sub>x</sub>R CDs) could then be fully characterized using HILIC LT-ELSD analysis.

In an effort to confirm the HILIC results, the KSP<sub>x</sub>R CDs must be effectively purified. The current purification process requires numerous steps and is a lengthy process. Interestingly, the HILIC separations performed here on the Luna HILIC column afforded

efficient separation of the impurities. However, the use of a preparative Luna HILIC column is quite costly. However, it is possible to use a silica based column HILIC separations that may afford similar separations. Optimization of this separation could then be applied to a medium pressure LC (MPLC) system currently set up in our lab. Once they are sufficiently purified, they could be analyzed using NMR integration and elemental analysis for validation of the HILIC results.

These KSP<sub>x</sub>R CDs could then be used to perform a more thorough study on the separation of the chiral alcohols analyzed briefly in this thesis. It would also be interesting to study variable DS with similar CDs on chiral resolution (comparison of KSP<sub>3.3</sub>  $\beta$ -CD, KSP<sub>4.6</sub>  $\beta$ -CD, KSP<sub>6.1</sub>  $\beta$ -CD and KSP<sub>8.4</sub>  $\beta$ -CD). This would provide a more insight into the mechanism of the chiral separation. Also, it would be beneficial to apply these KSP<sub>x</sub>R CDs to the hydroformylation studies and compared to those synthesized by Kirschner [17].

## References

1. Easton, C.J. and S.F. Lincoln, *Modified cyclodextrins : scaffolds and templates for supramolecular chemistry*. 1999, London: Imperial College Press. ix, 293 p.
2. Del Valle, E.M.M., *Cyclodextrins and their uses: a review*. Process Biochemistry, 2004. **39**(9): p. 1033-1046.
3. Kirschner, D.L. and T.K. Green, *Separation and sensitive detection of D-amino acids in biological matrices*. J Sep Sci, 2009. **32**(13): p. 2305-18.
4. Xiao, Y., et al., *Recent development of cyclodextrin chiral stationary phases and their applications in chromatography*. J Chromatogr A, 2012. **1269**: p. 52-68.
5. Zhang, X.P., et al., *Cyclodextrins and Their Derivatives in the Resolution of Chiral Natural Products: A Review*. Instrumentation Science & Technology, 2012. **40**(2-3): p. 194-215.
6. Zhao, W. and Q. Zhong, *Recent advance of cyclodextrins as nanoreactors in various organic reactions: a brief overview*. Journal of Inclusion Phenomena and Macrocyclic Chemistry, 2012. **72**(1-2): p. 1-14.
7. Khan, A.R., et al., *Methods for selective modifications of cyclodextrins*. Chemical Reviews, 1998. **98**(5): p. 1977-1996.
8. Dong, Z., Q. Luo, and J. Liu, *Artificial enzymes based on supramolecular scaffolds*. Chem Soc Rev, 2012. **41**(23): p. 7890-908.

9. Sinay, P. and A.J. Pearce, *Diisobutylaluminum- Promoted Regioselective De-O-Benzylation of Perbenzylated Cyclodextrins: A Powerful New Strategy for the Preparation of Selectively Modified Cyclodextrins*. *Angewandte Chemie International Edition*, 2000. **39**(20): p. 3610-3612.
10. Ortega-Caballero, F., et al., *Four orders of magnitude rate increase in artificial enzyme-catalyzed aryl glycoside hydrolysis*. *Journal of Organic Chemistry*, 2005. **70**(18): p. 7217-7226.
11. Lindback, E., et al., *Two Diastereomeric Artificial Enzymes with Different Catalytic Activity*. *European Journal of Organic Chemistry*, 2012(27): p. 5366-5372.
12. Varga, G., et al., *Chiral separation by a monofunctionalized cyclodextrin derivative: From selector to permethyl-beta-cyclodextrin bonded stationary phase*. *Journal of Pharmaceutical and Biomedical Analysis*, 2010. **51**(1): p. 84-89.
13. Laza-Knoerr, A.L., R. Gref, and P. Couvreur, *Cyclodextrins for drug delivery*. *J Drug Target*, 2010. **18**(9): p. 645-56.
14. Otero-Espinar, F.J., et al., *Cyclodextrins in drug delivery systems*. *Journal of Drug Delivery Science and Technology*, 2010. **20**(4): p. 289-301.
15. Fugedi, P. and P. Nanasi, *Synthesis of 6-O- $\alpha$ -D-Glucopyranosylcyclomaltoheptaose*. *Carbohydrate Research*, 1988. **175**: p. 173-181.

16. Kirschner, D.L. and T.K. Green, *Nonaqueous synthesis of a selectively modified, highly anionic sulfopropyl ether derivative of cyclomaltoheptaose ( $\beta$ -cyclodextrin) in the presence of 18-crown-6*. Carbohydrate Research, 2005. **340**(11): p. 1773-1779.
17. Kirschner, D., et al., *Fine tuning of sulfoalkylated cyclodextrin structures to improve their mass-transfer properties in an aqueous biphasic hydroformylation reaction*. Journal of Molecular Catalysis A: Chemical, 2008. **286**(1-2): p. 11-20.
18. Tait, R.J., et al., *Characterization of sulphoalkyl ether derivatives of beta-cyclodextrin by capillary electrophoresis with indirect UV detection*. J Pharm Biomed Anal, 1992. **10**(9): p. 615-22.
19. Harris, D.C., *Quantitative chemical analysis*. 6th ed. 2003, New York: W.H. Freeman and Co.
20. Snyder, L.R., J.L. Glajch, and J.J. Kirkland, *Practical HPLC method development*. 1988, New York: J. Wiley. xvi, 260 p.
21. Alpert, A.J., *Hydrophilic-interaction chromatography for the separation of peptides, nucleic acids and other polar compounds*. J Chromatogr, 1990. **499**: p. 177-96.
22. Guo, Y. and S. Gaiki, *Retention and selectivity of stationary phases for hydrophilic interaction chromatography*. Journal of Chromatography A, 2011. **1218**(35): p. 5920-5938.



23. Buszewski, B. and S. Noga, *Hydrophilic interaction liquid chromatography (HILIC)-a powerful separation technique*. Analytical and Bioanalytical Chemistry, 2012. **402**(1): p. 231-247.
24. Hemstrom, P. and K. Irgum, *Hydrophilic interaction chromatography*. Journal of Separation Science, 2006. **29**(12): p. 1784-1821.
25. Estrada, R., 3rd and G. Vigh, *Comparison of charge state distribution in commercially available sulfated cyclodextrins used as chiral resolving agents in capillary electrophoresis*. J Chromatogr A, 2012. **1226**: p. 24-30.
26. Mitchell, C.R., et al., *Comparison of the sensitivity of evaporative universal detectors and LC/MS in the HILIC and the reversed-phase HPLC modes*. Journal of Chromatography B-Analytical Technologies in the Biomedical and Life Sciences, 2009. **877**(32): p. 4133-4139.
27. Hjerten, S., *Free zone electrophoresis*. Chromatogr Rev, 1967. **9**(2): p. 122-219.
28. Jorgenson, J.W. and K.D. Lukacs, *Zone electrophoresis in open-tubular glass capillaries*. Analytical Chemistry, 1981. **53**(8): p. 1298-1302.
29. Terabe, S., et al., *Electrokinetic separations with micellar solutions and open-tubular capillaries*. Analytical Chemistry, 1984. **56**(1): p. 111-113.
30. Chankvetadze, B., *Enantioseparations by using capillary electrophoretic techniques. The story of 20 and a few more years*. J Chromatogr A, 2007. **1168**(1-2): p. 45-70; discussion 44.
31. Weinberger, R., *Practical capillary electrophoresis*. 1993, Boston: Academic Press. xv, 312 p.

32. Evans, C.E. and A.M. Stalcup, *Comprehensive strategy for chiral separations using sulfated cyclodextrins in capillary electrophoresis*. Chirality, 2003. **15**(8): p. 709-723.
33. Baum, K., *Reactions of Silver Perchlorate and of Silver Triflate with Alkyl Iodides. Solvent Inhibition of Isomerization*. The Journal of Organic Chemistry, 1974. **39**(26).
34. Gobbi, A., et al., *Metal-Ion Catalysis in Nucleophilic-Substitution Reactions Promoted by Complexes of Polyether Ligands with Alkali-Metal Salts*. Journal of Organic Chemistry, 1995. **60**(18): p. 5954-5957.
35. Gokel, G.W., et al., *Clarification of the Hole-Size Cation-Diameter Relationship in Crown Ethers and a New Method for Determining Calcium Cation Homogeneous Equilibrium Binding Constants*. Journal of the American Chemical Society, 1983. **105**(23): p. 6786-6788.
36. Corey, E.J. and M. Chaykovsky, *Methylsulfinylcarbanion*. Journal of the American Chemical Society, 1962. **84**(5): p. 866-867.
37. Corey, E.J. and M. Chaykovsky, Journal of the American Chemical Society, 1965. **87**(6): p. 1345-1353.
38. Suntornsuk, L., *Recent advances of capillary electrophoresis in pharmaceutical analysis*. Anal Bioanal Chem, 2010. **398**(1): p. 29-52.

39. Choi, S.-H., H.-J. Noh, and K.-P. Lee, *Chiral Separation of Arylalcohols by Capillary Electrophoresis Using Sulfonated  $\beta$ -Cyclodextrin and Ag Colloids as Additives*. Bulletin of the Korean Chemical Society, 2005. **26**(10): p. 1549-1554.
40. Takeo, K.i., K. Uemura, and H. Mitoh, *Derivatives of  $\alpha$ -Cyclodextrin and the Synthesis of 6-O- $\alpha$ -D-Glucopyranosyl- $\alpha$ -cyclodextrin*. Journal of Carbohydrate Chemistry, 1988. **7**(2): p. 293-308.
41. Takeo, K.i., H. Mitoh, and K. Uemura, *Selective Chemical Modification of Cylomalto-Oligosaccharides via tert-butylmethyilsilation*. Carbohydrate Research, 1989. **187**: p. 203-221.
42. Tongiani, S., et al., *Sulfoalkyl ether-alkyl ether cyclodextrin derivatives, their synthesis, NMR characterization, and binding of 6 $\alpha$ -methylprednisolone*. Journal of Pharmaceutical Sciences, 2005. **94**(11): p. 2380-2392.
43. Qu, Q., E. Tucker, and S.D. Christian, *Sulfoalkyl Ether  $\beta$ -Cyclodextrin Derivatives: Synthesis and Characterizations*. Journal of Inclusion Phenomena and Macrocyclic Chemistry, 2002. **43**: p. 213-221.
44. Stella, V.J., et al., *Evaluation of the utility of capillary electrophoresis for the analysis of sulfobutyl ether  $\beta$ -cyclodextrin mixtures*. Journal of Pharmaceutical and Biomedical Analysis, 1996. **15**: p. 63-71.
45. Li, D.M., S.L. Fu, and C.A. Lucy, *Prediction of electrophoretic mobilities. 3. Effect of ionic strength in capillary zone electrophoresis*. Analytical Chemistry, 1999. **71**(3): p. 687-699.

